DESIGN OF A MM-WAVE BEAMFORMING NETWORK AND ANTENNA ARRAY

BY

ALI TAWFIQ RASHED ALRESHAID

A Thesis Presented to the
DEANSHIP OF GRADUATE STUDIES

KING FAHD UNIVERSITY OF PETROLEUM & MINERALS

DHAHRAN, SAUDI ARABIA

In Partial Fulfillment of the
Requirements for the Degree of

MASTER OF SCIENCE

In

ELECTRICAL ENGINEERING DEPARTMENT

DECEMBER 2014

KING FAHD UNIVERSITY OF PETROLEUM & MINERALS

DHAHRAN- 31261, SAUDI ARABIA

DEANSHIP OF GRADUATE STUDIES

This thesis, written by **ALI TAWFIQ RASHED ALRESHAID** under the direction his thesis advisor and approved by his thesis committee, has been presented and accepted by the Dean of Graduate Studies, in partial fulfillment of the requirements for the degree of **MASTER OF SCIENCE IN ELECTRICAL ENGINEERING.**

Dr. Ali Ahmad Al-Shaikhi
Department Chairman

Dr. Mohammad S. Sharawi
(Advisor)

Dr. Salam A. Zummo
Dean of Graduate Studies

عمادة الدراسات العليا
DEANSHIP OF GRADUATE STUDIES

H. Masoudi 24-12-2014

Prof. Husain M. Masoudi
(Member)

5/2/15
Date

Sheikh Sharif 24-12-2014

Dr. Sheikh Sharif Iqbal
(Member)

To my parents, Maha and Tawfiq

ACKNOWLEDGMENTS

The author would like to thank his advisor, Dr. Mohammad Sharawi, for his effort in supervising the work done in this Thesis. His advises, corrections, and suggestions were essential to this work.

The effort done by Prof. Kamal Sarabandi in acquiring the measurements for the fabricated designs is acknowledged by the author. Dr. Kamal conducted the measurements at the University of Michigan, An Arbor, USA.

The author would also thank Mohammad Umar Khan and Rifaqat Hussain for their help in manufacturing and measuring the system in the Antenna and Microwave Structure Design Lab at KFUPM.

Finally, the author would like to express his appreciation to the National Science, Technology and Innovation Plan (NSTIP), represented by the Deanship of Scientific Research (DSR) at King Fahd University of Petroleum and Minerals for funding this project.

TABLE OF CONTENTS

LIST OF TABLES

LIST OF FIGURES

LIST OF ABBREVIATIONS

3D	**:**	Three Dimensions
AF	**:**	Array Factor
BW	**:**	Bandwidth
CMOS	**:**	Complementary Metal Oxide Semiconductor
dB	**:**	Decibel (Logarithmic ratio)
dB_i	**:**	Decibel (Compared to an isotropic radiator)
dBm	**:**	Decibel (Compared to 10^{-3} of a unit)
FEM	**:**	Finite element method
HFSS	**:**	High Frequency Structural Simulator
HPBW	**:**	Half-power Beam width
LTE	**:**	Long-Term evolution
MIMO	**:**	Multi-input Multi-output
MM-WAVE	**:**	Millimeter-Wave
MWO	**:**	Microwave Office
PCB	**:**	Printed-Circuit Board
RF	**:**	Radio Frequency
SIW	**:**	Substrate-integrated waveguide

ABSTRACT

Full Name : [Ali Tawfiq Al-Reshaid]

Thesis Title : [DESIGN OF A MM-WAVE BEAMFORMING NETWORK AND ANTENNA ARRAY]

Major Field : [Electrical Engineering - Electromagnetics]

Date of Degree : [December 2014]

Beam-Forming Feed Networks played major role in radar communications and directive antenna systems in beam scanning applications. One of the most desirable features of any radar system is to have directional high data rate communications. One of the powerful candidates is the Millimeter-wave Technology. Mm-wave communications has been used for a long time in the military and for point-to-point communication links. Recently, their consideration for short range communications and inclusion with 5G standards has been accepted by the research and industrial communities. It offers very large transmission bandwidth that is required to satisfy the expected 5G throughput, levels that are expected to be 1000 times more that its 4G counterparts.

In this work, the design of a Beam-Forming feed network based on the Butler matrix and an Antenna Array operating at mm-wave is presented. A step by step procedure is followed to design and fabricate the system that consists of a 4x4 Butler matrix feed network and a 16-element printed Antenna Array consisting of 4x4 planar slot based antenna elements. Every 4 slot antennas are series fed by a common microstrip line to reduce the complexity of the design. The integrated feed network and antenna array operated at 28.5 GHz with a simulated bandwidth of 1 GHz. In simulations, the maximum achieved gain was 12 dB and the beam was switched between four directions; -45˚, -20˚, +20˚ and +45˚. Several prototypes were fabricated and simulation and measurements results are compared.

ABSTRACT (Arabic)

ملخص الرسالة

الاسم الكامل: علي بن توفيق الرشيد

عنوان الرسالة:

التخصص: الهندسة الكهربائية - الكهرومغناطيسية

تاريخ الدرجة العلمية: ديسيمبر 2014

شبكات التغذية المكوّنة للأشعة الموجّهة لعبت دوراً كبيراً في قطاع الاتصالات وأنظمة الهوائيات التوجيهية. واحدة من أكثر السمات المرغوب فيها في أنظمة الإتصالات هي توفير وسيلة اتّصال ذات معدّل نقل بيانات عالي وذات توجيه قوي. وهذه المتطلّبات تجعل تقنية أشعّة المللميتر من أبرز المرشحين لتوفير قنوات الاتصال. تم استخدام تقنية أشعّة المللميتر منذ زمن طويل في القطاعات العسكرية وفي قنوات الاتصال بين مستخدم واحد إلى مستخدم واحد فقط. بدأت المجالات العسكرية والصناعية مؤخراً بالإهتمام بها في توفير الاتصالات ذات المدى القريب وفي تقنية التواصل الجديدة (5G). هذه التقنية الجديدة توفّر وسيلة اتصال ذات نطاق ترددي عريض لتوفير معدّل نقل البيانات كافي لتلبية متطلبات التقنية الجديدة (5G). الطاقة الاستيعابية لنقل البيانات تفوق 1000 مرّة الكميّة التي نحصل عليها من التقنية الحالية (4G).

في هذه الرسالة، سوف يتم تصميم نظام شبكة تغذية مكوّنة للأشعّة الموجهة باستخدام مصفوفة (بتلر) وسيتم إيصالها بمصفوفة هوائيّات وسيعمل النظام بتقنية أشعّة المللميتر. سيتم إيضاح التصميم والتصنيع والقياسات المعملية بالتفصيل للنظام الذي يتكوّن من شبكة تغذية مكوّنة من أربع مداخل وأربع مخارج متصلة إلى مصفوفة هوائيّات من 16 عنصر. كل أربع عناصر من الهوائيّات سيتم تغذيتها بشريط واحد ذو عرض 0.3 جزء من المليون من المتر لتبسيط تعقيد تركيب المصفوفة الهوائيّة على شبكة التغذية. تم تصميم النظام أولاً باستخدام نظام محاكاة للأنظمة عالية التردد وتم الحصول على نطاق ترددي ذو عرض 1 قيقاهرتز ويعمل على التردد 28.5 قيقاهرتز. أعلى قوة توجيهية تم الحصول عليها كانت بمقدار 12 ديسيبل وتم النجاح بتوجيه الأشعة عن محور النظام إلى أربع اتجاهات: $+20^{\circ}$, -20°, -45° $+45^{\circ}$. تم تصميم وتصنيع عدّة نماذج من النظام في هذه الرسالة وسيتم مقارنة النتائج من برامج المحاكاة مع نتائج القياسات المعملية.

CHAPTER 1

INTRODUCTION

The demand for the high data rate systems seems to grow tremendously in the near future. That is the major factor nominating millimeter-wave technology to be a powerful candidate for 5G standards. Mm-wave systems have been established decades ago, where the main focus was for the Military purposes and point-to-point applications. With the supporting factors of succeeding in manufacturing low-cost low-loss materials, and the recent potential research from the academia and commercial industry, mm-wave is trending to dominate the wireless technology in the coming years. Researchers and organizations started the move toward standardizing and licensing new bands, placing more attention toward this band from industrial and commercial firms [1].

The name of the technology; "mm-wave", comes from the operating wavelength of the systems' frequency band. Since the frequency spectrum ranges from 30 to 300 GHz, the operating wavelength will range from 10 to 1 mm.

A lot of focus was given to the 60 GHz band, because it is an unlicensed band. Many researches have been conducted in this frequency band. This high frequency technology offered a lot of promising features and advantages over other techniques. Unfortunately, one of the major affecting disadvantages is the high path loss, resulting in having a short range of communication. That is why this technology will be mainly targeted to work in indoor environments. Several positive points about this technology are:

- High Bandwidth: A large unlicensed bandwidth has been established, which is available in all countries. This bandwidth could reach up to 7 GHz.

- Low interference with current devices: Most of the wireless devices used nowadays are working on the region from 1 to 7 GHz. So, negligible interference is expected.

- Frequency Re-use: Since the mm-wave signal fades rapidly, the same used frequency can be used again in a near area without having interference between them.

- Compact System Size: Since the operating frequency is very high, the size of antennas and systems will be relatively small, easing the problem of integrating the design into small devices.

As mentioned earlier, high path loss is a major drawback of mm-wave technology. These losses are introduced in the channel due to the composition of the atmosphere. It can be noticed in Figure 1 that we have an attenuation peak at 60 GHz due to Oxygen molecules. This can be avoided by shifting the operating frequency down to 30 GHz instead. To be more exact, the lowest attenuation achieved was at around 28 GHz, and it was 0.12 dB/Km at sea level. This is the reason why we chose our center frequency to be 28.5 GHz. By setting this certain frequency, the path attenuation is heavily reduced by almost 9 dB at sea level. [1]

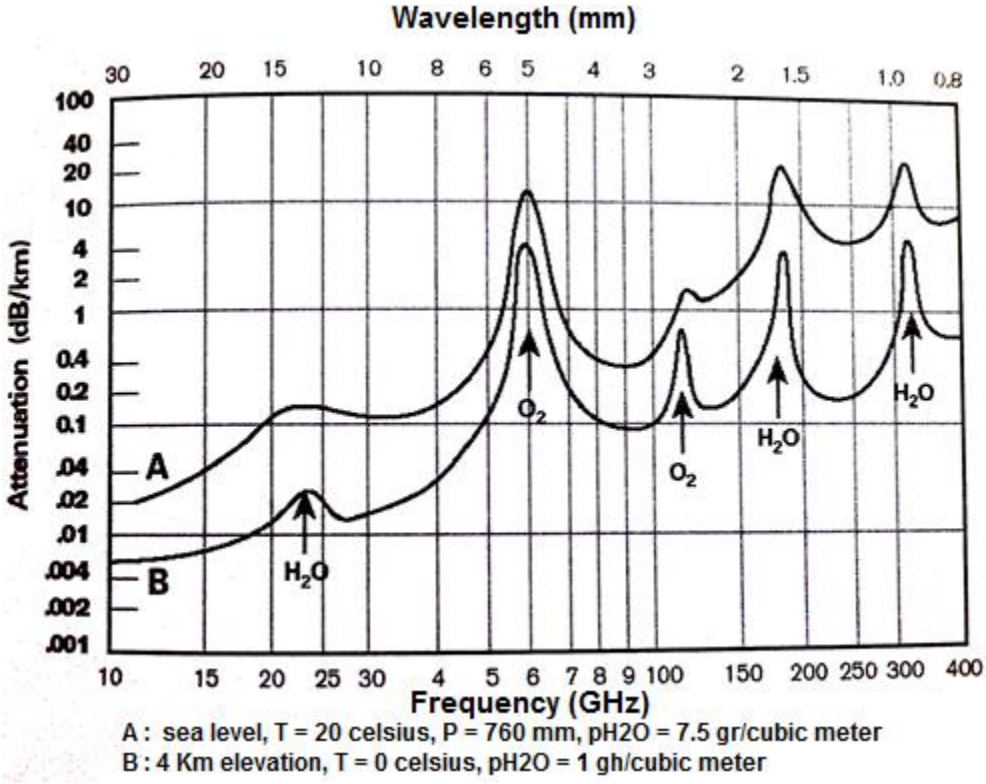

Figure 1 Average Atmospheric Absorption of millimeter waves [1]

According to reference [2], the life cycle of every wireless technology is a decade at most. So, there is point (estimated approximately at 2020) where the current 4G-LTE technology that offers 20 MHz channels for customers, will be insufficient to cover the BW need. This massive need can be satisfied by the BW offered when operating at high frequencies, such as mm-wave spectrum. Extensive measurements were conducted in [3]. The measurements show

promising results for two bands; 28 and 38 GHz, proposing them as the radio frequency carriers for 5G technology.

In this work, the 28.5-GHz band is targeted. A beam-forming feed network based on Butler matrix will be integrated with a planar 4x4 antenna array through power splitters and combiners as illustrated by Figure 2

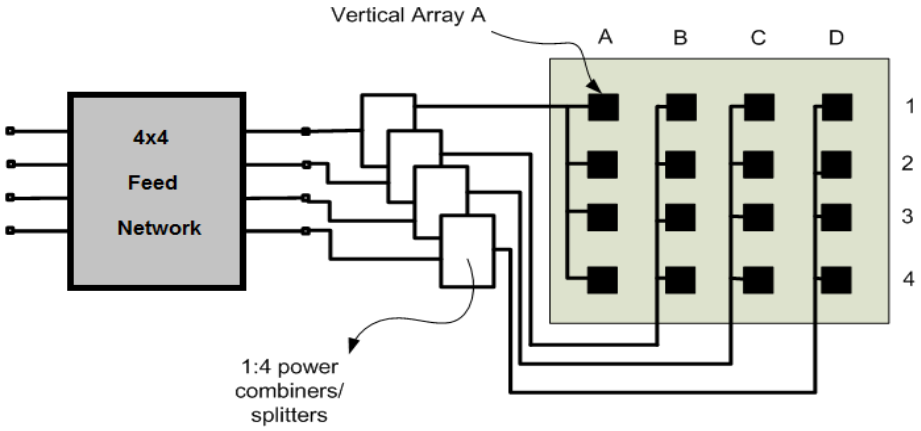

Figure 2 Overall Proposed System

1.1 Contributions

The contributions of this work are:

1. Design and simulation of a broadband Slot antenna array (4x4 planar) with a center frequency of 28.5 GHz and a bandwidth of 1 GHz.

2. Design of a broadband 4x4 Butler matrix feed network operating at 28.5 GHz with at least 500 MHz BW.

3. Detailed characterization of the performance of the fabricated antenna array and its feed network in the laboratory.

4. Characterization of the performance of the integrated array with its Butler matrix feed network and assess its beam switching performance for short range communication systems in an antenna testing facility.

1.2 Thesis Organization

This Thesis has 8 chapters to illustrate and show the work done to achieve the objectives. Chapter 2 covers the theoretical background needed to understand the behavior of the system. First, the Butler feed network will be explained and why it was chosen over other beam-forming networks. Also, consisting components of Butler network will be illustrated. Finally, microstrip-based antennas; slot and rectangular patch will be analyzed and illustrated.

A literature review is conducted in chapter 3, covering the previous work done about Butler network with more focus to papers proposed a complete system including the antenna array.

Chapter 4 shows the design steps and procedures that were applied to acquire the targeted system. The design procedure took several stages to get into the final design, but they will be summed up to 3 important stages. Stage I suffered from high loss, while stage II almost attained ideal performance. Stage III was to mitigate a problem occurred with measurements conducted on fabricated models of stage II. All of the focus of this chapter is given to Butler network alone.

The complete integrated system including Butler network and antenna array with their feed network is designed and optimized in Chapter 5. First, single antenna elements are designed individually; analyzing the radiation properties of the slot antenna as well as the patch antenna. Later, a linear 1x4 antenna array was built for the two antenna types to ensure the performance and the expected radiation when connect to Butler network. After that, the power splitter/combiner needed to connect Butler with the antenna array is discussed and designed. After that, the planar 4x4 slot antenna array is simulated; to guarantee the ability of the power splitter to feed the antenna elements properly so they will provide the expected radiation patterns when fed. Finally, the complete integrated system is simulated and analyzed.

In chapter 6, fabrications and measurements for designed Butler and antenna array will be shown. First, it will show the failed attempts to fabricate Butler network based on Stage I. Then, it will show measurements conducted on Butler model that is based on Stage II. Also, Butler network based on Stage III as well as the complete system design including the linear as well as the planar antenna array will be shown and their measurements will be analyzed. Finally, a plan for future work will be mentioned in Chapter 7.

CHAPTER 2

THEORITICAL BACKGROUND

2.1 Beam-Forming Networks

There are several configurations that can provide the desired phase and amplitude at the output ports for multi-beams antenna systems. They can be classified into different categories; Active and Passive, Steering and Non-Steering, Simple and complex. Each configuration has its own pros and cons.

Several beam-forming networks have been investigated in an earlier work [4]. The Butler feed network was preferred over other types as its behavior can modeled firmly and its design is of less complexity. This is the reason of giving all of the focus on Butler in this work. The most widely used networks are:

- Butler Matrix Feed Network
- Phased Array Network
- Rotman Lens
- Monopulse Network

2.2 Butler Feed Network

A beam-forming network based on the Butler Matrix is a reciprocal network. In other words, it can be used to combine the signals from an array Antenna or to split the injected signal into n-outputs with the corresponding phase shifts needed to feed the antenna array.

The Butler Network is an NxN network. It has N inputs and N outputs. For transmitting mode, depending on which input is injected with the signal, a certain direction of radiation will be generated. So a switch might be needed to control this process. In receiving mode, the array antennas will receive a signal in certain direction that will result in having one of the outputs acquiring most of the power of the signal. In other words, the port with highest power will be the one whose radiation configuration is used in receiving the signal. This can be used to determine the direction of the receiving signal.

For these networks, the number of inputs and outputs "N" is flexible. In literature review, one can find 4x4, 5x5, 6x6, 8x8 and 16x16 configurations.

Depending on this number, everything is designed accordingly; starting from number of components needed to the phase shifts required from fixed phase shifters.

The reasons of choosing Butler over other kinds of networks are:

- It is a Reciprocal network; it can be used for transmitting and receiving.
- It is a Passive circuit; no external biasing is needed.
- No need for external control.
- Compact Design.

Unfortunately, it has some drawbacks, such as:

- Beam patterns are fixed; it cannot be steered to other angles than the pre-defined ones.
- Power levels and phases of outputs cannot be modified.
- Many components are needed.

The components used to build this type of network are:

- 90° Hybrid Coupler
- Crossover
- Fixed Phase Shifter
- Quarter-wavelength transformer.

The number of these components is related to the number of inputs and outputs. For different values of "N", different numbers of components are needed. Taking a 4x4 Butler network in this work, there will be four Hybrid couplers, two crossovers, two phase shifters and several quarter-wavelength transformers for matching purposes. The system is shown in Figure 3.

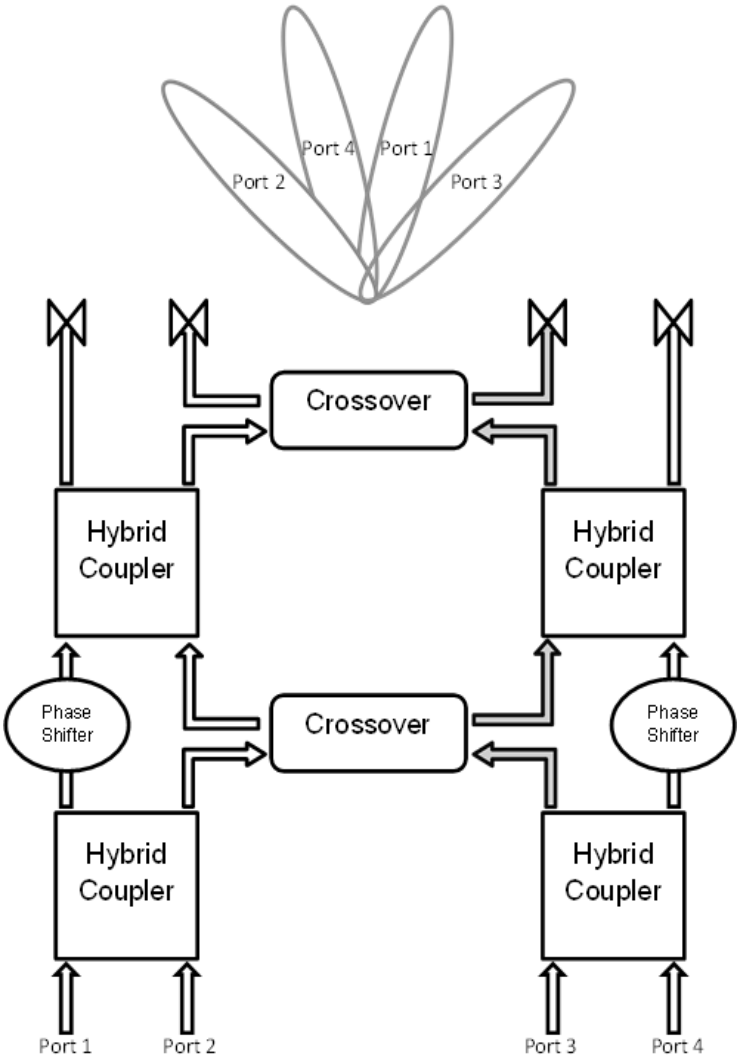

Figure 3 Block diagram of 4x4 Butler Feed Network

The number of required components can calculated based on the number of inputs 'N', which has to be two raised to the power of multiples of two. [5]

$$N_{Hybrid\ COupler} = \left(N/2\right) \times \log_2(N) \qquad (2.1)$$

$$N_{Phase\ shifters} = \left(N/2\right) \times \log_2(N-1) \qquad (2.2)$$

The radiation patterns are also determined by N. In this work, the Butler is 4x4, so the output phases should be -135, -45, +45 and +135 when port 1, 2, 3 or 4 is excited, respectively. In other words, when port 1 is excited, the phase

difference between adjacent outputs must be -45 degrees in order to have the desired constructive and destructive additions between the outputs. Considering Figure 3, if the leftmost port is used as input, we will have a radiation pattern similar to the one titled with "1R".

The pattern of the phase differences between the output ports can also be modeled. Depending on 'N', the network will generate N orthogonal beams. The model is described by the following relations, which is taken from the array factor illustrated in chapter 6 of [6]:

$$\sin\theta_i = \pm\left[i\,\lambda/2\,N\,D\right]; \quad i = 1, 2, 3, \ldots, N-1 \qquad (2.3)$$

$$\alpha_i = \beta\, d\, \sin\theta_i = \frac{2\pi}{\lambda} \times d\, \sin\theta_i = i\left(\pi/N\right) \qquad (2.4)$$

Where θ is the elevation angle from the Z-axis in the Cartesian coordinate system, λ is the wavelength, N is the number of elements in the array, D is the inter-elements spacing and β is 2π divided by λ.

Table 1 shows the values of the phases of each output port for four cases. Case 1 is when port 1 is excited. Case 2 is when port 2 is excited, and so on. For the case when port 3 is excited, Beam Port-3's column shows the values of phases for the four output ports. It can be noticed that the phase difference between the ports will -135 degrees as shown.

Table 1 Phase difference between output ports for 4x4 Butler

Output\Input	Beam Port-1	Beam Port-2	Beam Port-3	Beam Port-4
Port-5	135	45	90	0
Port-6	90	180	-45	45
Port-7	45	-45	180	90
Port-8	0	90	45	135
Phase Diff.	-45	135	-135	45

2.3 Butler Network's Components

2.3.1 Hybrid Coupler

The 90° Hybrid coupler is a block that is capable of splitting the signal into two equal parts with a phase difference of 90 degrees between them. This coupler is symmetrical and has four ports. It can be analyzed by even-odd method. A block diagram is shown in Figure 4.

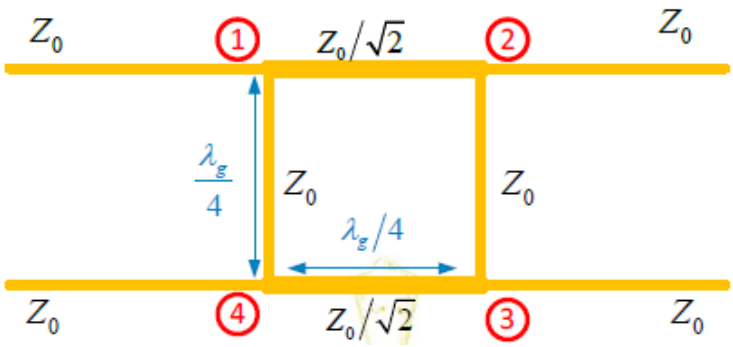

Figure 4 Block Diagram of Hybrid Coupler

In the hybrid coupler shown above, ports 1 and 4 are isolated; if a signal injected into port 1, nothing will arrive to port 4. It is expected that the power of the signals at ports 2 and 3 are equal. The benefit of this configuration over normal power divider is that it provides phase difference between the outputs; this will be used to have the required output phases at the outermost terminals. So, in terms of scattering parameters, S14 is expected to be zero and $S_{21}/S_{31} = \pi/2$.

$$\boldsymbol{S} = \frac{-1}{\sqrt{2}} \begin{bmatrix} \mathbf{0} & \boldsymbol{j} & \mathbf{1} & \mathbf{0} \\ \boldsymbol{j} & \mathbf{0} & \mathbf{0} & \mathbf{1} \\ \mathbf{1} & \mathbf{0} & \mathbf{0} & \boldsymbol{j} \\ \mathbf{0} & \mathbf{1} & \boldsymbol{j} & \mathbf{0} \end{bmatrix} \qquad (2.5)$$

The Hybrid Coupler can be built by connecting two pairs of quarter-wavelength micro strip lines of certain characteristic impedance with another pair of the same length but with impedance equal to the characteristic value divided by $\sqrt{2}$. Figure 5 shows examples of fabricated Hybrid couplers.

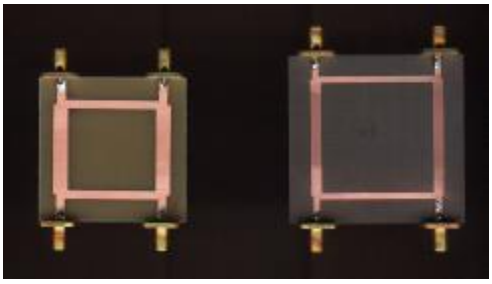

Figure 5 Fabricated Hybrid Coupler

2.3.2 Crossover

There are four outputs in the network, so we need to split the signal into four sub-signals. Thus, the signal is needed to pass through a second stage of hybrid couplers. This will result in having an intersection between the lines, which is a problem for micro-strip circuits. A line cannot jump over or go underneath another to pass through it.

There are two methods to solve this problem. One way to have a crossover between the lines is by etching the circuit on the surfaces of two substrates mounted on top of each other. So, the line can transfer into other layer when needed. An illustration is shown in Figure 6.

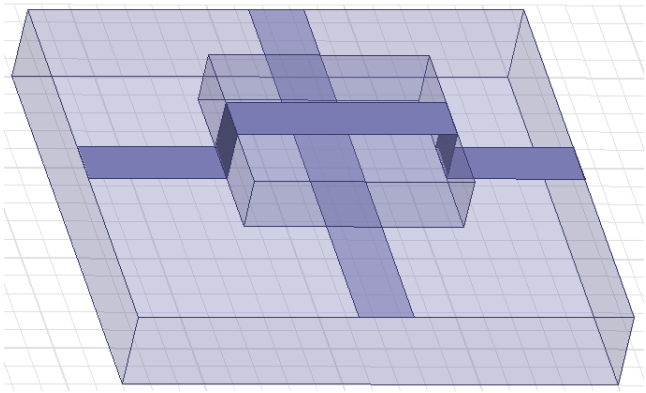

Figure 6 Crossover by several layers

Another way to do crossover is to cascade two hybrid couplers. This will result in passing the two signals across each other with some loss and phase shift. The two hybrid couplers are connected by two quarter-wavelength transmission line with the value of the characteristic impedance as illustrated in Figure 7.

Figure 7 Crossover on one layer

2.3.3 Phase Shifter

As can be noticed from previous components, the outputs will suffer from some undesired various phase shifts. The difference in the phase shifts between the outputs must follow a certain pattern. In order to achieve that, phase shifters are introduced to modify them. The geometry of the system will remain unchanged, thus, fixed phase shifters are preferred over steering shifters to have fixed radiation beams.

In the implementation, it can be simply accomplished by placing a transmission line with certain length that corresponds to the desired phase; this could be straight or bended line. For 4x4 Butler network, the phase shift needed is $\pi/4$ radian.

One of the major concerns is to provide this specific phase shift for a large bandwidth of operation. A simple line will provide the required phase shift but with relatively not wide bandwidth. Several designs of phase shifter are capable of offering this wide frequency range such as Schiffman Phase Shifters.

The Schiffman phase shifter used in this design consists of two sections; the first one is the reference transmission line, while the other is a single C-section of two parallel coupled transmission lines connected directly to each other at one end. In Figure 8, it shows how the C-section line will provide a phase shift of 90° over the other straight transmission line. [7]

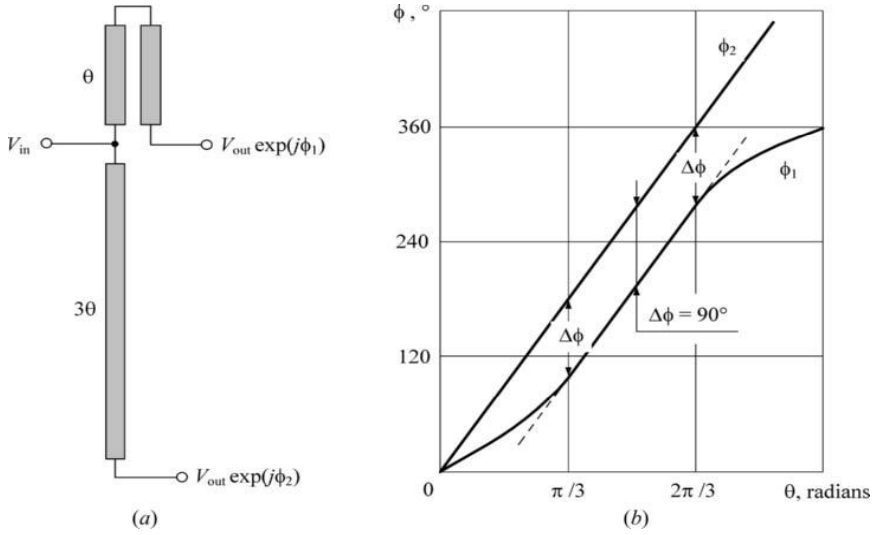

Figure 8 C-section vs straight line; (a) Diagram. (b) Phase Plot. [7]

2.4 Microstrip Antenna

Microstip-based antennas have received large attention in the last few decades due to several advantages. These low profile antennas can be mounted on different geometrical structures; planar and even non-planar designs. The manufacturing difficulty is at its least for this type of antenna, making it the most commonly used in several systems. Economically, the cost to fabricate these antennas in large amount is low; making them preferable to be used on certain commercial applications.

On the other hand, these types of antennas cannot handle high power signals. Their structures are close to the rectangular cavity. That is the reason behind having very high Q factor. Unfortunately, bandwidth is also limited and the polarization is not that pure.

Based on the shape of the radiating part, we could have many designs. The key is to have the antenna resonating; radiating all the power as much as possible. In order for that to happen, we need the fields to add up in phase. We could have shapes as square, rectangular, dipole, circular, elliptical, triangular, sector, ring or sector of a ring. In this work, the rectangular patch and the rectangular aperture will be considered for the integrated system. Both of them will be discussed, analyzed and designed.

2.4.1 Slot Antenna

The slot antenna, shown in Figure 9, is widely used in applications where it is desired to place an antenna on a very fast moving object, i.e. aircrafts and missiles. Since it is just an opening slot filled with certain dielectric, it will not introduce any interrupts to the aerodynamic properties of an object. Another point, as will be shown later, the slot antenna provides wider bandwidth compared to regular microstrip-based antennas.

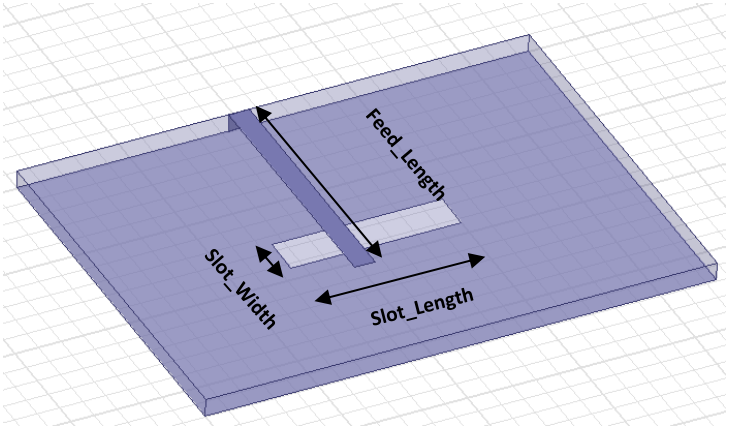

Figure 9 Slot Antenna and its dimensions

Let's have a half-wavelength slot; the feeding mechanism will be through aperture coupling. The slot will be placed on the ground plane where the microstrip line will be on the top layer. For the radiation to take place, we either need the current to add up in phase (like dipole antenna) or the voltage to add up in phase (like this case). The reason behind choosing the length of Lambda/2 is that when the slot is fed, half a period voltage signal will take place across it. This will ensure having all the electric fields to add up in phase in one direction and that will produce radiation as illustrated in Figure 10 [8].

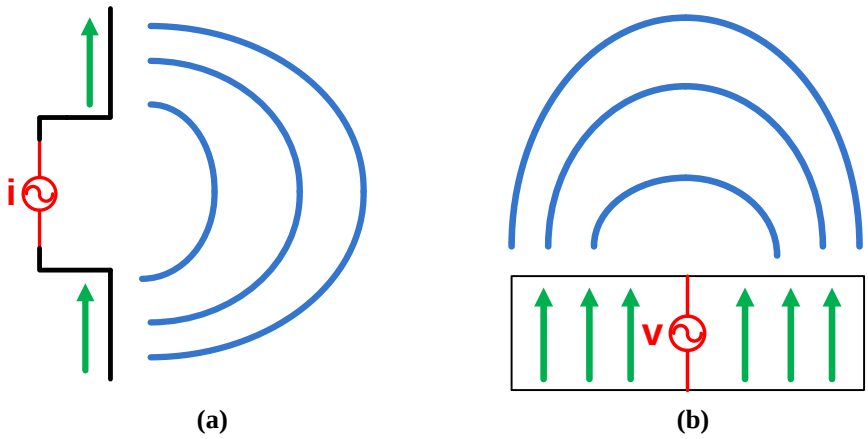

Figure 10 Radiation Mechanism for (a) Dipole Antenna (b) Slot Antenna

For the feeding point, if the slot was fed somewhere not in the middle, then the feeding point will be more than quarter-wavelength from one end and less than quarter-wavelength from the other side. As can be seen from Figure 11, the slot can be considered as a transmission line. At both terminals, the transmission lines are terminated by short circuits, making the voltage drop equal to zero between the two opposite sides surrounding the thin gap. From the Smith chart, when we move a distance greater than quarter-wavelength from the short circuit point (Smith Chart is used to represent impedance), we will end up with a negative impedance, in other words, a capacitive load. While when the distance is less than quarter-wavelength, it will be an inductive load. The key is to make the capacitive part cancel the inductive part in order for the antenna to resonate. It is found that the best place to feed is almost 0.05*Lambda away from one edge, which is a small distance. [8]

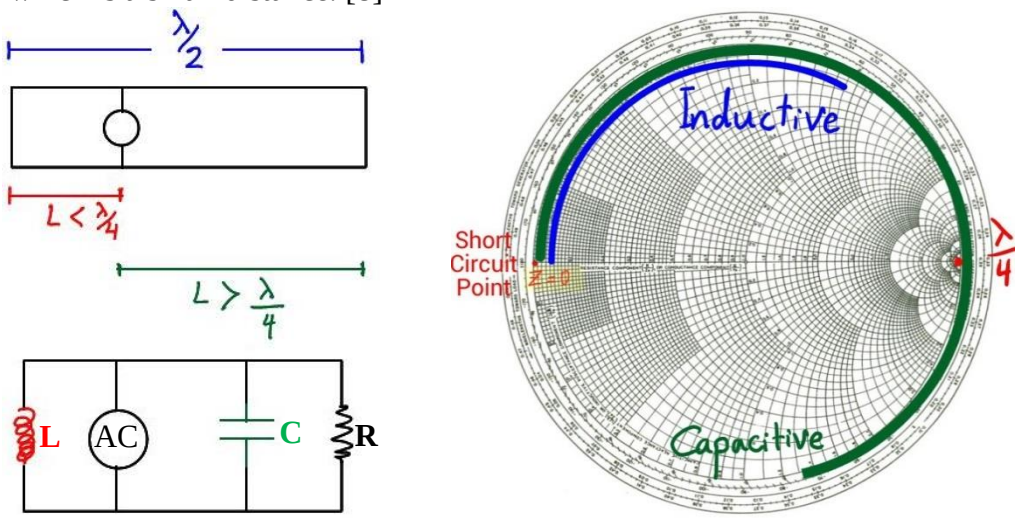

Figure 11 Slot Antenna as a transmission line

For the analysis, there are two ways to express the radiated electric and magnetic fields. The first way is by solving the wave equations and applying the proper boundary conditions, which is quite lengthy. The other way is by using Duality Theorem and Babinet's principle, [6], which will be illustrated here.

It can be noted that the slot antenna is nothing but the compliment of the dipole antenna as illustrated in Figure 12. In terms of radiation patterns, if the radiation pattern of a dipole is added to the radiation pattern of a slot that has the exact same dimensions, the total pattern will look like an isotropic sphere, approximately.

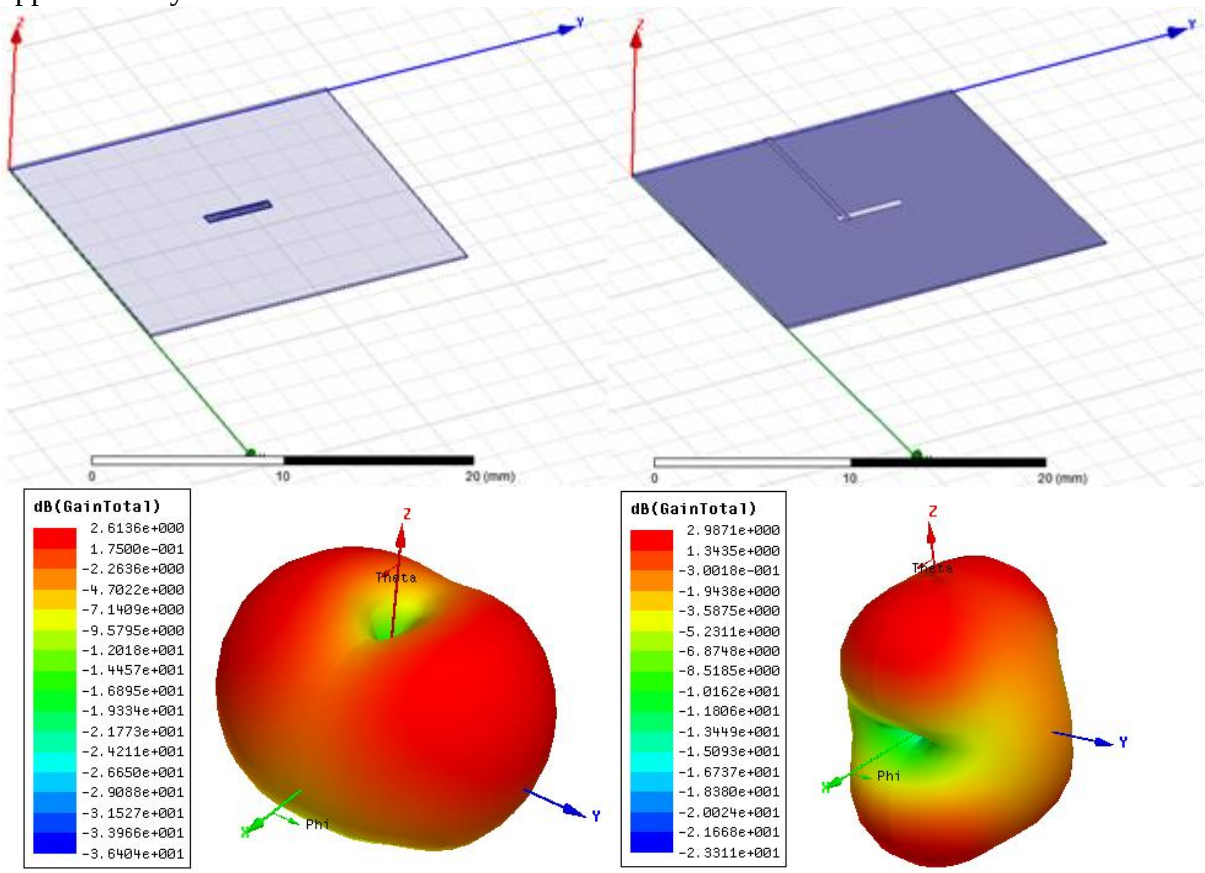

Figure 12 Comparison between the dipole and the slot antenna

By using the Duality theorem, mathematical expressions, that are alike but differ in the variable only, share the same solutions. So, if one is solved, the other can be obtained by proper variable replacement. Also, Babinet's principle states that the radiated fields of two complimentary radiating structures are related and governed by

$$Z_1 \times Z_2 = {\eta^2}/{4} \tag{2.6}$$

Where Z_x is the impedance of structure 'x'.

As a result, the radiating fields of the slot will be as a follows:

- $E_{\theta\_slot} = H_{\theta\_dipole} = Zero$ (2.7)
- $E_{\phi\_slot} = H_{\phi\_dipole} = j\frac{I_0 e^{-jkr}}{2\pi r}\left[\frac{\cos\left(\frac{kl}{2}\cos\theta\right)-\cos\left(\frac{kl}{2}\right)}{\sin\theta}\right]$ (2.8)
- $H_{\theta\_slot} = {-E_{\theta\_dipole}}/{\eta^2} = \frac{I_0 e^{-jkr}}{2j\eta\pi r}\left[\frac{\cos\left(\frac{kl}{2}\cos\theta\right)-\cos\left(\frac{kl}{2}\right)}{\sin\theta}\right]$ (2.9)
- $H_{\phi\_slot} = {-E_{\phi\_dipole}}/{\eta^2} = Zero$ (2.10)

Where η is the characteristic impedance of the medium, k is the wave number which is 2*pi/Lambda and r is the distance from the antenna's center to the observation point. E_i and H_j are the electric field in the i-axis and the magnetic field in the j-axis, respectively.

2.4.2 Patch Antenna

The microstrip patch antenna, shown in Figure 13, can be viewed as two slots connected by a low impedance transmission line. It can be analyzed by three different methods, which are transmission line model, cavity model and full wave numerical methods. The Cavity model will be considered to explain the radiation mechanism of the patch antenna.

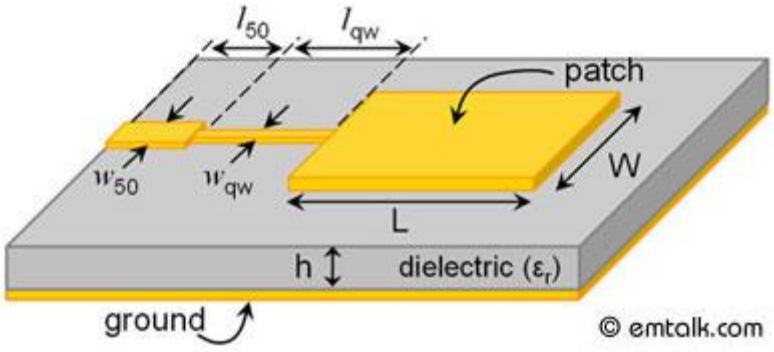

Figure 13 Mircrostrip Patch Antenna

In the analysis, the top and bottom layers will be considered as perfect electric conductors while the side walls are perfect magnetic conductors. The magnetic vector potential must satisfy the wave equation; $\nabla^2 A + k^2 A = 0$. The solution will contain a standing-wave term in each axis in the rectangular coordinates. Considering TM_x (Magnetic field is transverse), the solution is in the form of: [6]

$$A_x = [A_1 \cos(k_x x) + B_1 \sin k_x x]\left[A_2 \cos(k_y y) + B_2 \sin k_y y\right][A_3 \cos(k_z z) + B_3 \sin k_z z] \quad (2.11)$$

After solving it for the aforementioned boundary conditions, the expression will be as follows:

$$A_x = [A_1 \cos(k_x x)]\left[A_2 \cos\left(k_y y\right)\right][A_3 \cos(k_z z)] = A_{mnp} \cos(k_x x) \cos(k_y y) \cos(k_z z) \quad (2.12)$$

Where $k_x,\ k_y\ and\ k_z$ are wave numbers on their corresponding axes. They cannot be chosen to be zero all at once. The resonance frequency can be found by solving for k:

$$f_{r,mnp} = \frac{1}{2\pi\sqrt{\mu\varepsilon}} \sqrt{\left(\frac{m\pi}{h}\right)^2 + \left(\frac{n\pi}{L}\right)^2 + \left(\frac{p\pi}{W}\right)^2} \quad (2.13)$$

The lowest frequency generated for our structure is when m = p = 0 while n =1. It is called the dominant mode, given that h << L and h << W,

$$f_{rc(010)} = \frac{1}{2\times(L)\sqrt{\epsilon_{r\_eff}}\sqrt{\mu_0\epsilon_0}} \quad (2.14)$$

Given that ω is the angular frequency, μ is the dielectric permeability and ε is the dielectric permittivity, the electric and magnetic fields can be found from the magnetic vector potential and Maxwell equations by the next set of equations: [6]

$$\boldsymbol{E_x = -j\frac{(k_2 - k_r^2)}{\omega\mu\varepsilon} A_{mnp} \cos(k_x x) \cos\left(k_y y\right) \cos(k_z z)} \quad (2.15)$$

$$\boldsymbol{E_y = -j\frac{k_x k_y}{\omega\mu\varepsilon} A_{mnp} \sin(k_x x) \sin\left(k_y y\right) \cos(k_z z)} \quad 2.16)$$

$$\boldsymbol{E_z = -j\frac{k_x k_z}{\omega\mu\varepsilon} A_{mnp} \sin(k_x x) \cos\left(k_y y\right) \sin(k_z z)} \quad (2.17)$$

$$\boldsymbol{H_x = 0} \quad \textbf{(TMx mode)} \quad (2.18)$$

$$\boldsymbol{H_y = -\frac{k_z}{\mu} A_{mnp} \cos(k_x x) \cos\left(k_y y\right) \sin(k_z z)} \quad (2.19)$$

$$\boldsymbol{H_z = -\frac{k_y}{\mu} A_{mnp} \cos(k_x x) \sin\left(k_y y\right) \cos(k_z z)} \quad 2.20)$$

The fields under dominant mode will follow Figure 14. It can be noticed that the field will pass through a zero point in Length side of the patch and then it will become the opposite of the previous sign. This will create opposite charge distribution on the ground

plane. Almost an opposite distribution will be formed on the bottom layer of the patch antenna that will result in having electric fields that add up on the Width side of the patch, but they will not add up in phase on the Length side.

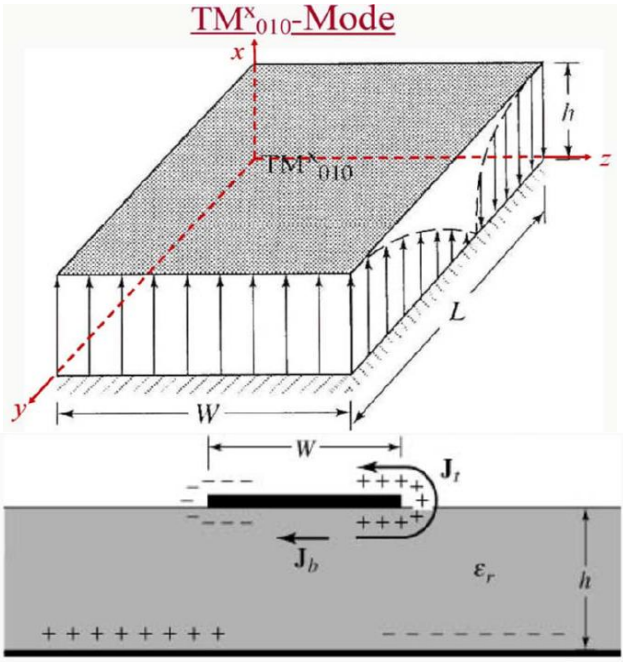

Figure 14 TM_{010} mode of the patch antenna [6]

The radiation pattern of a patch is the sum of the radiations emitted by the two slots in the patch's structure. The patch pattern is analytically given as (assuming an infinite ground plane):

$$E_\theta = \frac{2\times\sin(0.5\times kW\sin\theta\sin\phi)}{kW\sin\theta\sin\phi}\times\cos(0.5\times kL\sin\theta\cos\phi)\cos\phi \quad (2.21)$$

$$E_\phi = -\frac{2\times\sin(0.5\times kW\sin\theta\sin\phi)}{kW\sin\theta\sin\phi}\times\cos(0.5\times kL\sin\theta\cos\phi)\cos\theta\sin\phi \quad (2.22)$$

2.5 Conclusions

In this chapter, the Butler beam-forming network has been discussed in details; showing its advantages over other types of networks. Each component inside the Butler network has been explained and how it functions within the system. After that, antennas based on microstrip structures were presented. Finally, a focused view has been shed on patch and slot antenna, explaining their radiation mechanisms.

CHAPTER 3

LITERATURE REVIEW

3.1 Literature Review Introduction

Since the introduction of Butler Matrix Network in 1961 by Butler and Howe [9], researchers started to analyze and criticize the classic design. The first issue with the original Butler design was the relatively limited bandwidth. That was due to bandwidth limitation for some components. So, they started to introduce new designs for the hybrid coupler, crossover as well as the phase shifter which can carry larger capacity in terms of bandwidth. The Second point with the classic design is the problem of crossings, which was one of the major drawbacks in the Butler network. Several innovative ideas have been designed to overcome this hassle. Due to the problem of the crossover, people started to come up with new geometry for the network where they can reduce the number of crossings needed. Some new designs for the crossover achieved higher bandwidth. Other designs succeeded in totally avoiding the use of crossovers.

Regarding the bandwidth limitation, Researchers implemented new designs with relatively wider bandwidth for the phase shifter as they did in [4]-[11]. These new designs have higher bandwidth compared to the classic design presented in [18] for example. One paper avoided the use of phase shifter resulting in a higher bandwidth network [19]. Also different structures were used for the Hybrid Coupler to increase its bandwidth as was done in [10], [12], [13], [15], [16], [17], [20], [21], [22], [23], [24], [25], [26]. Also the same was made with the crossover as in [10], [12], [13], [17], [21], [22], [25], [26].

For the crossing issue, a number of papers introduced several designs to solve this problem. Some used Multi-layers structure to overcome it like [10], [12], [16], [20], [21], [22], [24], [25], [26], [27], [28], [29], [30], [31], [32]. One paper; [33], introduced a different layout on one layer to reduce the number of crossings. Some papers succeeded to build the butler network without using a crossover [34], [35].

3.2 Butler Matrix & Antenna Array Literature Review

First, the focus of the review will be on Butler matrix networks, where previous work is analyzed. Knowing advantages and disadvantages of several

designs and structures, it will aid us to decide which configurations and components to be used. Later, a dedicated review on antenna array integrated with these Butler networks will be presented and discussed.

3.2.1 Butler Matrix Literature Review

In this literature review, the main classification chosen to categorize the work done for Butler Matrix Network is the number of metal layers used in the structure. There are three groups in this review:

i. *Bilateral Structure*

ii. *Trilateral Structure*

iii. *Tetra lateral Structure*

The classic design is a bilateral-structure Network. The two layers are the metallic conducting layer and the ground. Other classifications can be applied such as the operating frequency, geometry of the network and the size of the network. The size of the network can be 3x3, 4x4, 6x6, …, 32x32. The smallest size found was 3x3 (2x2 is just a Hybrid Coupler) and the largest one designed was 32x32. One paper [23] designed 3x4 Butler Network. All details will be shown in the following sections.

3.2.1.1 Bilateral Structure Design

The papers which implemented a two-layer (Bilateral) design were [18], [11], [15], [17], [23], [35], [36], [5], [37], [38], [39], [40], [41], [42], [43]. In these papers they were restricted with one layer. As a result, all of them were forced to use the classic crossover where they cascade two Hybrid couplers with a quarter-wavelength transformer. Different designs were used for the Hybrid Coupler as well as the phase shifter.

In [5], a 4x4 Butler was proposed where a Genetic Algorithm (GA) was implemented to select the optimum dimensions of all components of the Butler network with the same layout as the classic design. The operating frequency was 3.15 GHz but the bandwidth was narrow.

A 4x4 Butler Network with a bandwidth of around 5.3 GHz operating at 60 GHz was designed and implemented in [18]. Since the operating frequency was high, the wavelength is very small that posed a limit where the components might overlap in the design. So, the characteristic impedance was changed from 50 Ω to 100 Ω to have

narrower. Quarter-wavelength transformers were needed at the input terminals. Figure 15 shows this Butler matrix that was applied to a linear antenna array of 4-elements.

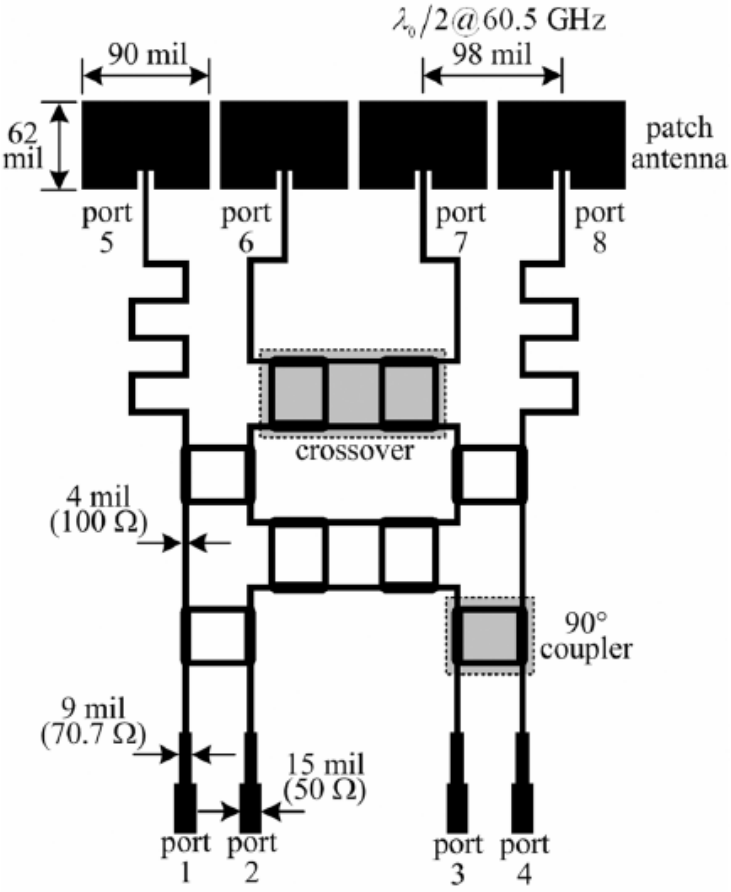

Figure 15 4x4 Butler at 60 GHz [18].

Due to fabrication tolerance, the frequency was shifted to 62 GHz instead of 60 GHz. The size of the overall system was 9.75x13.1 squared mm as shown in Figure 16. Figure 17 shows the shift introduced in the frequency domain due to fabrication.

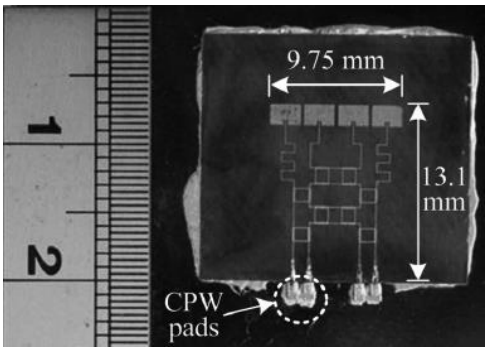

Figure 16 Fabricated 4x4 Butler at 62 GHz [18]

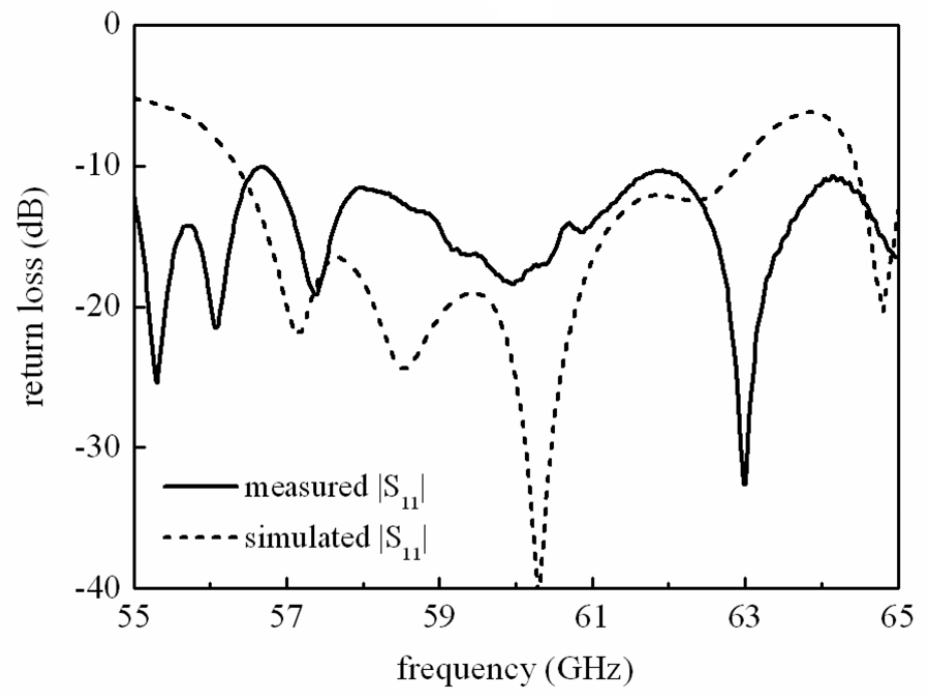

Figure 17 Measured and simulated return loss [18]

Another design was fabricated and built at 60 GHz in [37]. The bandwidth achieved was higher and it was covering the band from 56.7 GHz to 63.7 GHz with a BW of 7 GHz. In this work, a Butler network alongside with a quasi-Yagi 4x1 array antenna as well as a 4x1 switch were demonstrated as shown in Figure 18. Here, the characteristic impedance was increased from 50 Ω to 70 Ω because of the high frequency. The fabricated system's size was 1.4 cm by 1.75 cm.

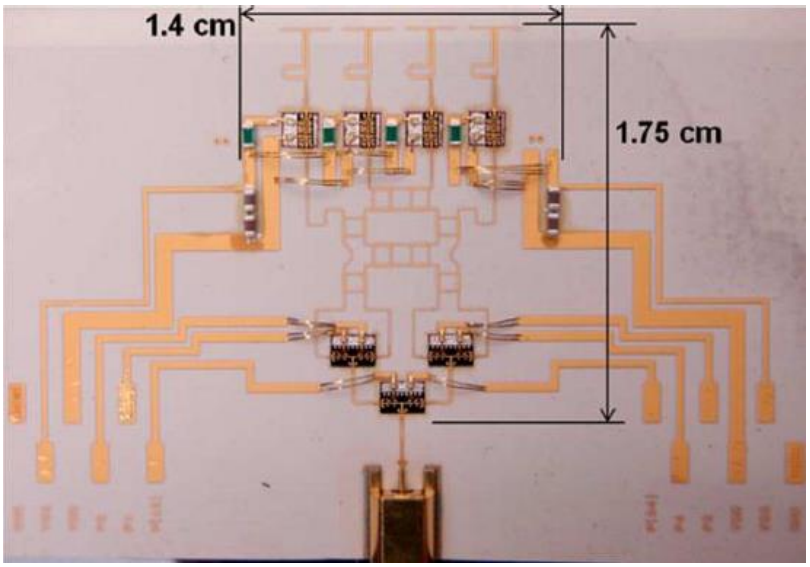

Figure 18 Fabricated 4x4 Butler at 60 GHz [37]

In [38], a 4x4 Butler that achieved a bandwidth of 3.4 GHz at an operating frequency of 60 GHz was presented. The new idea in this work was to separate the antenna from the Butler Network and put it on another layer. The array antenna was fed by the Butler network though coupling via holes in the common ground between the two layers. This design prevents surface waves and mutual interaction between the array antenna and the network. This idea is further explained in Figure 19 (a) and (b). The size of the network was 20.56 x 14 mm^2. The thickness of the separating layer was 0.2 mm. Figure 19 (b) shows the Butler network while (a) shows the overall design.

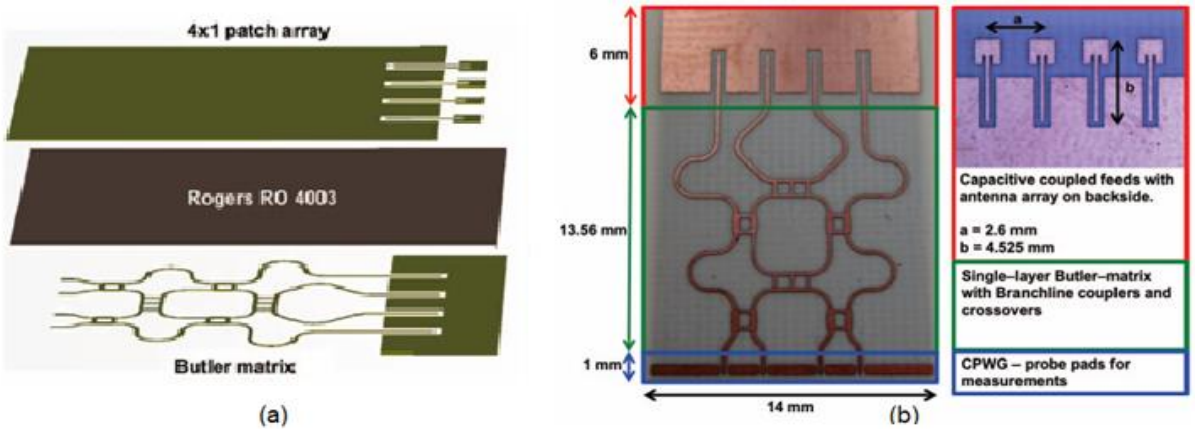

Figure 19 Array Antenna on another layer [38]

While in [11], they have used Schiffman phase shifter instead of a regular reference line. This technique is supposed to provide broader bandwidth of operation. This design presented a 4x4 Butler network operating at a frequency of 6 GHz. The bandwidth was about 400 MHz, which is relatively low. The fabricated size of the system was 115 mm x 115 mm as shown in Figure 20. The substrate used was Rogers5880 with relative dielectric constant of 2.2 and loss tangent equal to 0.0009. The thickness was 0.508 mm

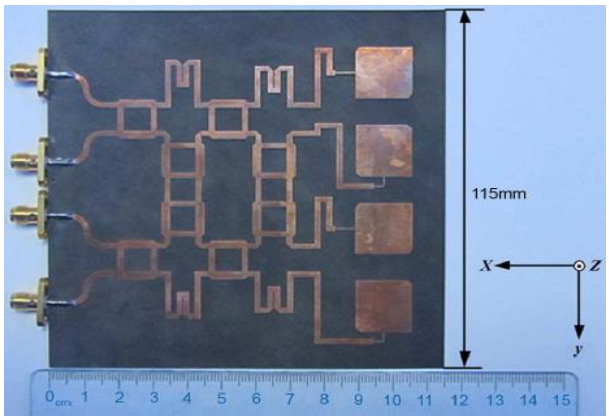

Figure 20 4x4 Butler with Schiffman phase Shifter [11]

A novel design of a Hybrid coupler was implemented in [23]. In this paper, a 4x4 Butler network operating at 1.85 GHz with a bandwidth of 300 MHz was designed and fabricated. The contribution of this paper resides in reducing the size of the network significantly. The paper took a new design of the Hybrid Coupler done by Sakagami and added some parasitic capacitance to solve the problem of frequency shifting in the design. The novel design succeeded to reduce the size of the network by 80% which results in having a compact system achieving the feeding task. The novel design is shown in Figure 21 with a comparison with other structures. Figure 22 (a) shows the fabricated models of Hybrid Couplers. It can be noticed that the size was reduced significantly when observing the whole structure of Butler Network implemented based on the novel design compared to the classical one.

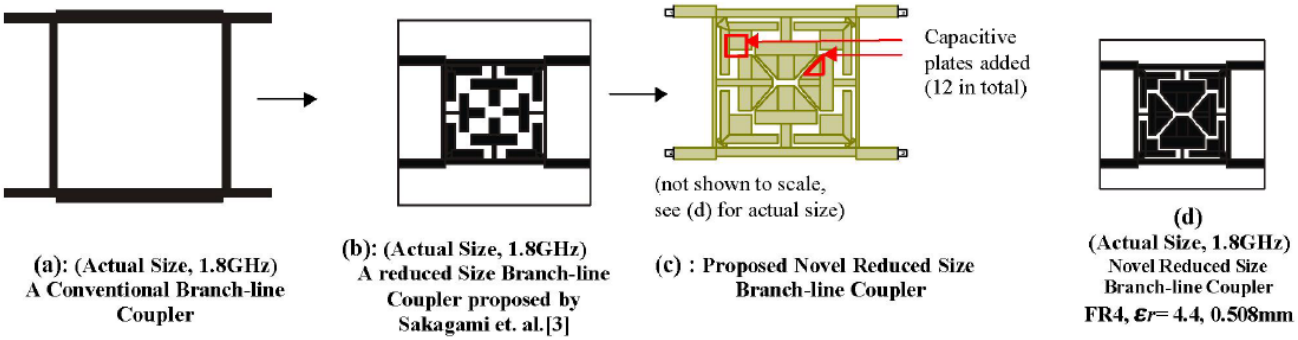

Figure 21 Novel Design of Hybrid Coupler [23]

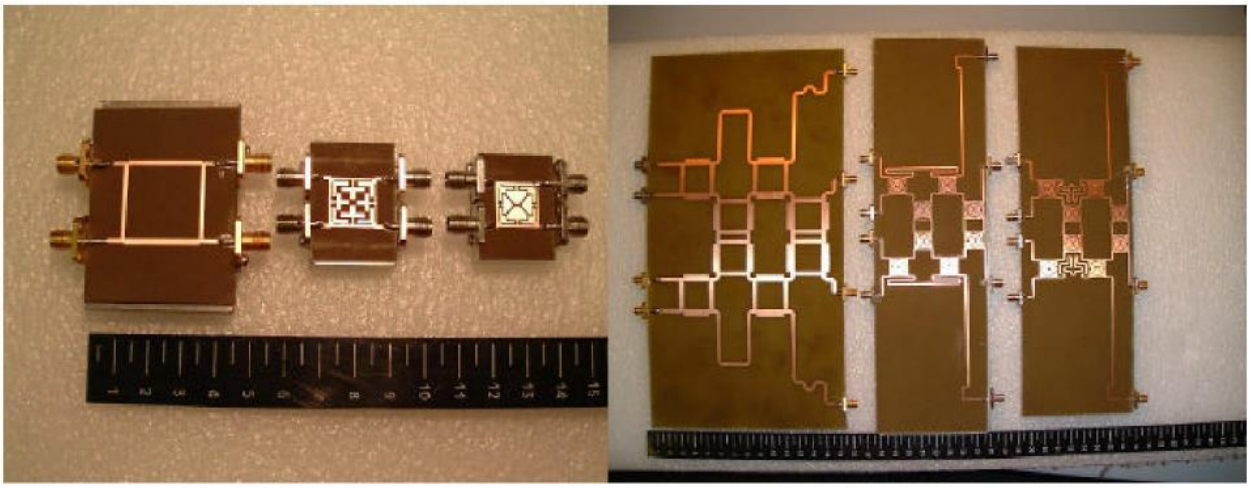

Figure 22 Butler Network based on 3 Hybrid Coupler designs [23]

Another design for the Coupler was shown in [15]. In this paper, they designed a 4x4 Butler network without fabrication. The simulated operating frequency was 5 GHz with a 6 GHz bandwidth. For the Coupler, they designed a

Tapered-coupled-line Directional Coupler as shown in Figure 23. For the phase shifter, the paper designed a two-section Schiffman phase shifter. The overall simulated structure is shown in Figure 24. In this paper, they ignored the problem of the crossover. They just did the simulation for the whole system to analyze the performance of their network.

Figure 23 Tapered-line-Directional-Coupler [15]

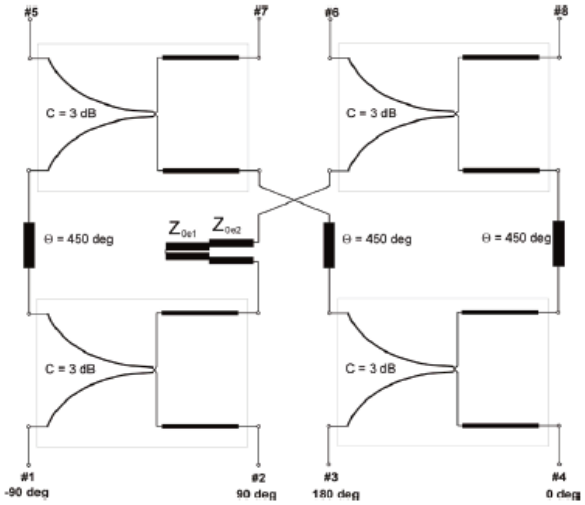

Figure 24 Schematic of 4x4 Butler [15]

In [41], a regular 4x4 Butler network operating at 2.4 GHz was designed. The bandwidth was about 200 MHz. The main idea of this paper was to prove that using mitered bends is better than using circular bends in terms of performance and provides more compact size. The system dimensions based on mitered bends was 18.137 cm by 6.127 cm. The overall design with mitered bends is shown in Figure 25. When compared to the circular-bend design, the bandwidth of the late one was 140 MHz and its size is larger.

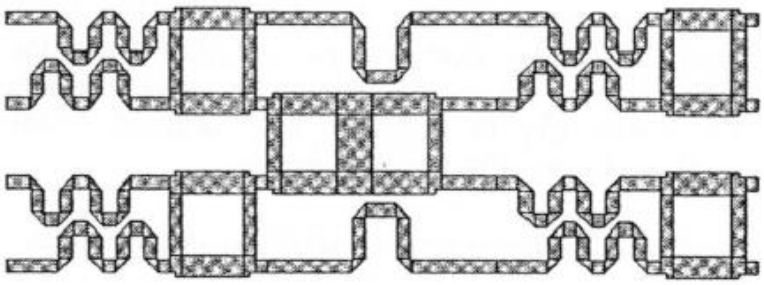

Figure 25 4x4 Butler with mitered bends [41]

A dual band Butler Feed Network was designed and implemented in [17]. The 4x4 Butler network operated at two frequencies; 2.45 GHz and 5.8 GHz. Each component in the network must be re-designed to operate at these two frequencies. For the building blocks, the Hybrid Coupler consisted of two branch lines connected to each other forming a rectangle, because their lengths are not equal. In the classic design, the shape of the Hybrid coupler was like a square where the length of the side is quarter wavelength. Now, one of the sides is slightly larger than quarter-wavelength in order for the Hybrid coupler to resonate at two different frequencies. The dual-band crossover was designed by cascading two dual-band Hybrid Coupler with a quarter-wavelength line. For the phase shifter, it was implemented using a Schiffman broadband design where it provides the required phase shift over a wide bandwidth covering the two operating frequencies. Schematics of the three components are shown in Figure 26. The overall fabricated design was 107 mm by 157 mm and it was connected to a dual-band antenna array as shown in Figure 27.

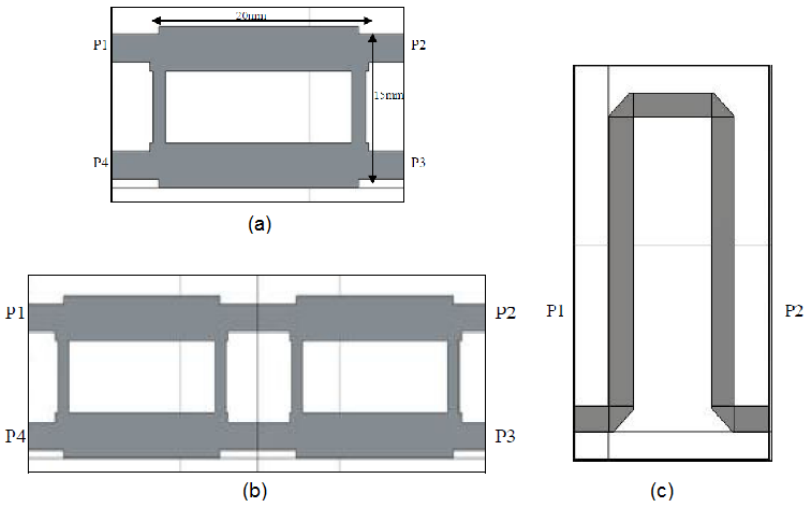

Figure 26 Dual-Band Butler (a) Hybrid Coupler (b) Crossover (c) Schiffman Phase Shifter [17]

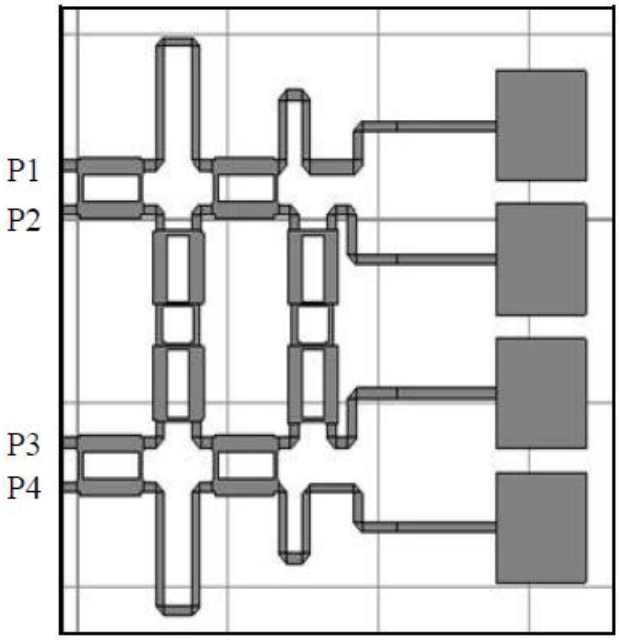

Figure 27 Dual-Band Butler with Dual-Band Array Antenna [17]

In [42], the smallest Butler Network in terms of input/output ports operating at 1.7 GHz was designed. It was a 3x3 Butler matrix. The overall fabricated size was relatively big, which covered 13 x 13 cm^2 as shown in Figure 28. It was fabricated on an FR-4 with dielectric constant of 4.25 and thickness of 1.5 mm.

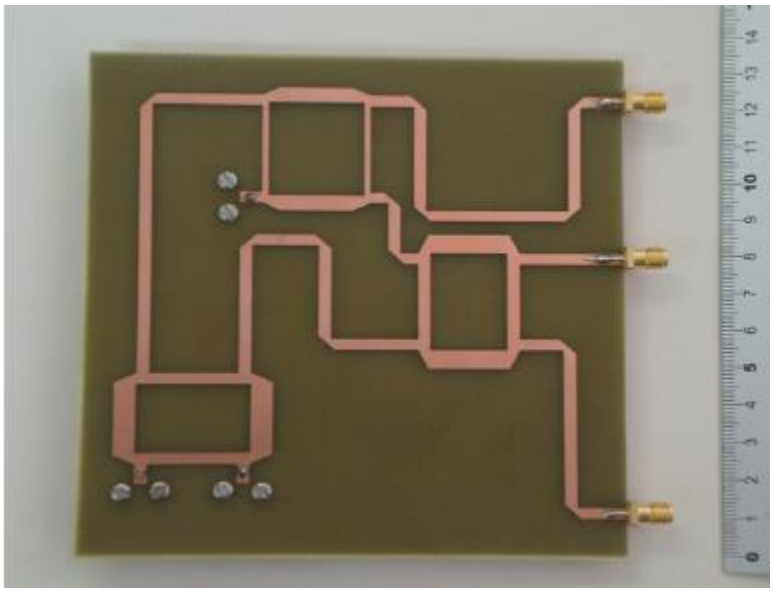

Figure 28 3x3 Butler Network [42]

A very clever design was implemented in [35], where the 4x4 Butler Network avoided the crossover problem. This system operating at 910 MHz, with a bandwidth of 100 MHz, succeeded to overcome the need of crossing the

two lines coming from the adjacent Hybrid Couplers. That was achieved at the expense of scattering the input and the output all over the system as shown in Figure 29. So, the network was not well organized to all inputs at one side and the outputs at the other side.

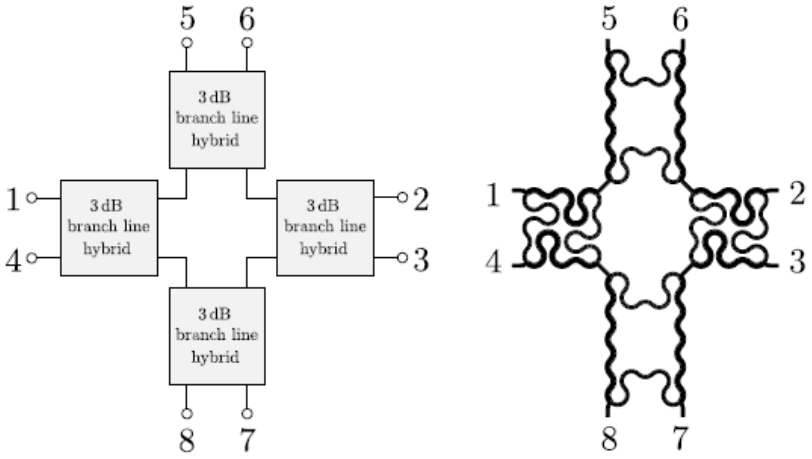

Figure 29 4x4 Butler with no crossover [35]

3.2.1.2 Trilateral Structure Design

The papers listed in this section had taken the advantages of having more than one layer. They used these layers to solve the problem of crossover, where they just let one line passes over one layer and the other passes on the second layer. New designs for the Coupler were found, where they separated the coupler into two parts, each one on different layer. The two parts interact with each other through coupling. The same thing goes for the phase shifter. Sometimes it is being done by a coupling route between different layers. Also a new task has been added which is the technique to switch between the two layers. This task can be achieved by using vias. But this will work for lower frequencies. For higher frequencies, other techniques are needed.

These three layers of metal can be separated into two groups depending on the position of the ground layer. On one hand, the papers [16], [24], [30], [32] placed the ground layer in the middle between the two conducting metallic layers as shown in Figure 30. On the other hand, [12], [26] and [31] have placed the ground layer on the edge as illustrated by Figure 31.

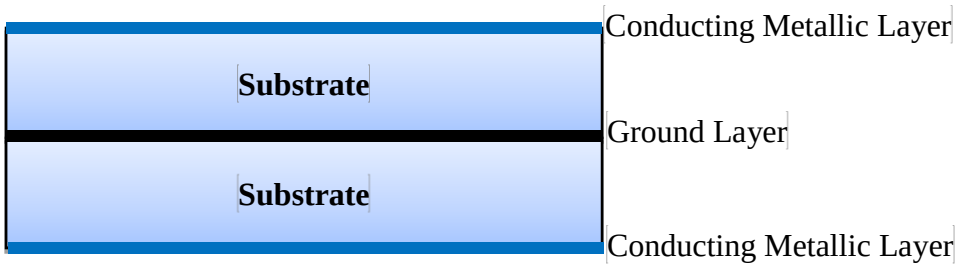

Figure 30 Metal-Ground-Metal Structure

Figure 31 Metal-Metal-Ground Structure

A. Common Middle Layer

One of the remarkable papers which violated the rule of having the number of inputs equal to the number of outputs is [30]. It showed a 3x4 Butler network with a frequency of 12 GHz. They integrated the three inputs with the network by using a power divider. One of the inputs passes through a power divider in the first stage, while the other passes through a branch-line coupler. The interconnection between layers is done by having an open slot in the ground layer, allowing coupling to take place between the two layers as shown in Figure 32. The overall implemented design occupied an area of 1.945 x 1.945 mm^2. The overall design is shown in Figure 33. The black-filled lines are etched on one layer while the white-filled ones are on the other layer. One layer has two couplers, two phase shifters and a power divider. The second layer has one coupler and two phase shifters.

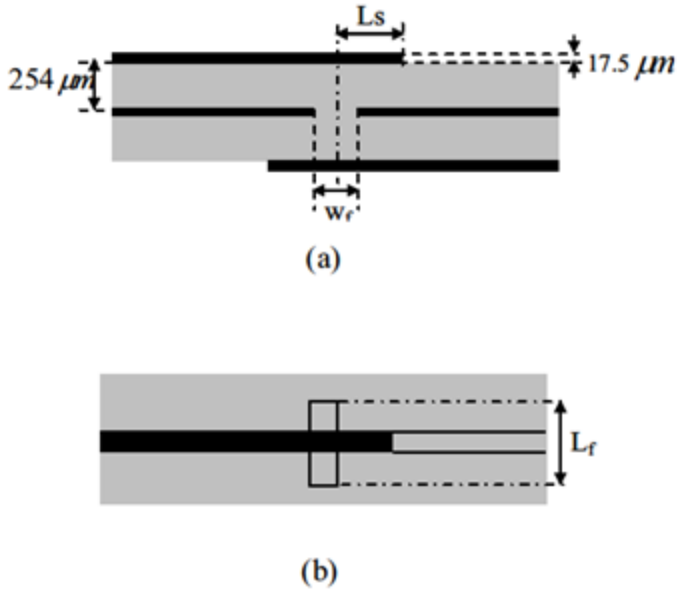

Figure 32 Layer Switching [30]

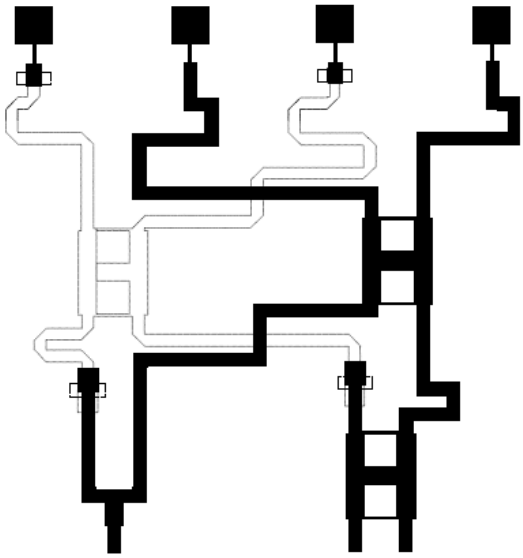

Figure 33 3x4 Butler Feed Network [30]

In [24], an ultra-wide band 4x4 Butler was designed and fabricated. It operated at 6.85 GHz. The novel idea in this work was the shape of the butterfly designed for layer interconnection, which is also used in the coupler. The Hybrid Coupler was designed using two transmission lines on different layers where the connection between them is accomplished by the butterfly interconnection design. The concept of the coupler is illustrated in Figure 34. The feeding and the direct ports are etched on one layer while the coupled and the isolated ports are implemented on the other side. There is an open hole in the common ground

layer to allow the coupling between the two layers. The final product is shown in Figure 35.

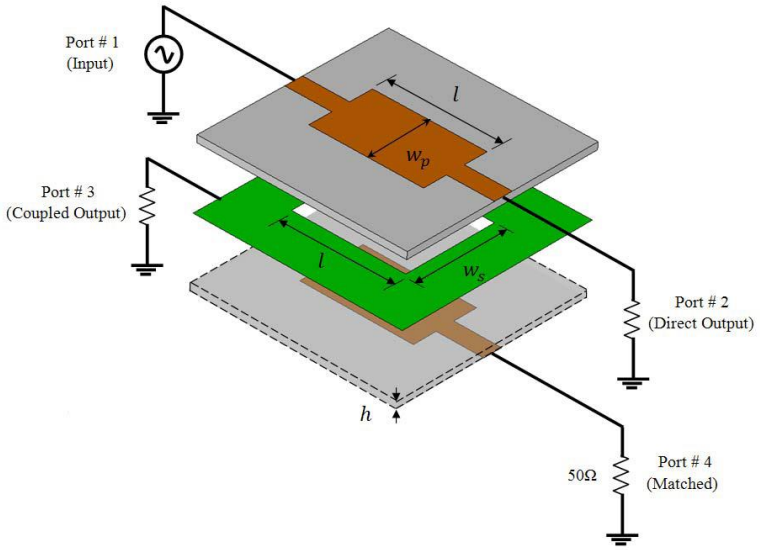

Figure 34 Two-Layer Hybrid Coupler [24]

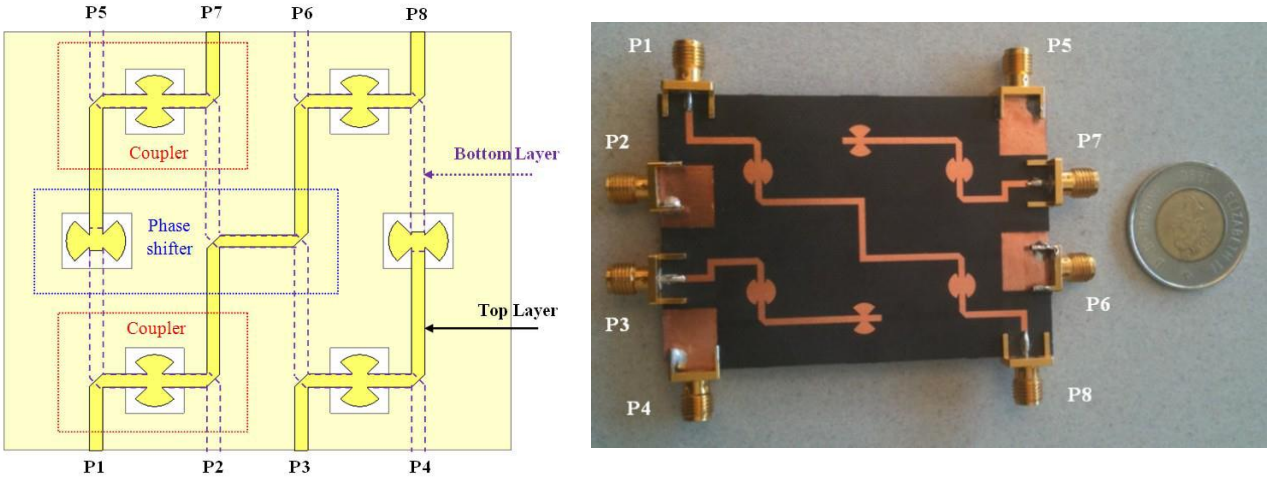

Figure 35 Bilateral 4x4 Butler Network [24]

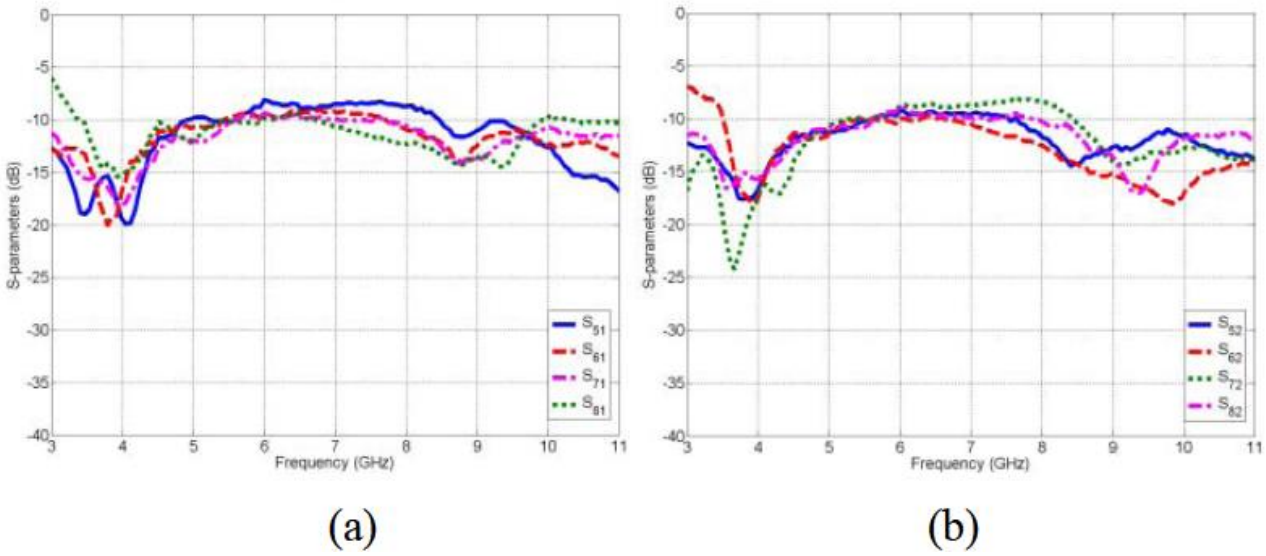

Figure 36 Measured transmission magnitudes of the butterfly 4×4 Butler matrix: (a) port 1 is fed (b) port 2 is fed [24]

In [16], a bandwidth of 1.1 GHz was achieved by an 8x8 Butler operating at 4.75 GHz. They succeeded to increase the bandwidth significantly by using wide-band designs for the components. For the coupler, they used a three-branch-line coupler instead of the common two-branch-line coupler, known as the classic Hybrid coupler. This new design of Hybrid coupler achieved 40% more bandwidth compared to the classic one. It operated from 3.9 GHz to 5.8 GHz. Also, for the phase shifter, the paper used two-section Schiffman phase shifters, which has relatively a large bandwidth of 2.8 GHz; from 3 to 5.8 GHz. The thickness of the substrate used in the design was 0.8 mm with a dielectric constant of 2.55. The hole in the common layer has a diameter of 3.6 mm.

In [32], they achieved wider bandwidth than [16]. The bandwidth obtained in this paper was 7.6 GHz; from 3 to 10.6 GHz. They achieved this with a different design for the Hybrid coupler. The idea was exactly the same as [24]. They just used a different shape other than the butterfly. The overall size was 9 x 4 cm^2 on a Rogers RO4003 substrate with thickness of 0.508 mm and dielectric constant of 3.38.

B. Common Bottom Layer

The 4x4 Butler Network in [12] consists of six three-section couple-line directional couplers. Two of these couplers will be used for the crossover. Schiffman C-section phase shifter is implemented in the design where it assists the system to have a bandwidth of almost 2 GHz. The center frequency of operation was 3 GHz.

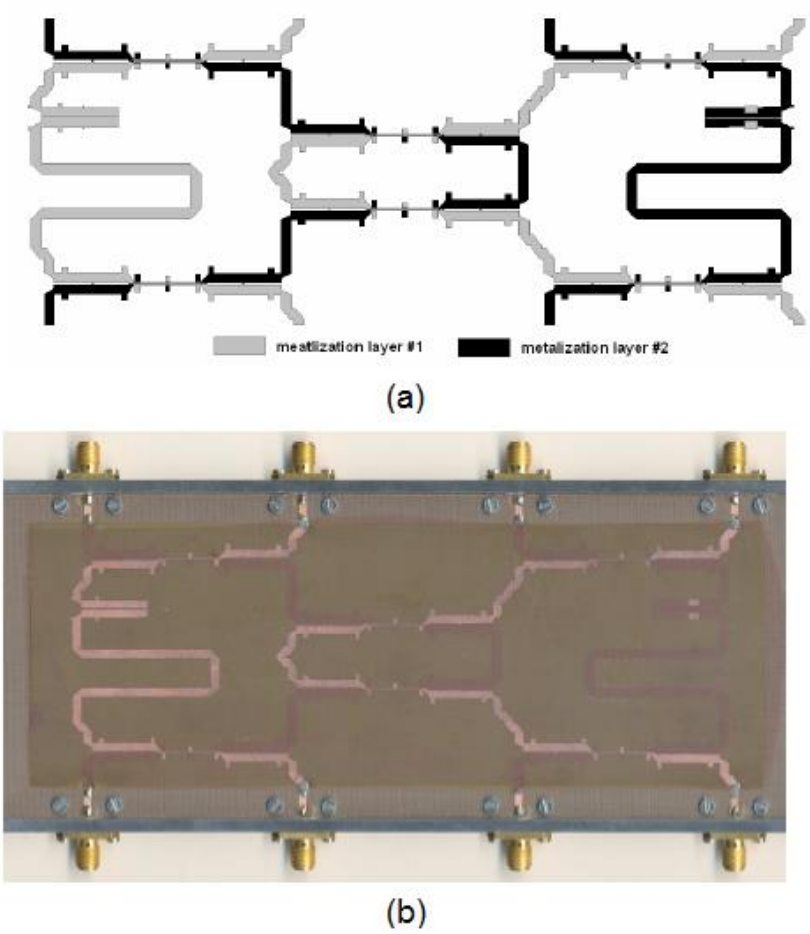

Figure 37 (a) Layout (b) Assembeled model of 4x4 Butler Matrix [12]

In [31], an 8x8 Butler matrix was used as a tool to measure the frequency response of any two port device. It gives accurate measurements for the transmission and the reflection coefficients in the range from 2 to 3.5 GHz. It utilizes the Butler matrix with an isolator to perform the measurements. The block diagram of the system is illustrated in Figure 38. The input signal is connected to port 1 while power measuring devices are connected to ports 2 – 8. Another power-measuring tool is needed at port 16 to act as a reference level. The device under test is connected to port 9. A switch in port 11 is needed to interchange between the measurements of transmission and reflection coefficients. Ports 12 – 15 are not used.

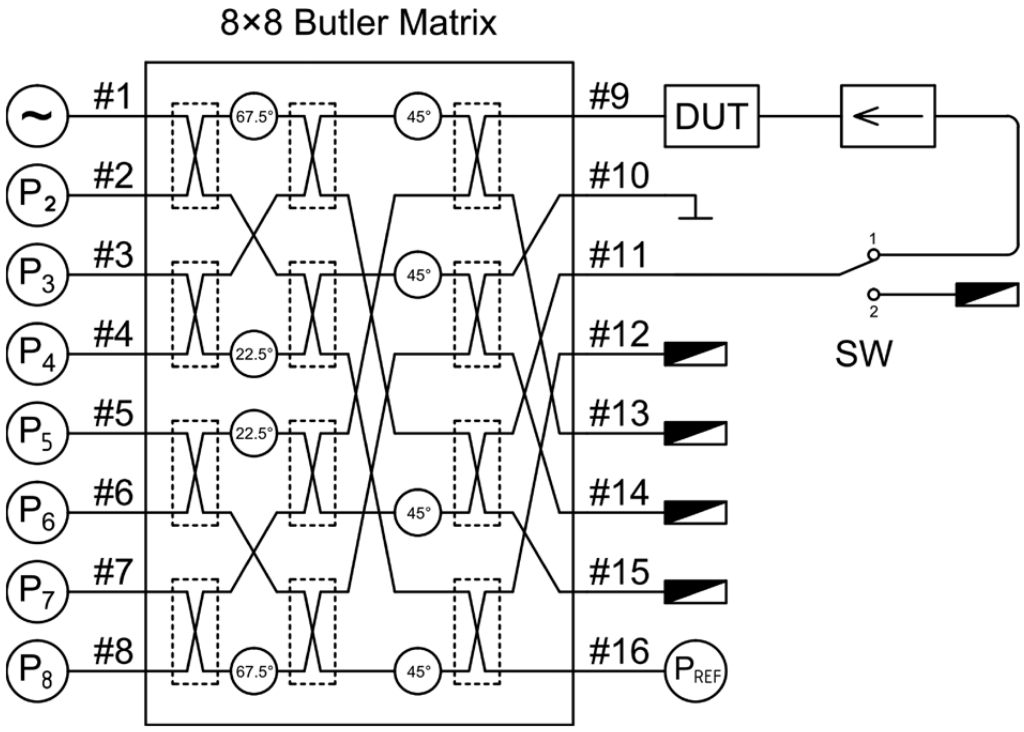

Figure 38 Schematic of the proposed multiport measuring system with a single 8x8 Butler matrix allowing for reflection and transmission coefficient measurement [31]

3.2.1.3 Tetra-lateral Structure Design

Quite few papers followed a tetra-lateral structure. It is as the "Common Bottom Layer" structure with an extra ground layer on the top, as illustrated in Figure 39. This structure had been used in [10], [20], [22] and in [25].

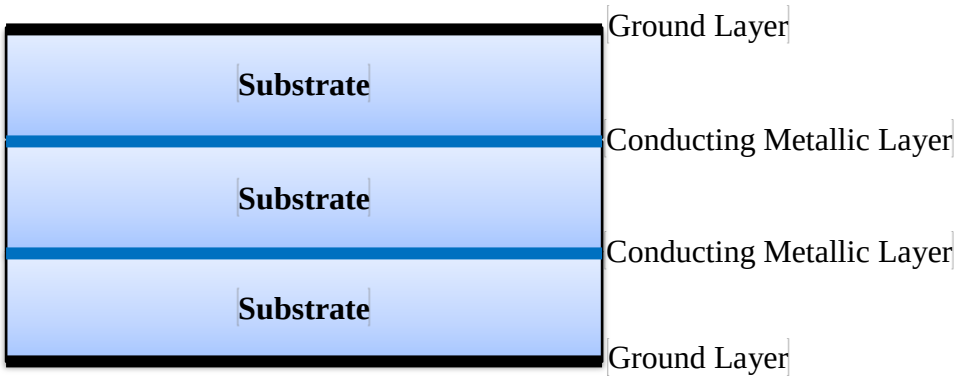

Figure 39 Terta-lateral Structure

In [20], an 8x8 Butler matrix was implemented to operate at 920 MHz with a very narrow bandwidth of 80 MHz. The design of the coupler was quite similar to the tapered-line directional-coupler shown in the Tri-lateral structure [12] but with some stubs attached near the terminals for impedance matching. This Butler gets fed by two differently polarized signals; one at -45 degrees and the other at +45 degrees. There are two modes of operations; odd and even. The

even mode takes place when the amplitude and phase of the two signals on the two opposite layers are the same. So, the field will be generated from the two conducting layers to the ground plates facing them. Thus, no coupling will take place between the two conducting layers. While in the odd mode, the phases will be different resulting in having the field originated from one layer to the other layer as well as the ground plate facing it. So, odd mode is preferred over the even mode so that the coupler as well as phase shifter will function. Figure 40 illustrates the concept.

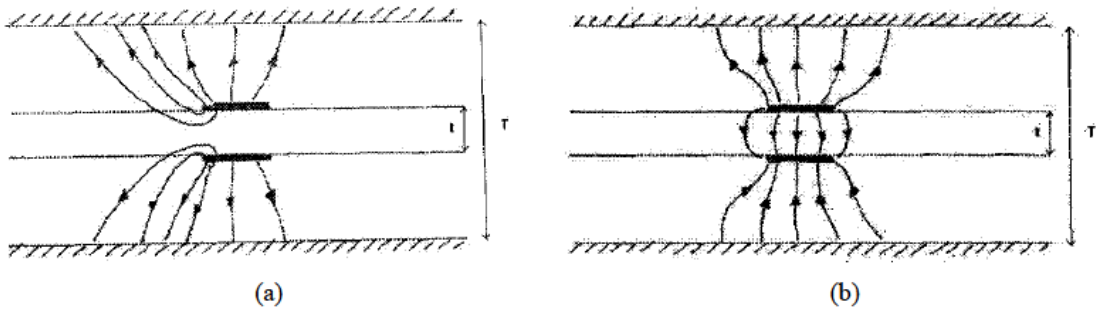

Figure 40 (a) even (b) odd modes of operations [20]

Another more complicated 8x8 Butler Matrix was designed in [10]. It used a 3-dB broadside coupler with Schiffman phase shifter. Due to these components, the bandwidth reached 1.2 GHz at a center frequency of 2.2 GHz. This design was fabricated on a board of dimensions 160 x 100 mm^2. The coupler was of the same type illustrated in [12] previously. Regarding the phase shifter, they used the design of one-section Schiffman phase shifter. The overall design is shown in the Figure 41. The dielectric constant of the substrate was 3.38 with a loss tangent of 0.0025

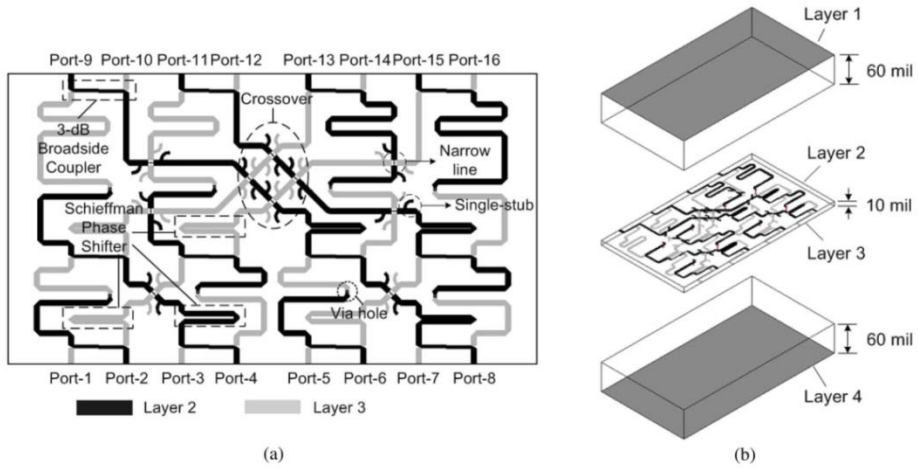

Figure 41 8x8 Butler Matrix [10]

3.2.2 Literature Review of Antenna Array Integrated with Butler Network

Different types of antenna elements have been used as antenna arrays integrated with feed networks as mentioned in section 3.2.1. The types used were patch, quasi-Yagi and SIW slot antenna arrays. The most common type of microstrip antenna that has been used with Butler networks as well as other beam-forming networks is the patch antenna due to its design simplicity and higher gain compared to others. Even though patch antenna arrays have been used a lot, each paper tried to enhance the performance and introduce something unique from other patch designs.

In [44], a planar 9x9 and 11x11 patch antenna arrays have been simulated to analyze the 3D topologies when using them with a phased network. Their target was to acquire a low-cost receive-only Ku-band antenna operating at 11.7 GHz. The inter-spacing distance between the elements was set to half a wavelength. By simulation, the gain obtained for the 11x11 antenna array was from 17.6 to 20.6 dB inside the elevation sector from 30˚ to 70˚. Trying to investigate the effect of having larger array size, a 16x16 planar patch antenna array has been simulated, where it gave a gain range from 16.9 to 23.7 dB over the same elevation sector but the 3dB bandwidth was narrower than before. They concluded that increasing the size of the array will not improve the coverage of the radiation pattern, actually, it will results in having more gain variation in the desired direction. This issue of gain variation can be solved by using larger sizes of Butler networks.

A linear 1x4 patch antenna array was designed, simulated and measured in [18]. The linear patches were designed and simulated to operate at 60.5 GHz, but since its butler network was found to operate at 62 GHz due to the aforementioned reasons in 3.2.1, these linear patches were measured at 62 GHz. The patch dimension was 2.286 x 1.575 mm^2 while the inter-element spacing was 2.49 mm that corresponds to half a wavelength. As shown in Figure 42, the patch antenna had a return loss of -35 dB centered at 60.5 GHz with a 10dB BW of almost 1.5 GHz. The beams were steered at ±14˚ and ±40˚. The maximum gain achieved was 8.9 dB and that was when port 1 of Butler network is excited. While when port 2 is excited, a gain of 7.7 dB is obtained.

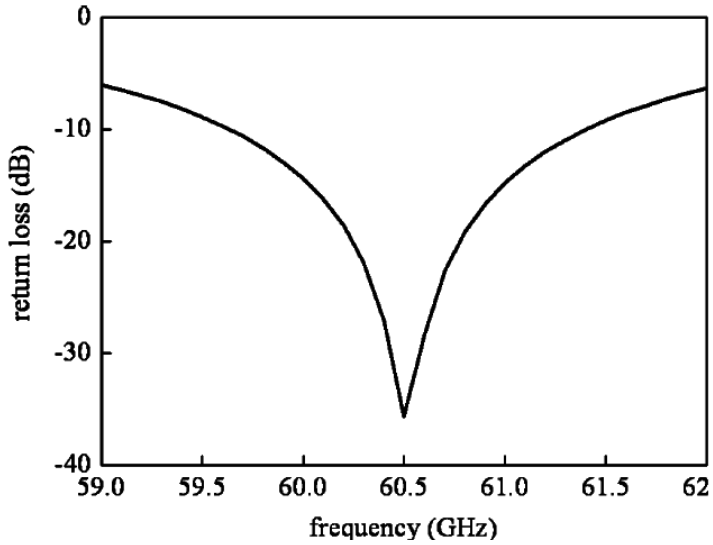

Figure 42 Simulated Return loss for the patch antenna [18]

A new antenna array design was proposed in [37], where the antenna element was the Quasi-Yagi antenna operating at 60 GHz with 5.8% bandwidth (3.5 GHz). The design and dimensions of the quasi-Yagi antenna element are shown in Figure 43. The inter-element spacing was again set to $\lambda/2$.

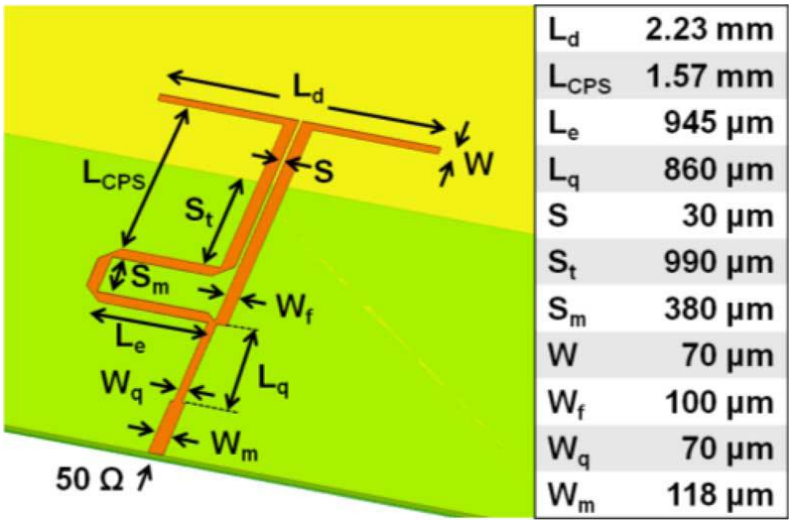

Figure 43 Sinle Quasi-Yagi antenna element operating at 60 GHz [37].

In [10], a linear 1x8 patch antenna array was attached to a phased network. In order to have better directivity, a reflector plane was attached to the back of the radiating elements to force the patterns to be pointed in one hemi-sphere. The antenna array was designed to operate at 2.45 GHz with dimensions of 41x26 mm^2. The reflector is placed 30 mm away from the system's structure as illustrated in Figure 44.

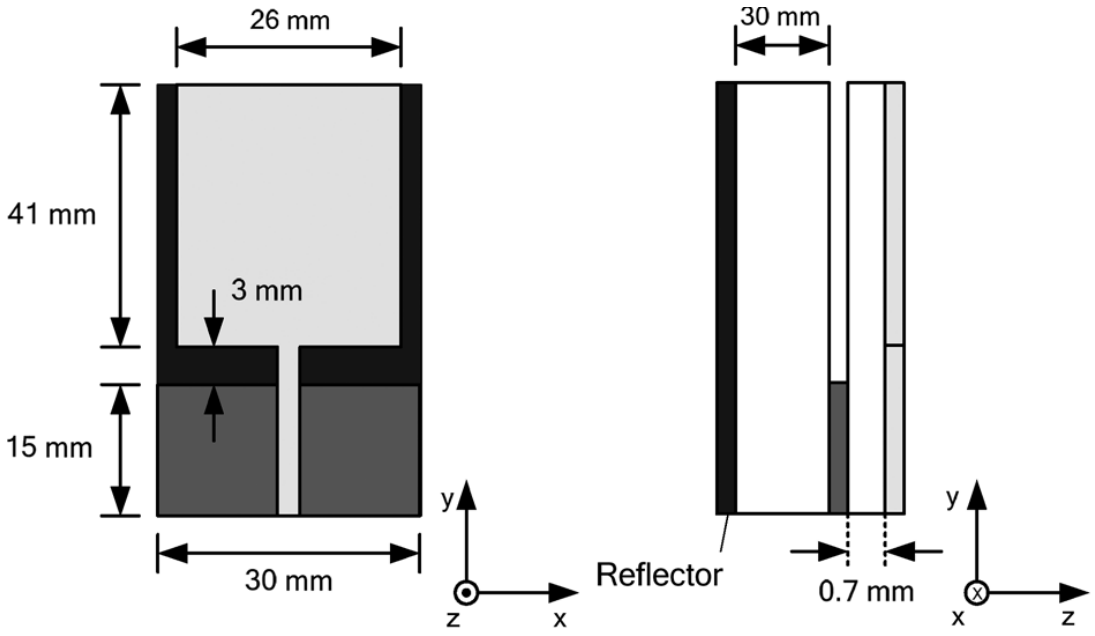

Figure 44 Configuration of the linear patch antenna with its reflector [10].

A 1x4 patch antenna array is designed at 2.45 GHz in [28]. The inter-element spacing was as usual; $\lambda/2$. The beams were radiated to ±15˚ and ±45˚ depending on which input of its Butler network is excited. While another 1x4 patch antenna array is operating at 60 GHz as the one in [38]. The novel idea presented in this paper was in how they fed their antenna array. It was accomplished by connecting the outputs of Butler network to a single conducting sheet that will couple into another upper conducting layer which is connected to the linear antenna array. The design is illustrated in Figure 19. The maximum gain achieved was 10.2 dB_i and that was when port 1 is excited. While 9.7 db_i is obtained by exciting port 2. In this antenna array, all side lobes were lower than -9dB and the 3dB BW was 3.4 GHz.

Beams directed to three angles instead of the usual four were provided by a 1x4 antenna array which was fed by a 3x4 Butler network, as shown in [30]. The three angles were 0˚ and ±25˚. The patch antenna array is designed to operate at 12 GHz with an inter-element spacing of 0.45*λ. The patch was a square with a side length of 1.945mm.

A dual band 1x4 Patch antenna has been design in [17]. The system operated at 2.45 GHz with a maximum gain of 11.5 dB_i, and at 5.8 GHz with gain peak of 6 dB_i. The performance is summarized in Table 2. Another dual band concept is presented in [25]. It attached two linear 1x4 patch antenna arrays, operating at two different frequencies, to a broadband Butler network via a diplexer for each

output. By this way, more focus was given to each array to enhance its performance.

Table 2 Gain and angles of the fabricated system in [17]

		Port 1	*Port 2*	*Port 3*	*Port 4*
At 2.45 GHz	*direction of maximum lobe (Degrees)*	8	39	-40	-11
	Gain (dB)	6.8	11.4	11.5	7.2
At 5.8 GHz	*direction of maximum lobe (Degrees)*	12	-25	26	-13
	Gain (dB)	5.3	5.8	6	5.2

Finally, a linear slot antenna array mounted on substrate-integrated waveguide (SIW) has been designed, simulated and measured in [45]. The bandwidth achieved was 4.5 GHz where the antenna was designed to operate at 60 GHz. The maximum gain achieved was 22 dB_i with a HPBW greater than 120˚. Even though the antenna array has achieved relatively high gain, its efficiency was 68%. The good performance of this antenna array was achieved via the complex geometry and design of the antenna array that was based on the SIW technology.

3.3 Literature Review Summary

Figure 45 shows the classification followed in this report and how much work is done under each category. It can be noticed that most of the work has been done using the bilateral structure design, where the complex geometry is avoided. Our proposed system will also be bilateral. Because of the same factor, Figure 46 shows that people focused on the 4x4 Butler instead of any higher size network. Also, according to Figure 47, very few papers were dedicated for the frequencies higher than 15 GHz. There are a bundle of papers operating at 60 GHz. But only one was operating at 77 GHz and no paper did it at 28.5 GHz, the frequency of our proposed system that has the least path attenuation.

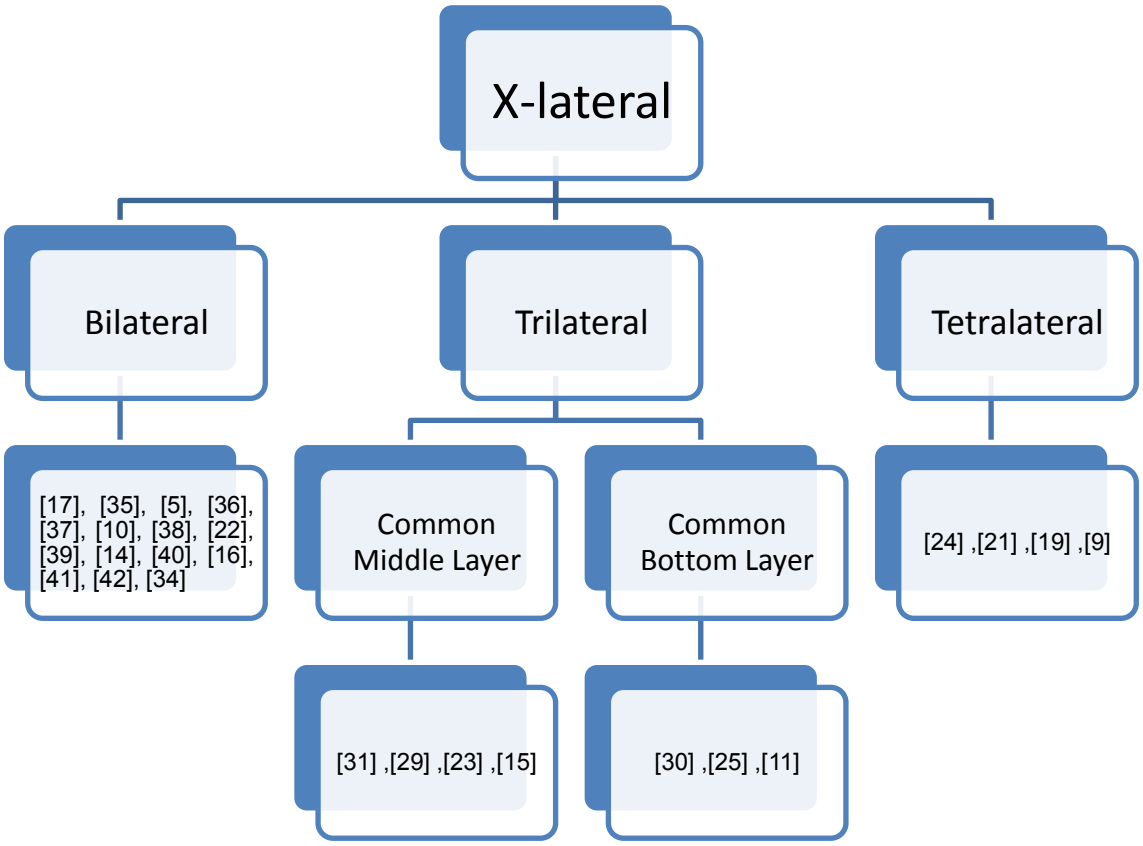

Figure 45 Classification based on number of layers

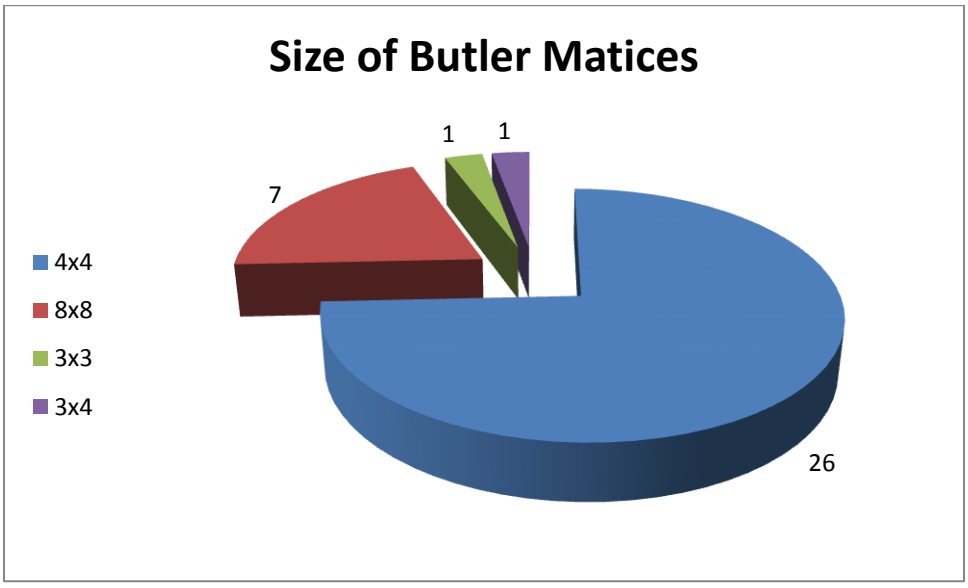

Figure 46 4x4 Butler captured most of the attention

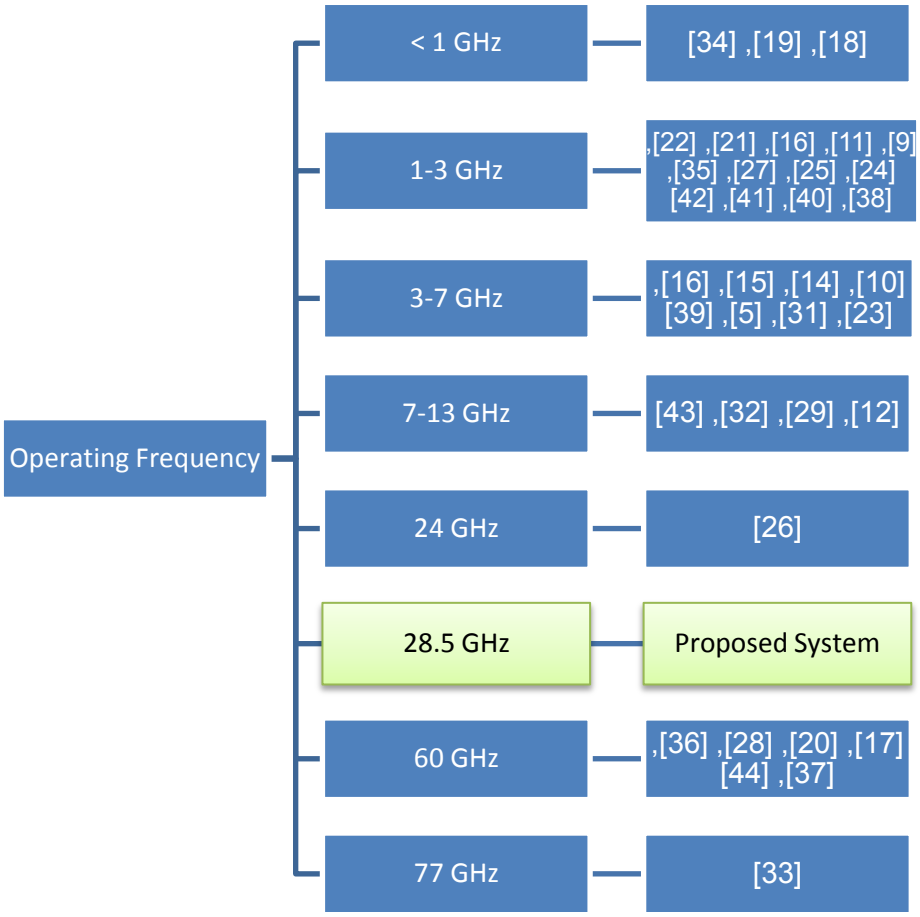

Figure 47 Classification based on operating frequency

In Figure 48, it is clear that a lot of attention is given to linear the patch antenna array. Design easiness, antenna size and high antenna gain played a major role of making the patch antenna very common with Butler networks. Still, different antennas have been proposed and designed in previous work. Slot antenna based on microstrip structures have not been used yet. One reason people avoided the slot antenna is the low gain acquired by them, that even having higher-order array will complicate the problem more due to the need to design power splitters and combiners.

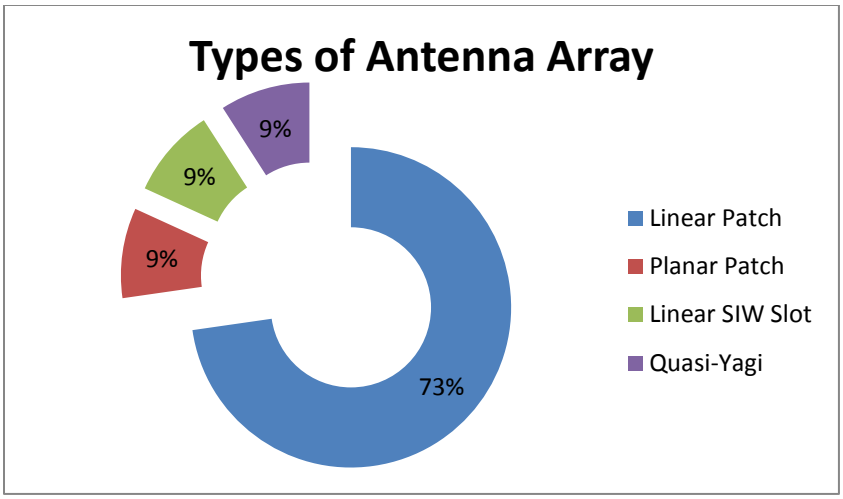

Figure 48 Antenna Array types integrated with Butler Networks

3.4 Conclusions

In this literature review, all work and researches conducted for the development of Butler feed network have been investigated. Starting with the limitations of the original Butler network introduced in 1961, people tried to solve the aforementioned problems and improve the performance. Some designs have improved the bandwidth, while some succeeded in shrinking the size significantly. New designs using multi-layers have been proposed and implemented. Regarding the problem of crossover, some papers came up with a novel design and they avoided the need for this component.

Since the Bilateral structure is the simplest geometry available, and since the problem of crossover is solved in a compact way using Hybrid couplers, this structure is chosen for our proposed system. Also, it can be noticed that no papers have been implemented to operate in the range from 25 to 60 GHz. Our system will operate at 28.5 GHz which has the lowest path attenuation as mentioned before. This band has a potential to be used for the 5G technology, especially after the experimental measurements that shown promising performance of this band as discussed in [3]. Also, no paper has implemented the use of slot antennas. A new 2D slot antenna array with its feed network will be presented in this work.

CHAPTER 4

BUTLER NETWORK DESIGN AND ANALYSIS

For our system, there are two main parts: Butler Feed Network and the Antenna Array. The focus first will be on designing the Butler Network. This feed network will be decomposed into its basic components. Each component will be designed and analyzed individually to give its maximum performance under the given conditions and requirements. They will also undergo fine tuning and modifying to force them operate at the desired operating frequency. After that, all components will be connected together to form the network. Then, tuning and resizing will be applied again to compensate for the deficiencies introduced when combining the components.

In this work, two simulation tools will be used; Microwave Office (MWO) and High Frequency Structure Simulator (HFSS). We will start with the design of the Hybrid Coupler, followed by the Crossover, Schiffman Phase Shifter and finally with the complete Butler Network. MWO simulation will be shown for stage 1 as a proof of concept only since the output responses of HFSS models were not up to the accepted level. At later stages, we succeeded to acquire satisfactory results using HFSS models, which are closer to real conditions, avoiding the need to prove the concept in MWO for the new parameters used.

In the following sections, the design procedure of the complete integrated system will be illustrated in stages, where each stage has its own material characteristics and design specifications. In this Thesis, we will have a total of three stages; the first one will be the first attempt, where we selected the material of RO3003 of thickness 1.76mm. Second stage will be based on a thinner substrate of 0.13mm for reasons explained later. Finally, third stage is similar to the second but we had to change the frequency response of constituent components to fix some further issues identified during the first fabricated model.

4.1 Stage I (Butler Design on RO3003 substrate of thickness 1.76mm)

For a microwave system operating at 28.5 GHz, the wavelength will be very small; about 10 mm. For some components, like the Hybrid coupler, the spacing between elements is quarter wavelength. In other words, the spacing between the component's elements' centers will be 2.5 mm apart. So, having RO3003 as a substrate with dielectric constant of 3.0 and loss tangent of 0.0013, if the

characteristic impedance is set to be 50 ohm after choosing the thickness of 1.76mm, the width of the line will be larger than 2.5/2 = 1.25 mm causing the elements to overlap. Because of this, the characteristic impedance was set to 100 ohm instead.

In the market, all available ports working at 30 GHz are 50 ohm. Therefore, a quarter-wavelength transformer will be used to match our micro-strip ($Z_o = 100\ \Omega$) line to the ports at the input and the output, where $Z_{transformer} = \sqrt{Z_{in} \times Z_L}$. Figure 49 shows a diagram of the quarter-wavelength transformer. The design details of each component of the Butler matrix will be explained in this sub-section. In sub-sequent sections, such details will be omitted and only the final optimized parameters will be shown with a focus on the results.

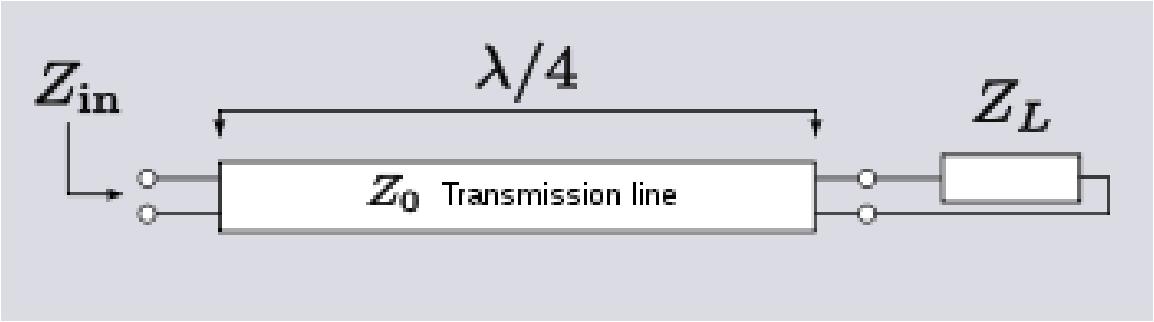

Figure 49 Quarter Wavelength Transformer

4.1.1 Hybrid Coupler

4.1.1.1 Microwave Office Simulation

The design of the Hybrid coupler in MWO is shown in Figure 50. After that, the S-parameters and the phase graph are plotted in Figure 51 and Figure 52, respectively. As can be seen the coupler is operating at 28.5 GHz with equal power split between ports 2 and 3 and a 90 degrees phase difference. The calculated values of the coupler arms followed equation

$$\boldsymbol{S} = \frac{-1}{\sqrt{2}} \begin{bmatrix} 0 & j & 1 & 0 \\ j & 0 & 0 & 1 \\ 1 & 0 & 0 & j \\ 0 & 1 & j & 0 \end{bmatrix} \qquad (2.5).$$

The insertion loss was around 3 dB and the inputs were matched to 50 ohms.

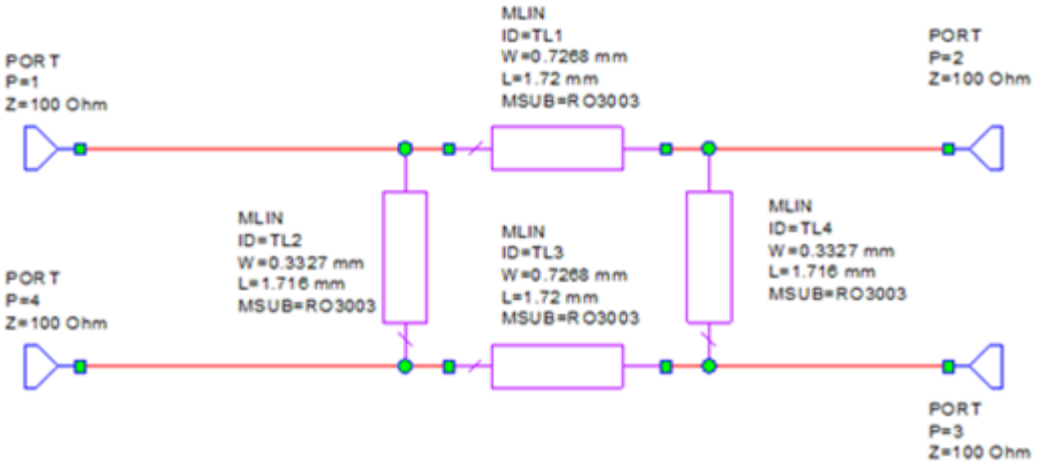

Figure 50 MWO Diagram of Hybrid Coupler

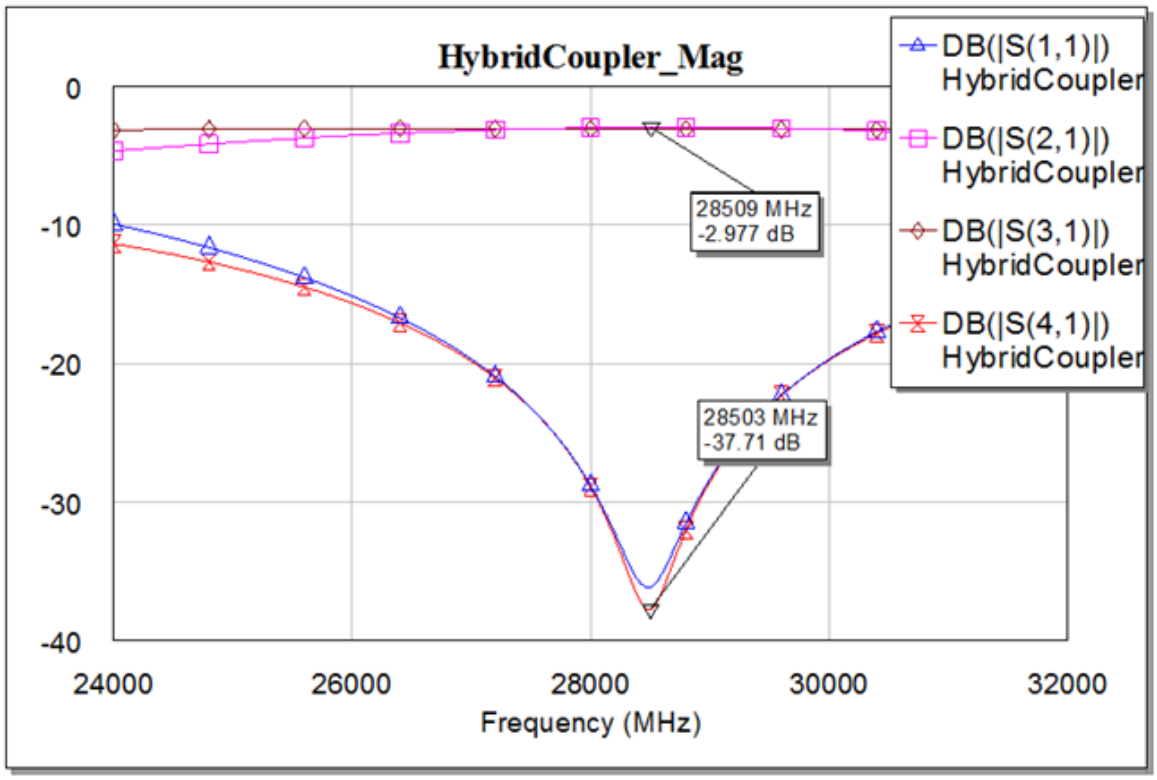

Figure 51 MWO S-parameters from Port 1 of the Hybrid Coupler

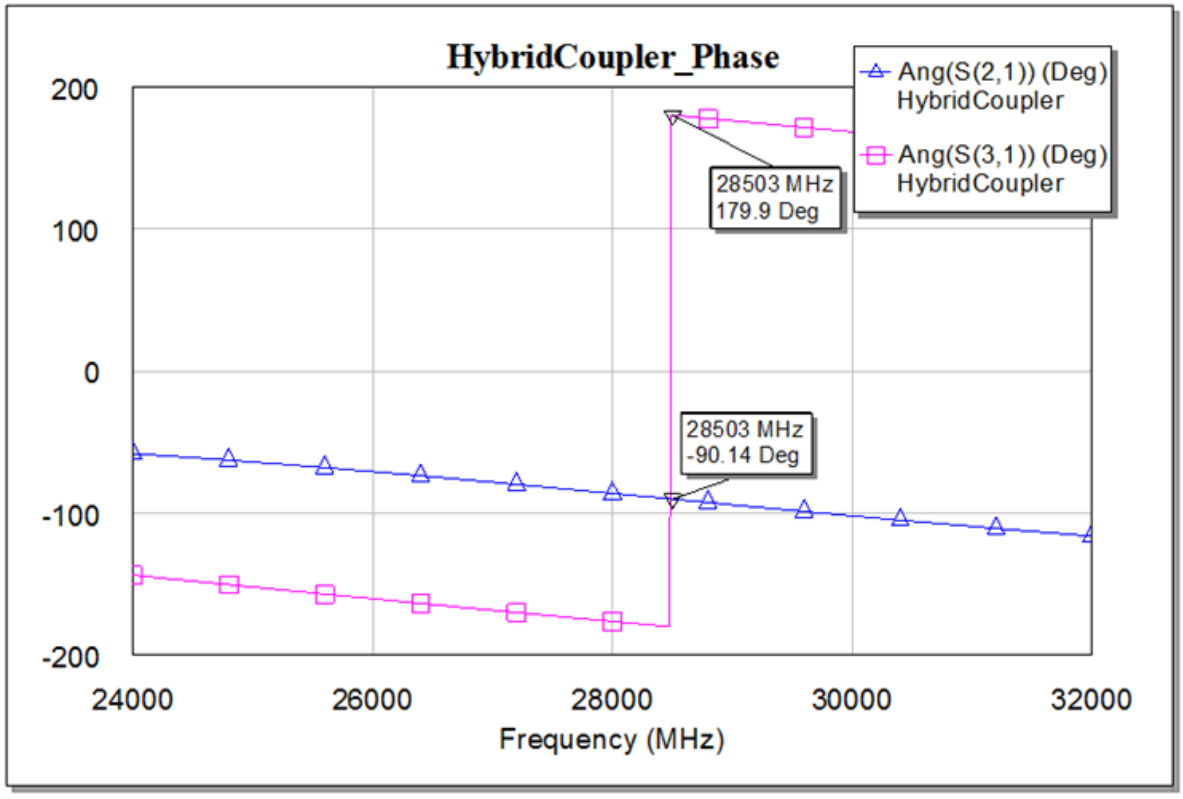

Figure 52 MWO Phase Plot lot of the Hybrid Coupler

4.1.1.2 High Frequency Structure Simulation

In HFSS, some points were noticed that affected the design from its theoretical dimensions. It was noticed that extending the length of both arms of the coupler will result in a narrower bandwidth of operation and an unequal power split between the two output ports. But the reflection coefficient S_{11} will be lower. Also extending the width of the thick arm will lead to a flatter response and wider bandwidth on one hand. It will also split the power more equally between the output ports. On the other hand, the reflection coefficient will increase and the operating frequency will be shifted downward. So, a trade of between the previous factors must be considered until approaching the design with the most efficient performance. When designing the coupler, having equal power split was given the top priority followed by the operating frequency.

In Figure 53, the Hybrid coupler model is shown in HFSS. The simulation results shows that at 28.5 GHz, the power levels at the output ports are -3.8 dB and -4.3 dB. These values are the closet levels acquired in HFSS. The phase difference between the two output ports are around 90 degrees as shown in Figure 55. A flat insertion loss is seen from 28.5 GHz up to 31 GHz.

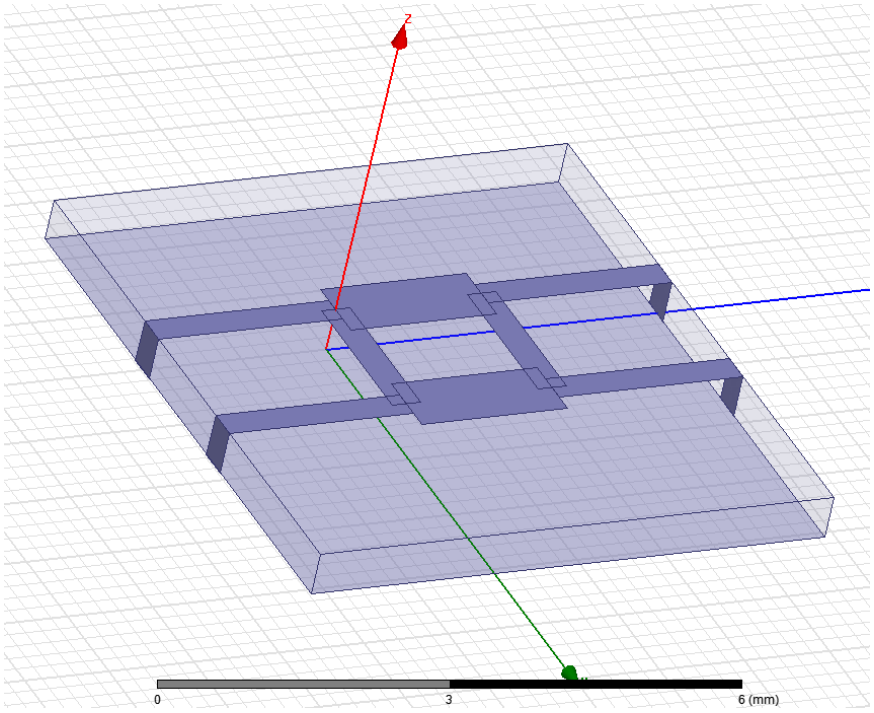

Figure 53 HFSS Design of the Hybrid Coupler

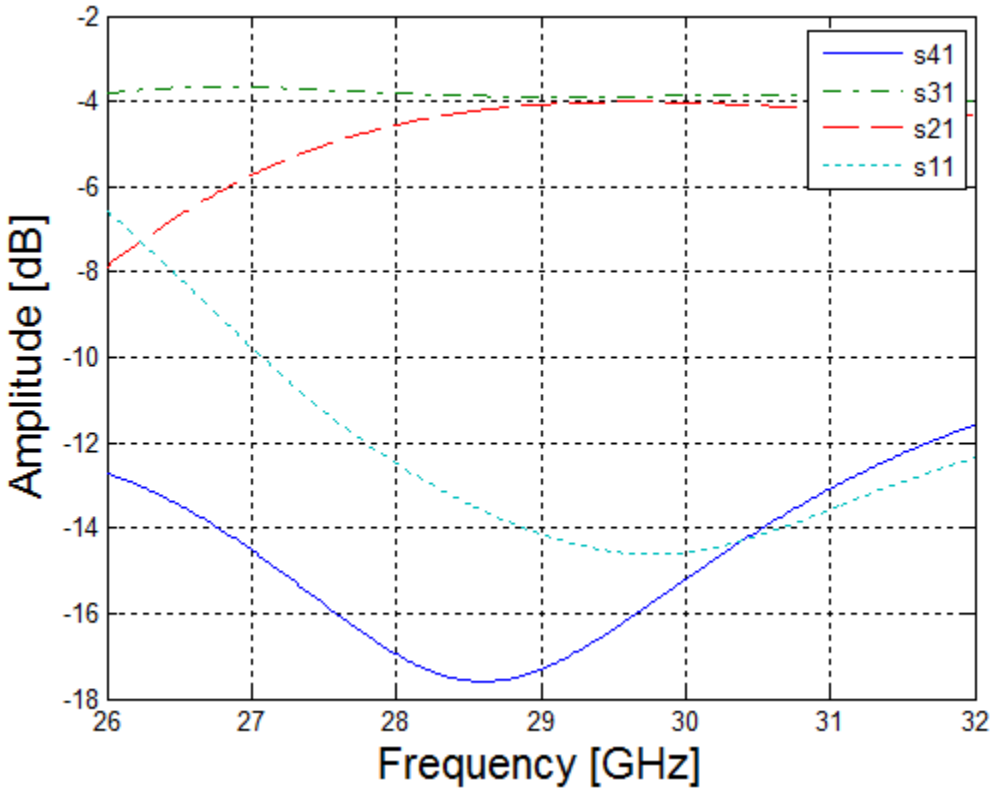

Figure 54 HFSS S-parameters from Port 1 of the Hybrid Coupler

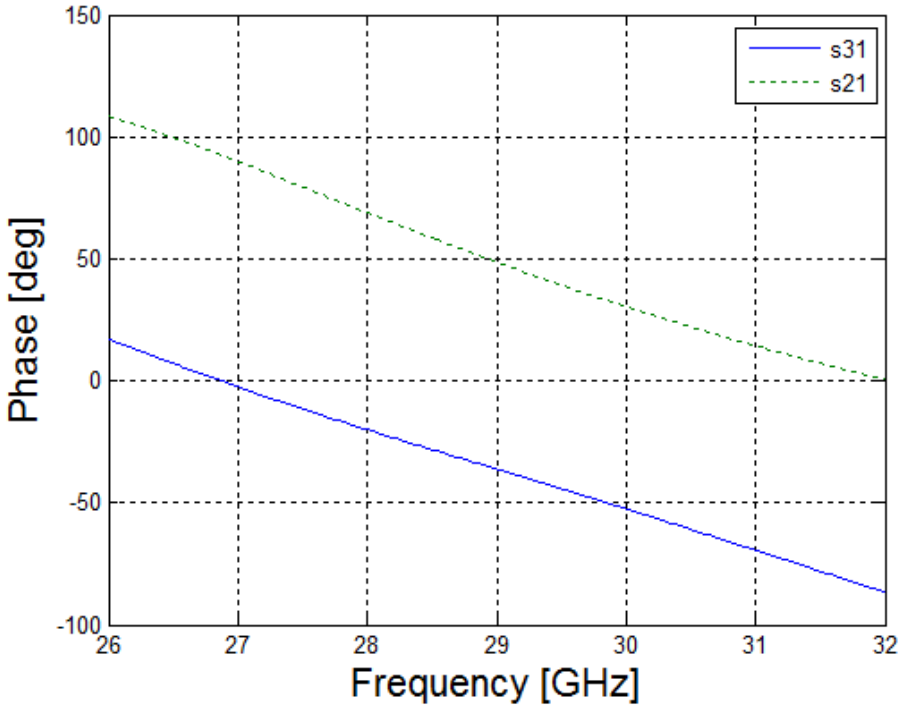

Figure 55 HFSS Phase Plot lot of the Hybrid Coupler

4.1.2 Crossover

4.1.2.1 Microwave Office Simulation

The crossover's diagram in MWO is shown in Figure 56. The dimensions here are exactly the same as the values acquired from theoretical quantities. In MWO, the insertion loss introduced by the crossover to the two paths; S41 and S23, are very negligible. The simulated insertion loss is -0.05 dB at our operating frequency as shown in Figure 57. Also the phase shift introduced is very small. As Figure 58 shows, the phase shift is only 1.5 degrees at 28.5 GHz.

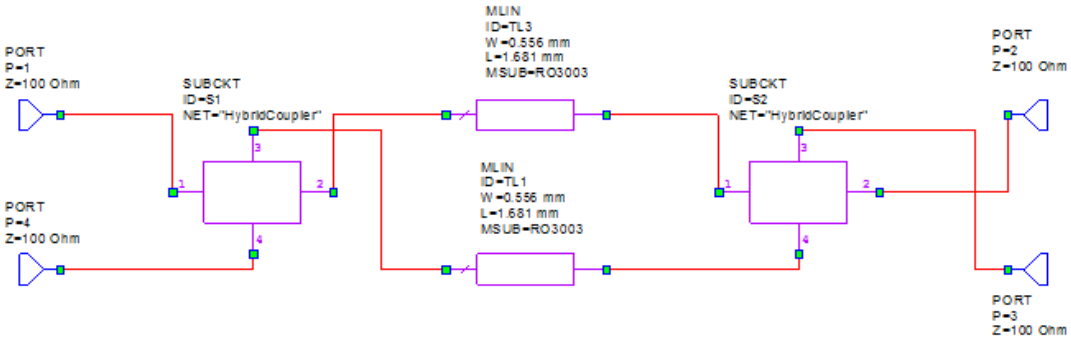

Figure 56 MWO Diagram of the crossover

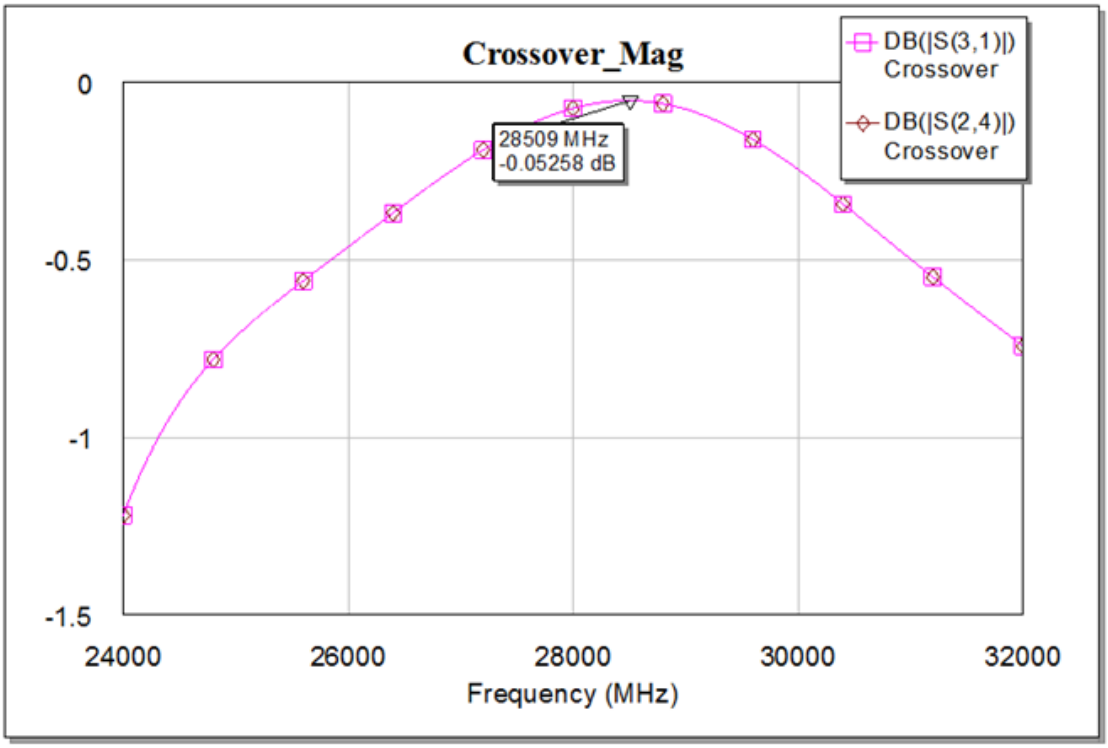

Figure 57 MWO S-parameters of the crossover

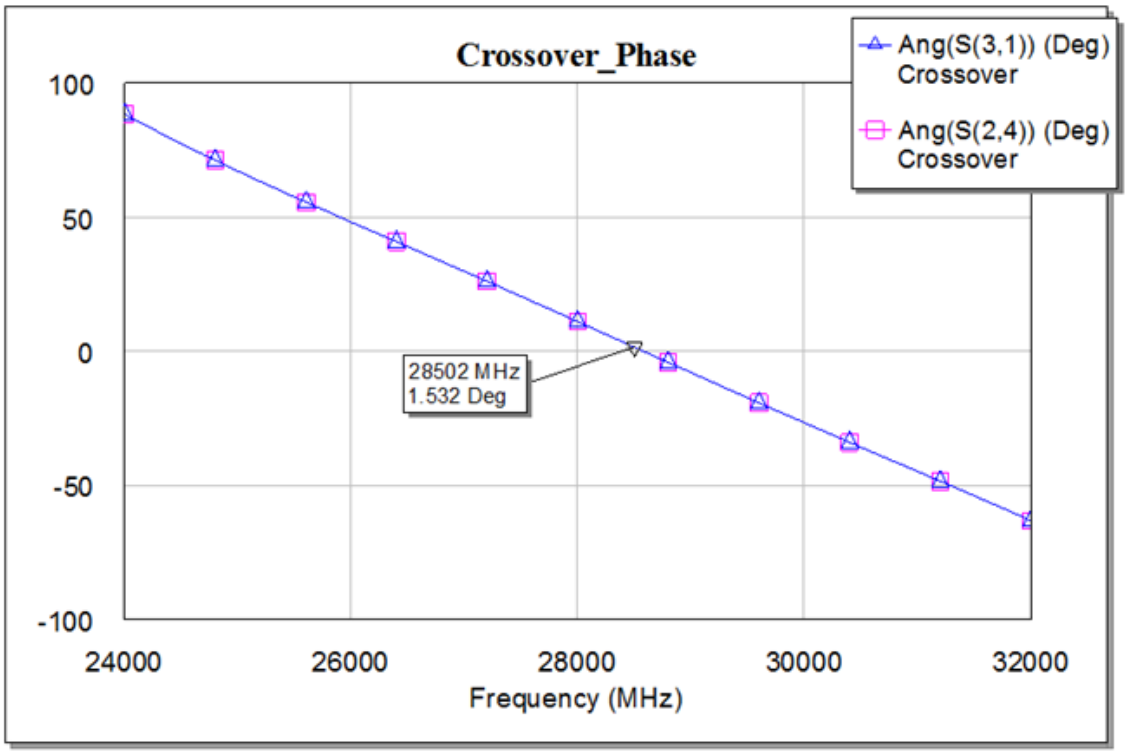

Figure 58 MWO Phase Plot of the crossover

4.1.2.2 High Frequency Structure Simulation

In HFSS, the crossover needed little tuning. The design is presented in Figure 59. The simulation result shows an insertion loss of -1.31 dB and it can go up to 30 GHz with less loss as illustrated by Figure 60. It should be noticed that although the design was intended to be at 28.5 GHz, results show good performance at 29.5 GHz as well. The phase difference between the two paths is -0.55 degrees as shown in Figure 61.

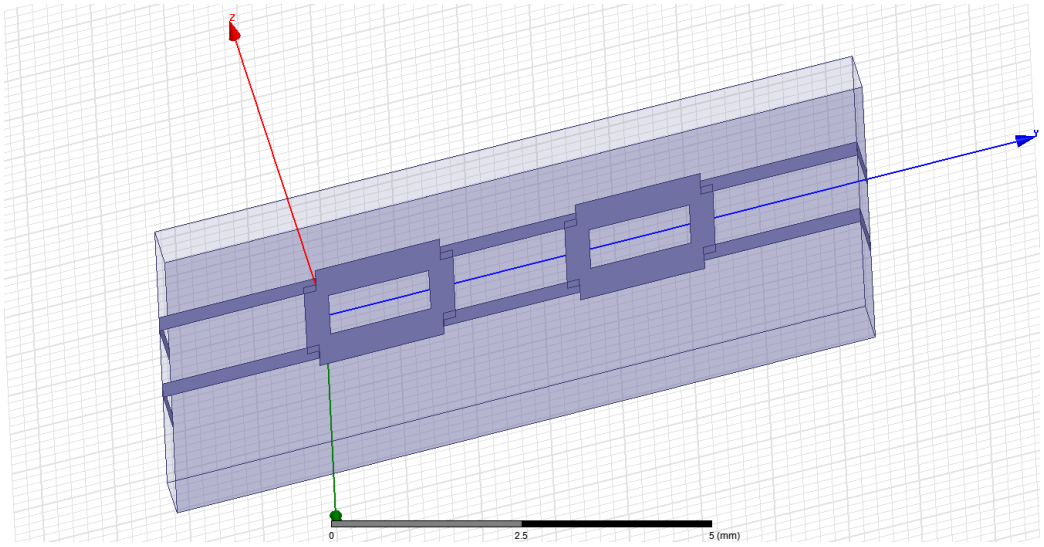

Figure 59 HFSS Design of the crossover

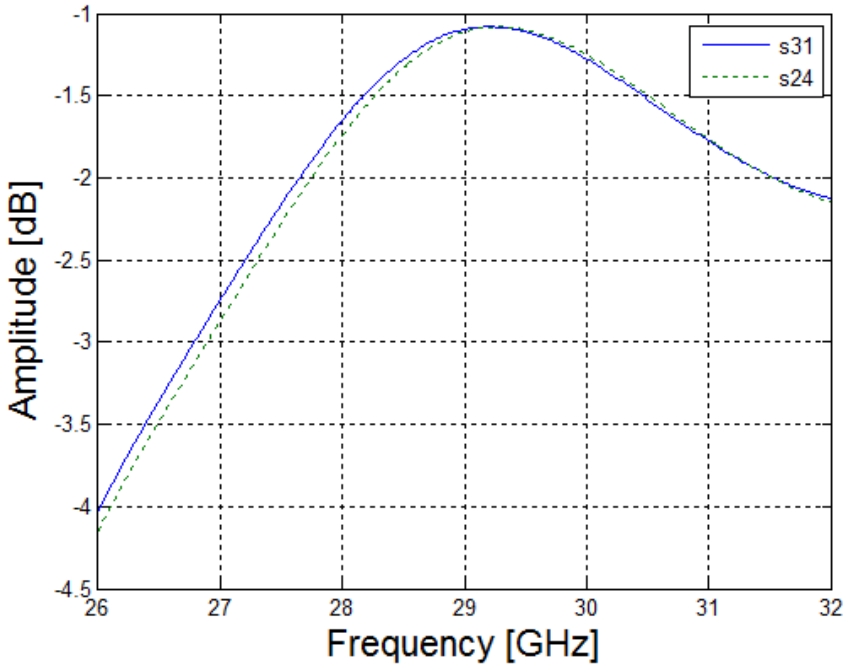

Figure 60 HFSS Insertion loss of the two paths of the crossover

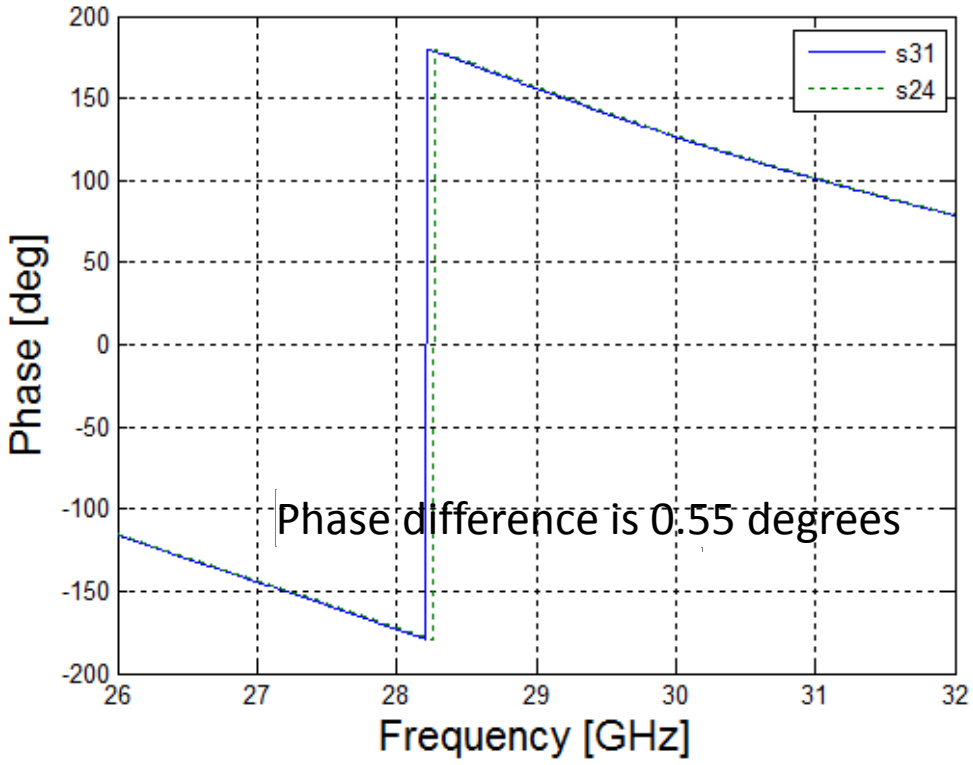

Figure 61 HFSS Phase shifts introduced by the crossover

4.1.3 Schiffman Phase Shifter

For the phase shifter, MWO simulation will be skipped since it is only a straight microstrip line providing the required phase shift. The HFSS design of Schiffman phase shifter is shown in Figure 62. As Figure 63 shows, the insertion loss at 28.5 GHz is about -1.7 dB and the reflection coefficient is around -17 dB, which is desirable.

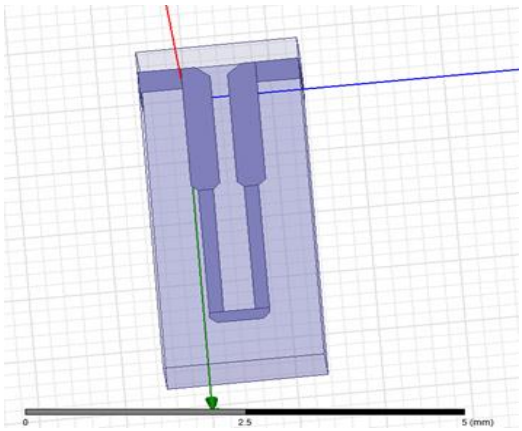

Figure 62 HFSS Design of Schiffman Phase Shifter

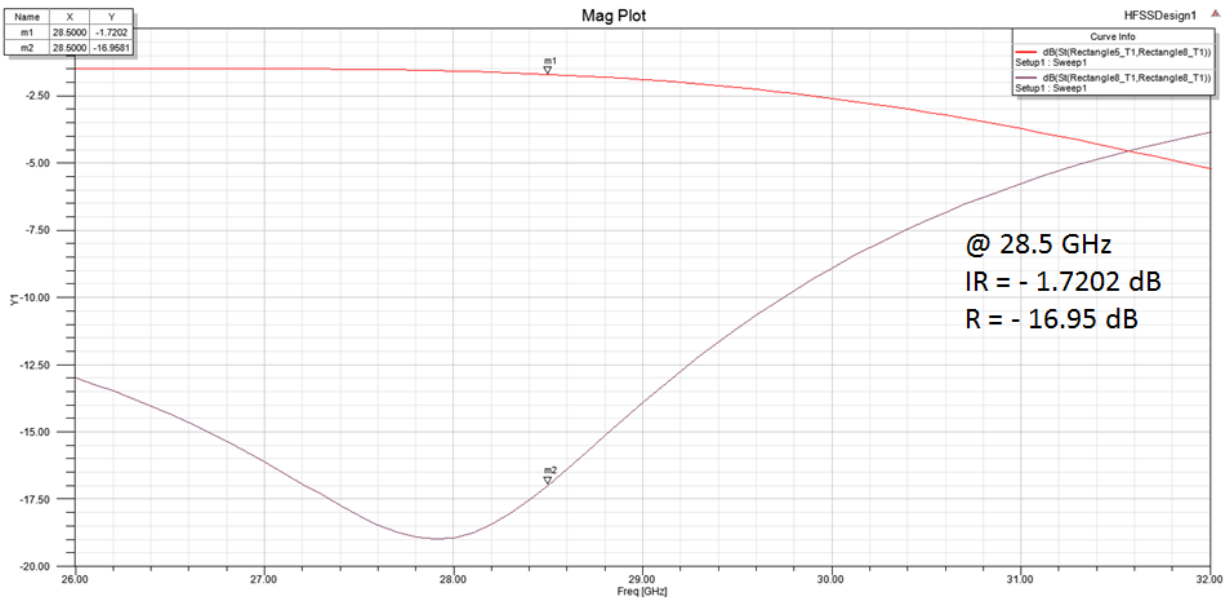

Figure 63 HFSS Insertion Loss and Rerlection Coefficient of the proposed shifter

Tuning the shifter will be needed to provide the required phase shift in the design for a wide bandwidth, which is 45 degrees in our case. The shifter needs to be tuned to provide 45 degrees shift with respect to the other line. Now, it will be tuned and compared to the phase shift introduced by a straight line. Further tuning will be needed once the complete system is connected. So, since the phases of the output ports of the Hybrid coupler is known and previously simulated, it will be used as reference in the procedure, as illustrated in Figure 64. It is found that the length needed for the C-section of the phase shifter is about 3.7 mm. Also the same length is needed for the base section. Making the width of the C-section half of the base section will provide the required performance in terms of insertion loss and reflection coefficient. After tuning, the phase difference is about -45 degrees for the range from 27.6 to 30 GHz as shown in Figure 65.

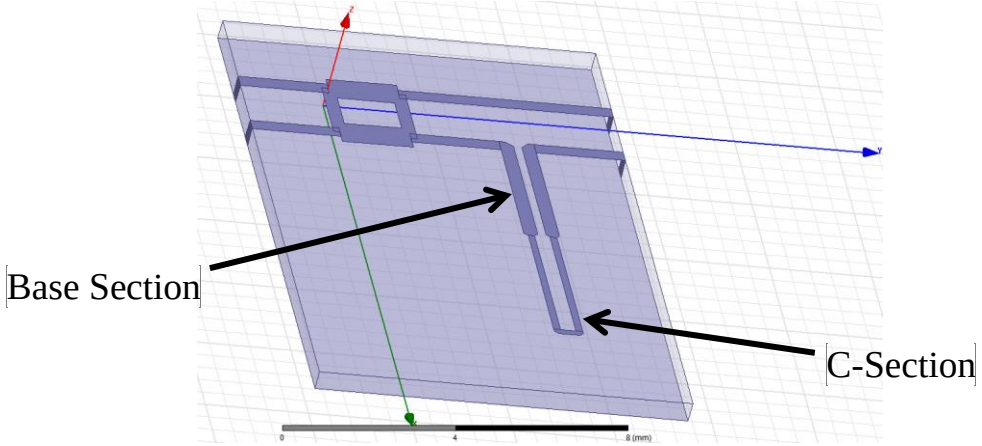

Figure 64 HFSS Diagram of the tuning system

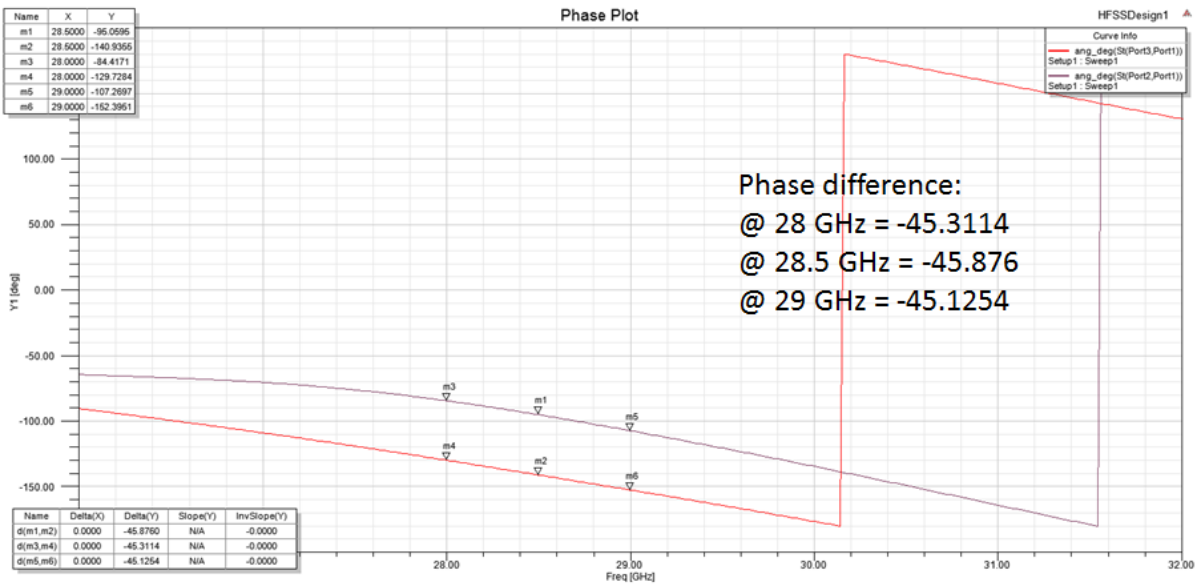

Figure 65 Schiffman Phase Shifter of 45 degrees

4.1.4 The Complete Butler Network

After simulating all the components individually, they will be connected together to form the complete Butler network operating at 28.5 GHz. First, the MWO-based model will be presented, then the HFSS one. Results are compared and conclusions are made.

4.1.4.1 Microwave Office Simulation

Figure 66 shows the block diagram in MWO of our Butler Network. In MWO, all results were close to the ideal case (i.e. One fourth of the input power) as shown in Figure 67 and Figure 68. We have almost -6 dB at each output and the phase differences were very close to 45 degrees.

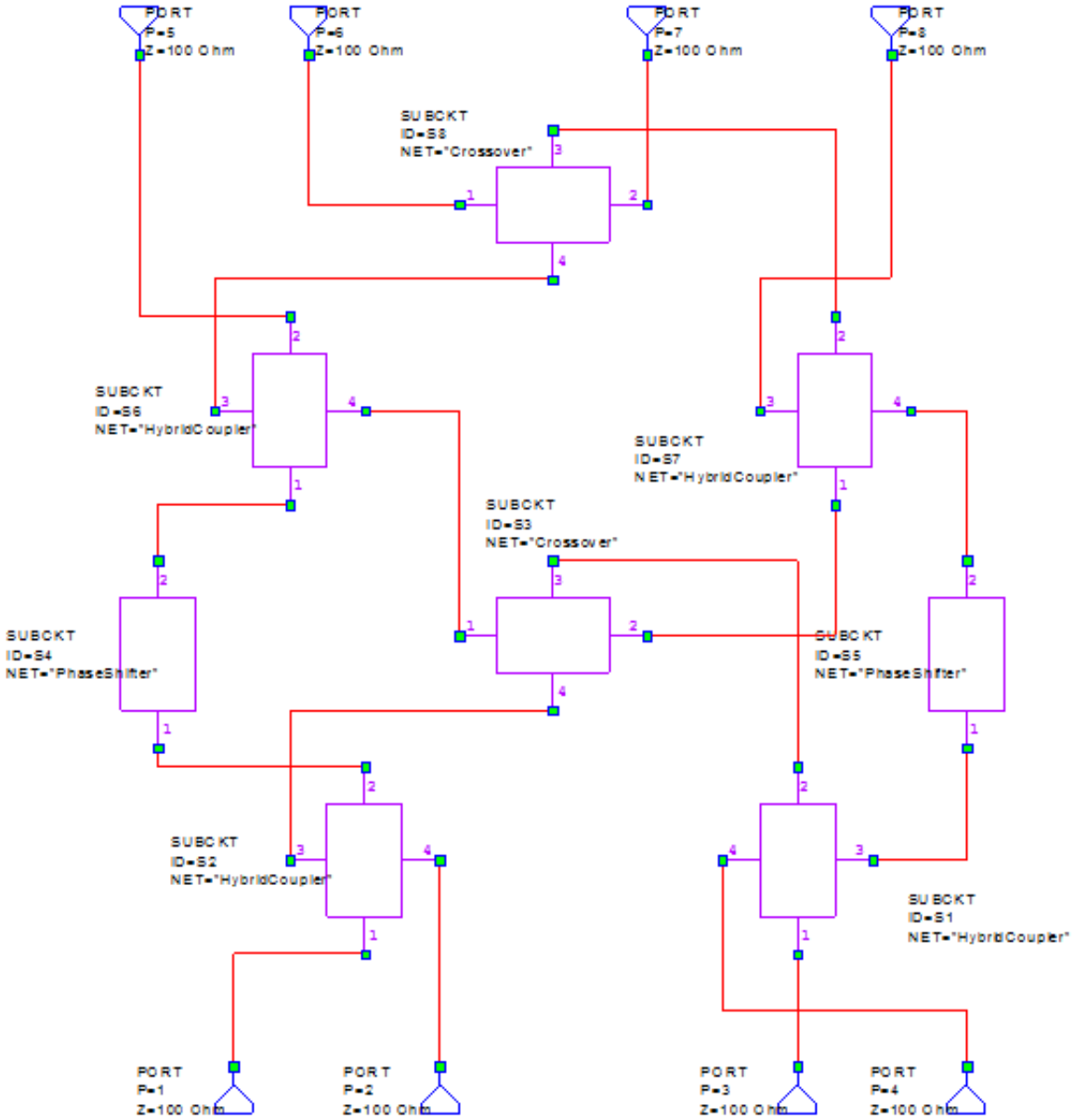

Figure 66 MWO Diagram of the proposed 4x4 Butler

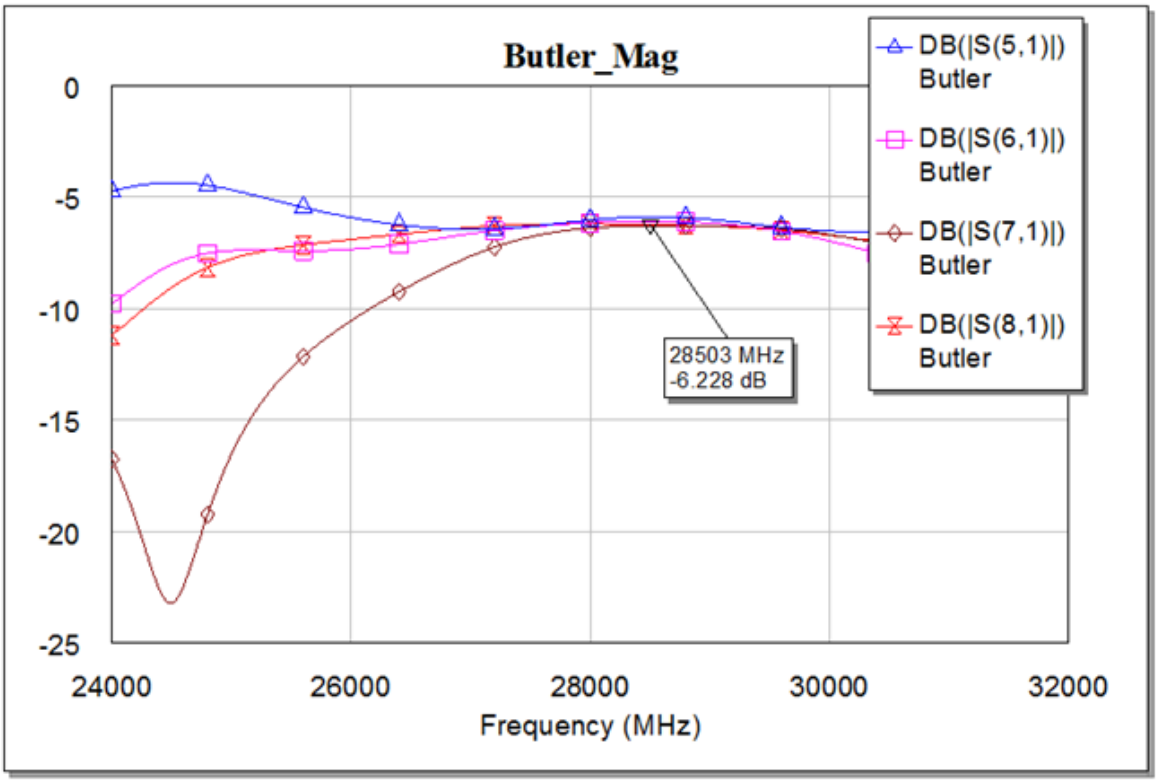

Figure 67 MWO S-parameters of Butler Nework when port 1 is excited

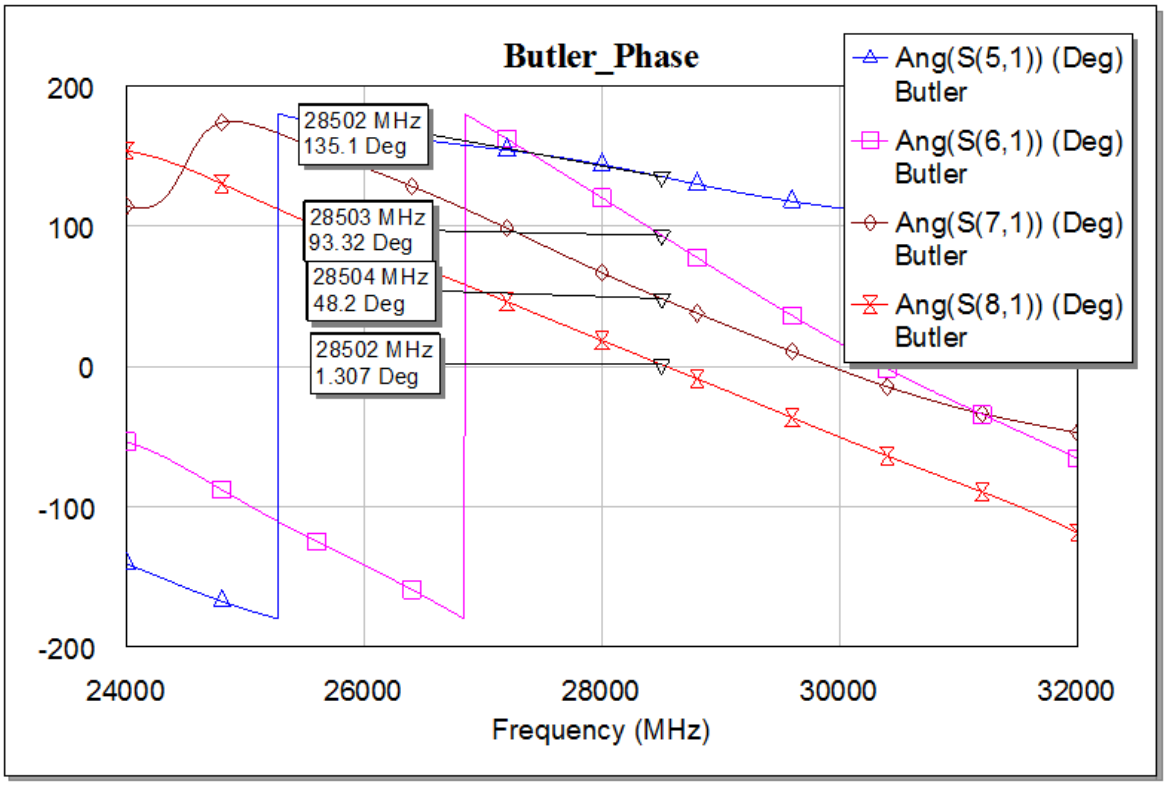

Figure 68 MWO Phase Plot of Butler

4.1.4.2 High Frequency Structure Simulation

In HFSS, constructing the complete Butler was a hard task. The system layout is shown in Figure 69. The amplitude responses at the output ports were approximately close to each other for wide bandwidth as shown in Figure 70 when port 1 is excited.

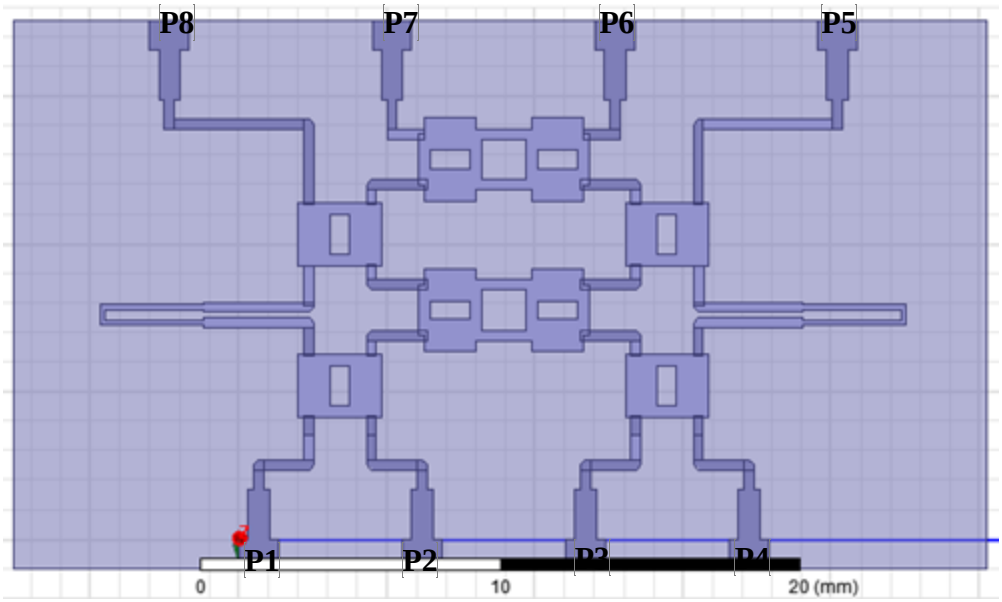

Figure 69 Butler Network with modified Hybrid Couplers

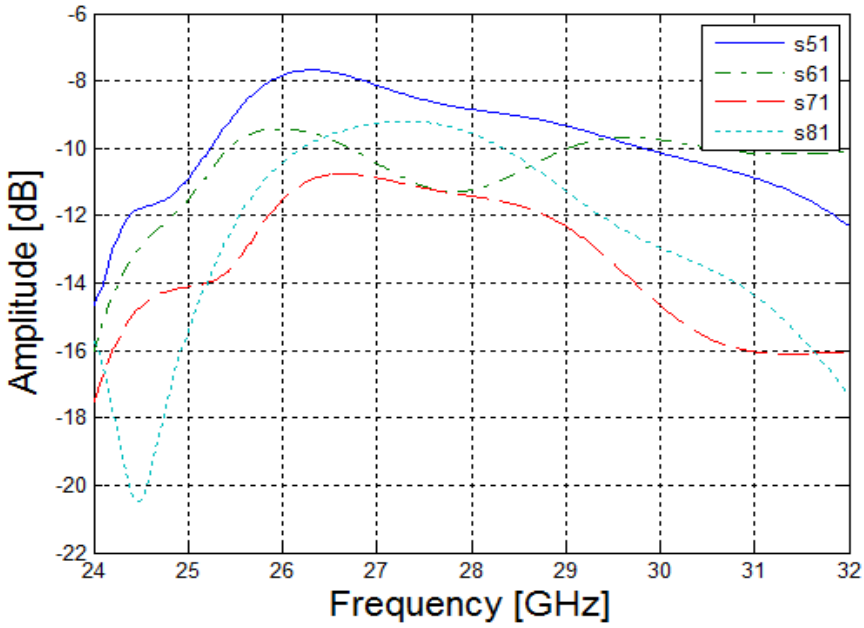

Figure 70 S-parameters for the proposed Butler Netwotk

The power level at port 5 was -9.058 dB, while it was -11.111 dB for port 6 and -11.66 dB for port 7. Port 8 had a power level of -10.145 dB. These power levels are the case when port 1 is excited. Having all the focus on reducing the power loss, the phases of the output ports are considerably mistuned. Phases at the output did not offer the required phase difference between adjacent ports as can be noticed from Figure 71.

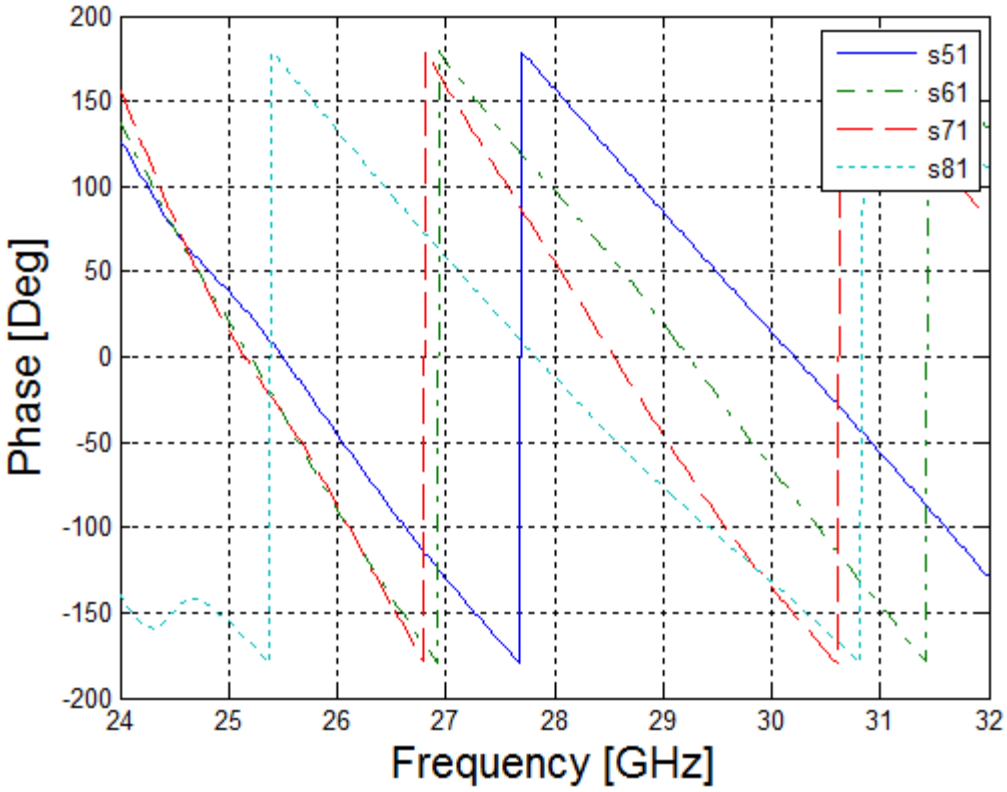

Figure 71 Phase Plot of the proposed Butler Network

When tuning the phase shifters, it sometimes degraded the amplitude so badly at the outputs. So, either having accepted amplitude and undesired phase differences, or having the desired phase difference but with a very weak signal unequally divided at the output. It has been noticed that Schiffman phase shifter was the reason behind this problem. That is due to the small distance gap between the lines in the small C-section of the shifter, which could introduce coupling and other effects. It must be mentioned that the Schiffman Phase Shifter has not been used for frequencies as high as 28.5 GHz. That is why we decided to remove this shifter and replace it with a normal microstrip line which will do the job of introducing the required phase shift.

The geometry of the input ports has been reconsidered to match the physical connector that will be used during measurements. A 50 ohm mini-SMP connector provided by Pasternack Company [46] is chosen as a physical port to our network. This port operates from DC up to 65 GHz. At our frequency,

28.5GHz, the insertion loss is expected to be 0.52 dB and 14dB for the return loss. A diagram of the port dimension is shown in Figure 72.

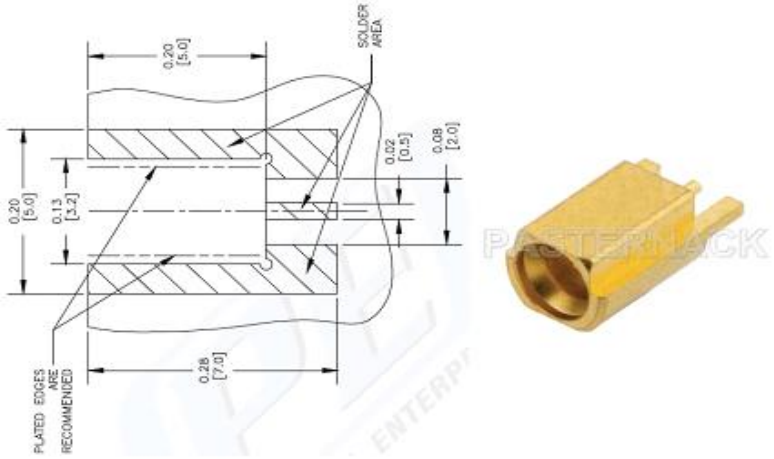

Figure 72 Diagram for the physical port [46]

As a result, the new Butler, shown in Figure 73, with regular transmission lines as phase shifters and with pads next to the ports which are connected to the ground through vias. Amplitude and phase responses are shown in Figure 74 and Figure 75, respectively. The results shown are for port 1. The amplitude responses were not acceptable. The phase differences between adjacent output ports should be -45 degrees. The errors were 3.4, 3 and 21.5 degrees for the output ports, giving an average error of 9.3 degrees. The average error when port 2 is excited was 16 degrees.

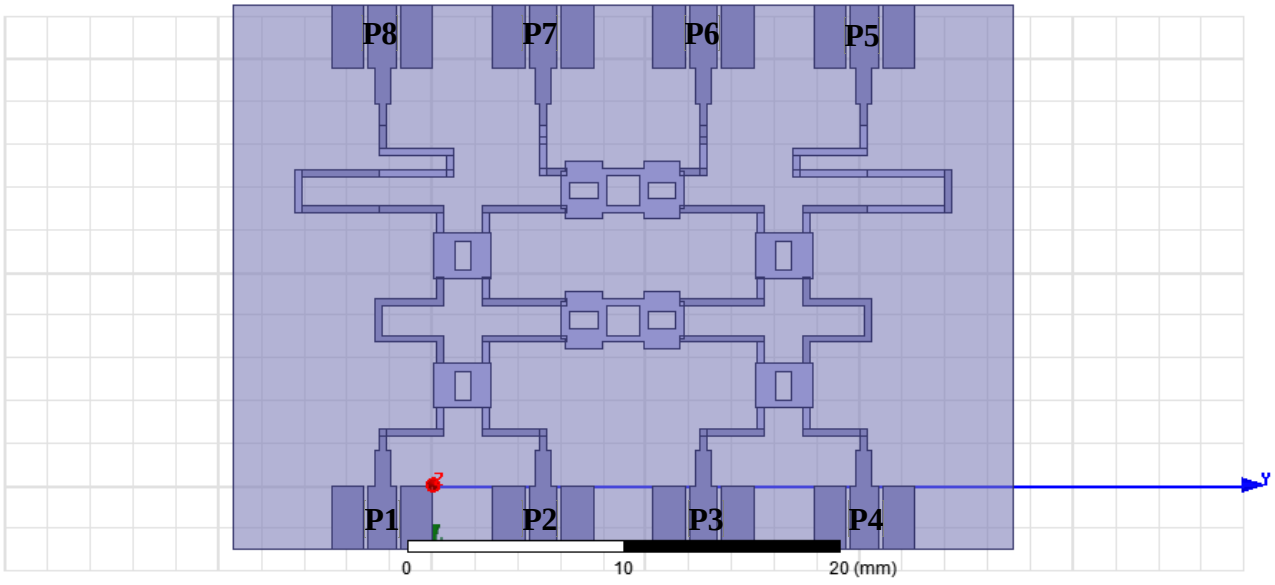

Figure 73 Layout of Butler wit GND pads

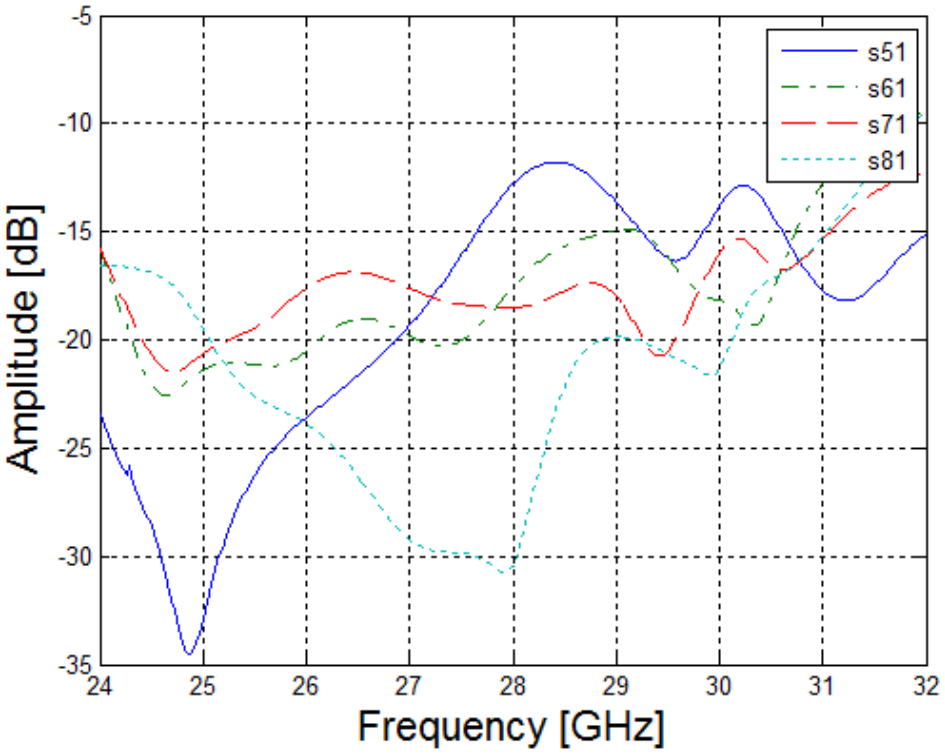

Figure 74 Amplitude response when port 1 is excited

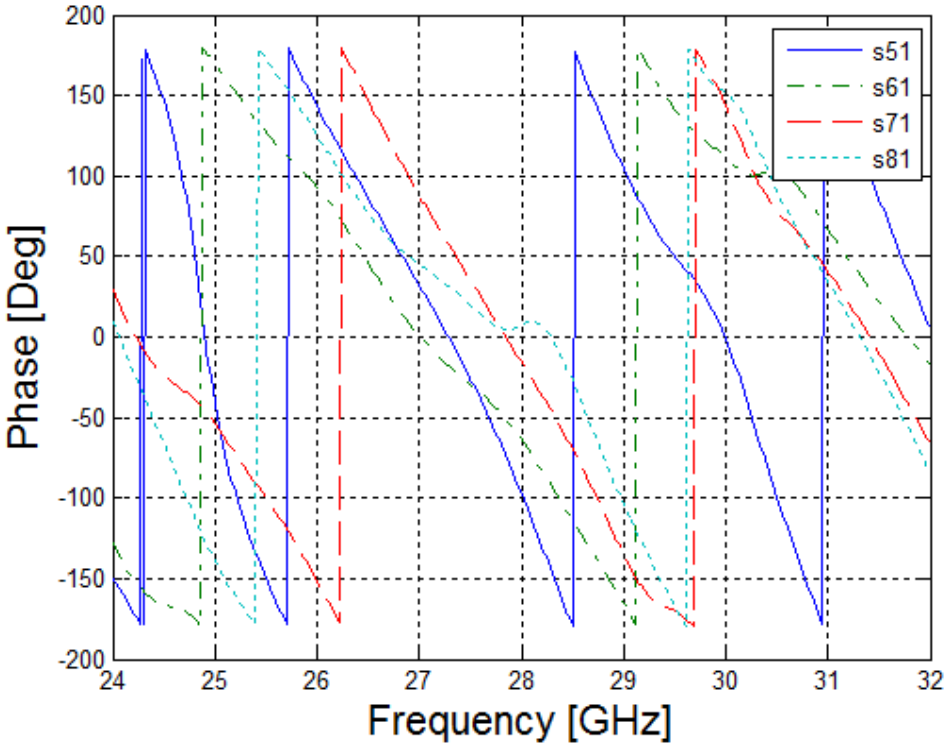

Figure 75 Phase response when port 1 is excited

4.2 Stage II (Butler Design on RO3003 substrate of thickness 0.13mm)

After observing the results of the designs from stage I, we noticed that we are still suffering from high loss at the output. Also, the power was not well divided between the ports (10 dB difference as in Figure 74) which was something not accepted. Taking a second overview over other references, we noticed that equal power split had been achieved at higher frequency using very thin substrates. So, it has been decided to go on with the thinnest substrate available for RO3003 material which was 0.13mm. So, a new Butler has been built through the same procedure mentioned in Stage I. It also known that for network microstrip structures, the thinner the substrate the better the performance due to tight coupling of the fields between the line and its ground. Opposite can be done for antenna based microstrip structures.

Also, moving to a thinner substrate has eliminated the need for Quarter-Wavelength impedance transformer at the ports. That is because the 50 and 70.7 Ohm stubs needed for the Hybrid couplers are thin and will not overlap with their corresponding widths when the thickness is 0.13mm.

Moving to the thinner substrate has solved the two aforementioned major problems. The new layout of the Butler network is shown in Figure 76. The output responses when port 1 and 2 are excited are shown in Figure 77 to Figure 80. It can be noticed that power level at the output are much closer to the ideal value of -6dB. When port 1 is excited, -6.7dB is detected at port 5, 7 and 8, while -8dB is detected at port 6 since it has travelled the longest distance compared to the other paths; two couplers and two crossovers. The phase difference between adjacent ports should be 45˚ in ideal case. In this simulation, phase difference was 41.7 degrees between port 5 and 6, 56.3 degrees between ports 6 and 7 and 20.7 degrees between ports 7 and 8. So, the errors were 3.3, 11.3 and 24.3 degrees introducing an average error of 13 degrees. Similarly, when port 2 is excited, around -7.5 dB is detected at the output ports. But in this case, port 6 will suffer the lowest attenuation of -5.5 dB. For phases, an average error of 15.5 degrees takes place. Simulation results when ports 3 and 4 are identical to ports 1 and 2. The dimensions of this Butler are 18.72 by 34 mm^2.

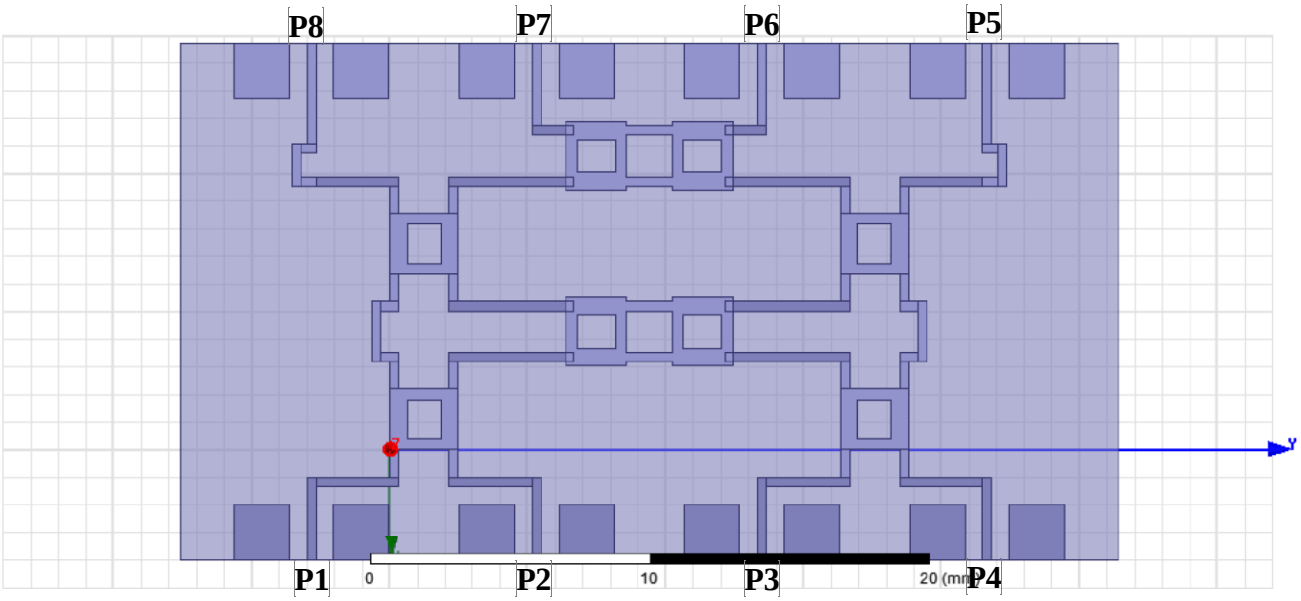

Figure 76 Butler Network on a 0.13mm substrate

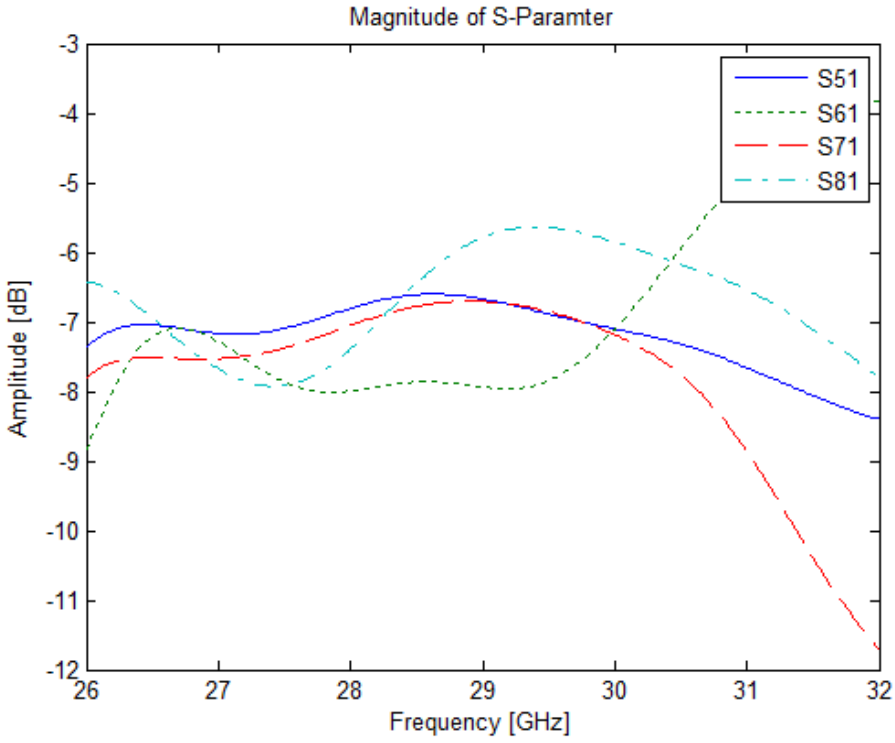

Figure 77 Amlitude response when port 1 is excited for Butler-Stage II

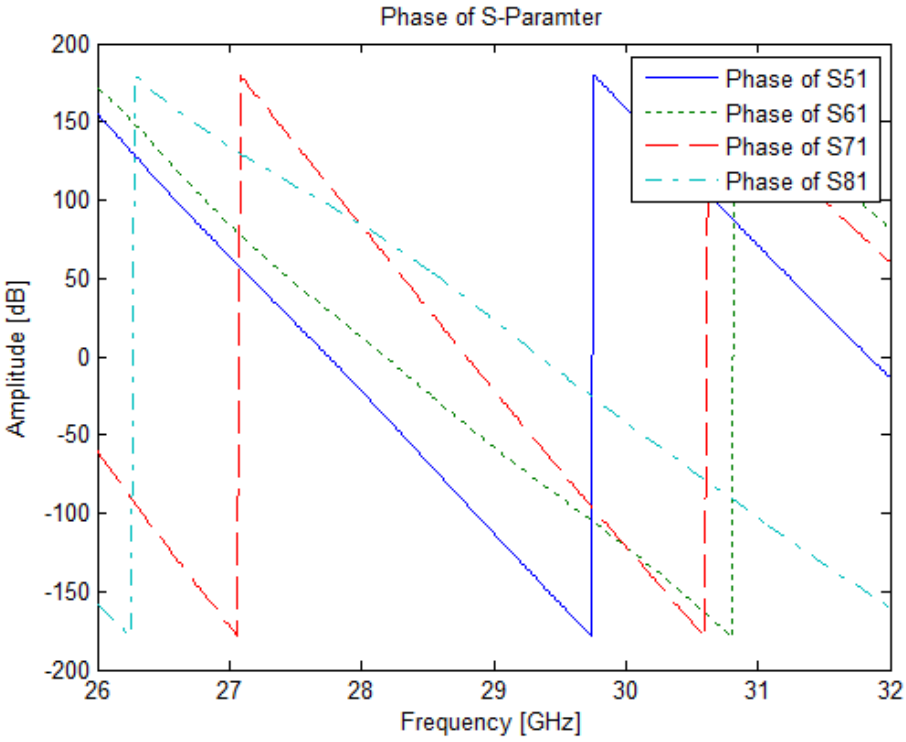

Figure 78 Phase response when port 1 is excited for Butler-Stage II

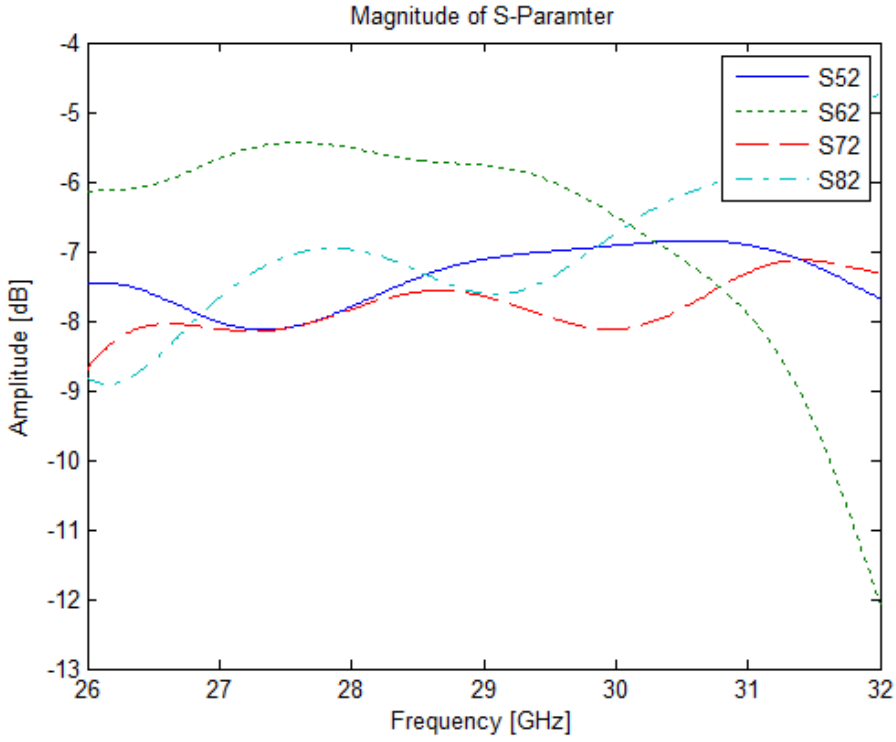

Figure 79 Amplitude response when port 2 is excited for Butler-Stage II

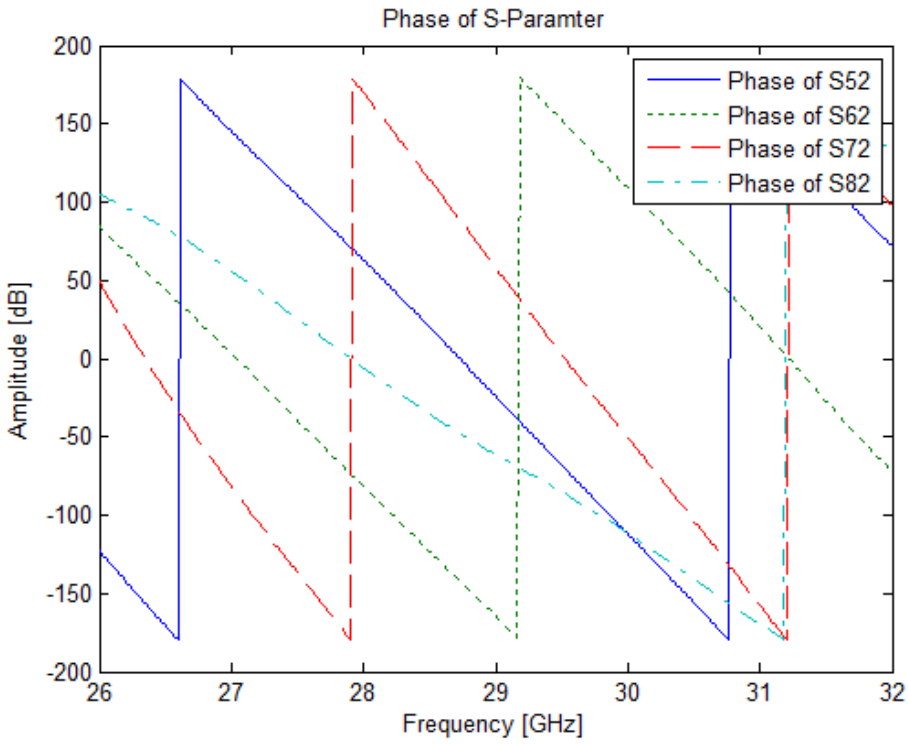

Figure 80 Phase response when port 2 is excited for Butler-Stage II

Having good output behavior affected the reflection coefficient of the system. At 28.5 GHz, the reflection coefficients are -12 dB for ports 1 and 4, and it is -15 dB for ports 2 and 3, as shown in Figure 81. This Butler network is somehow resonating at 31.4 GHz with good reflection coefficient of -20 dB for ports 2 and 3 and -30dB for ports 1 and 4. Nevertheless, since we got at least -12 dB at our point of interest, we proceeded with our design and integrated it to our system (i.e. integrated with antenna array).

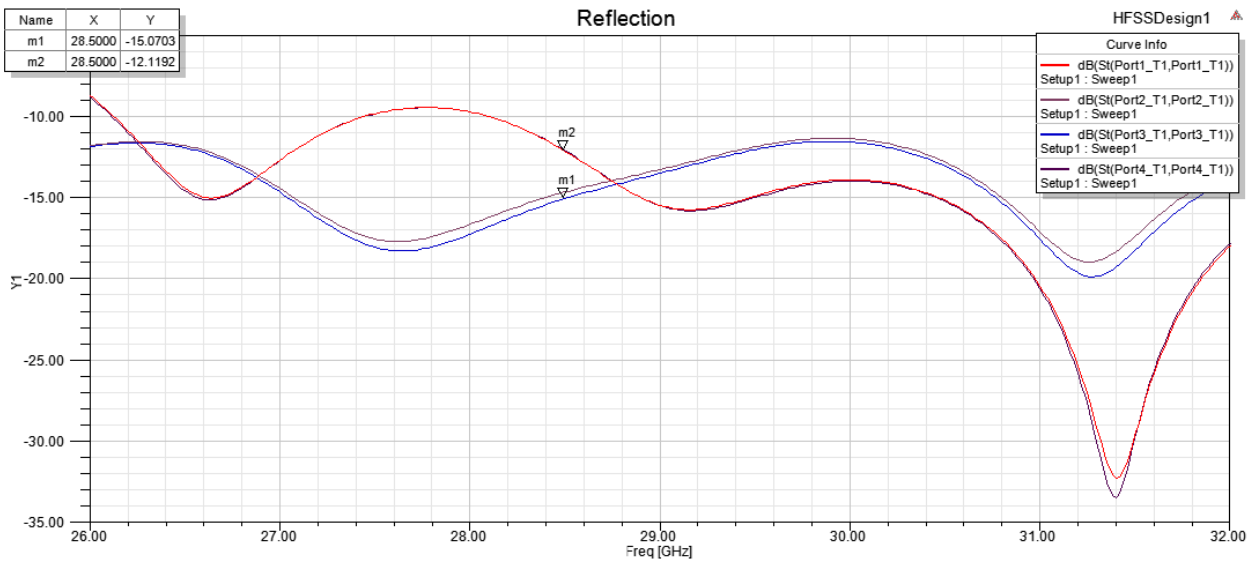

Figure 81 Simulated reflection coefficients for Butler-Stage II

4.3 Stage III (Second Butler Design on RO3003 substrate of thickness 0.13mm)

The reason of entering this stage will be justified and illustrated in chapter 6; Fabrication & Measurement. In short words, we needed to redesign our Butler to have better reflection coefficients for all ports at 28.5 GHz. In the first and second stage, all components were designed to operate at 28.5 GHz, and we ended up having a system with its reflection coefficients centered at 31.4 GHz. In order to have the complete system resonating at 28.5 GHz, individual components were redesigned a third time.

Shown next in Figure 82 and Figure 83, simulation results for the new Hybrid Couplers and Crossovers are displayed. The new coupler is now resonating at 27.2 GHz, while the crossover is resonating at 28 GHz with in insertion loss of 0.2 dB and reflection coefficient lower than -45 dB. Using these new designs, a new Butler is constructed with a regular phase shifters as in stage II.

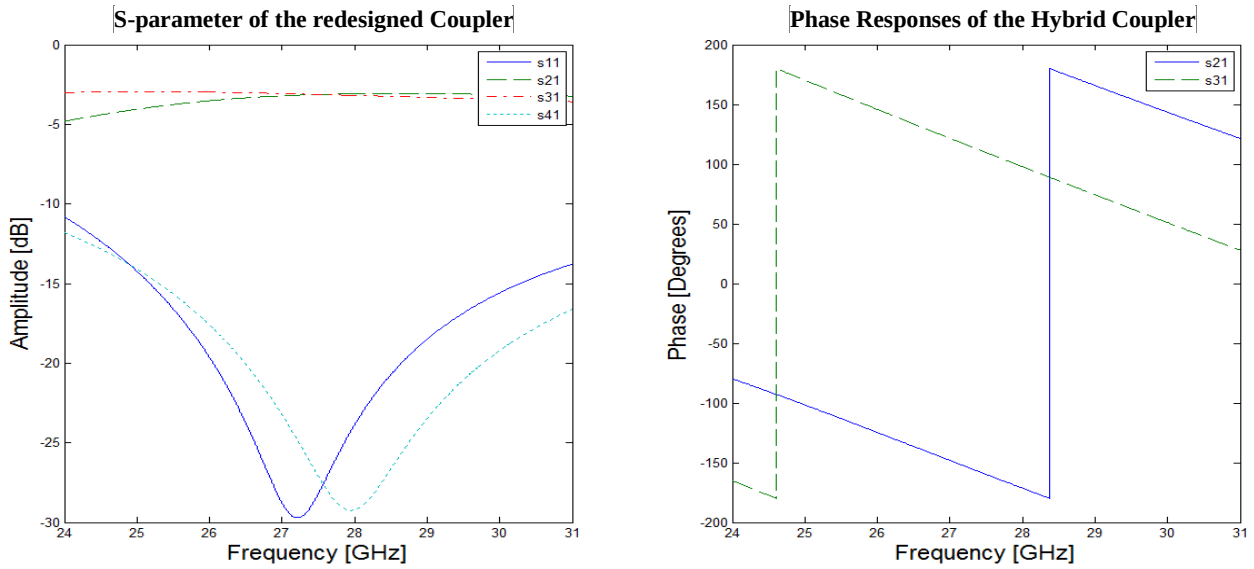

Figure 82 S-parameter for the redesigned Hybrid Coupler

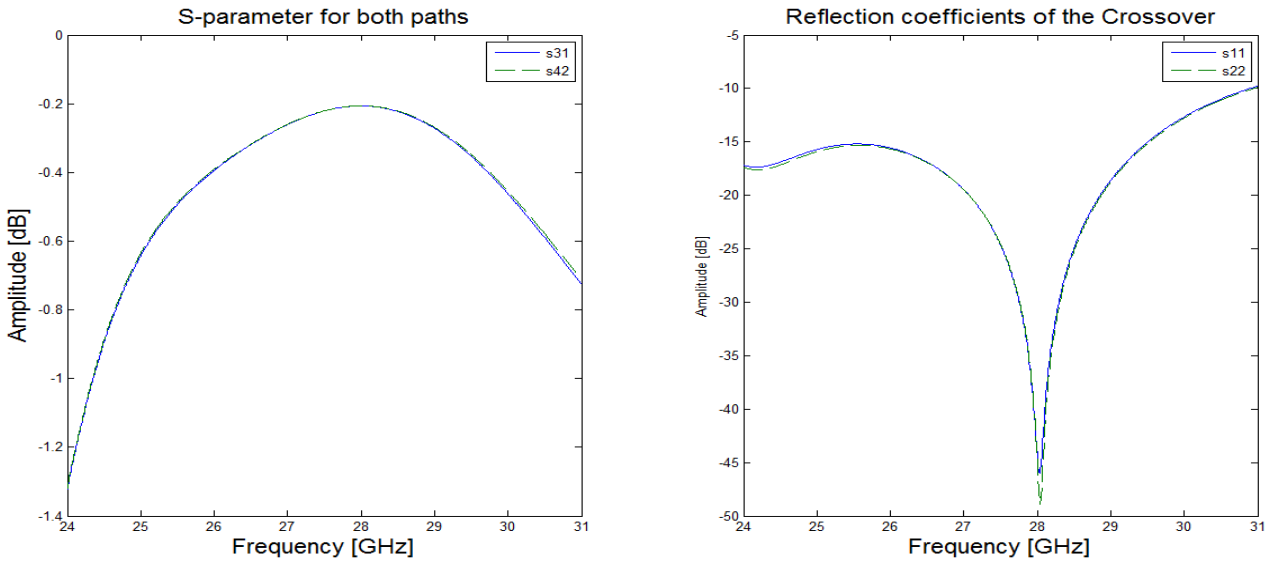

Figure 83 S-parameter of the redesigned Crossover

New Butler layout is shown in Figure 84 where the overall dimensions are 19 by 35 mm^2. With this design, the reflection coefficients for all ports are lowered below -20dB as illustrated in Figure 85. Fixing the reflection coefficients happened with an expense; output amplitudes are not close to each other as in stage II, but to the limit that it will not damage the performance of the final integrated system. Each pad near the ports is connected to the bottom ground plane by five 0.1mm-diameter vias.

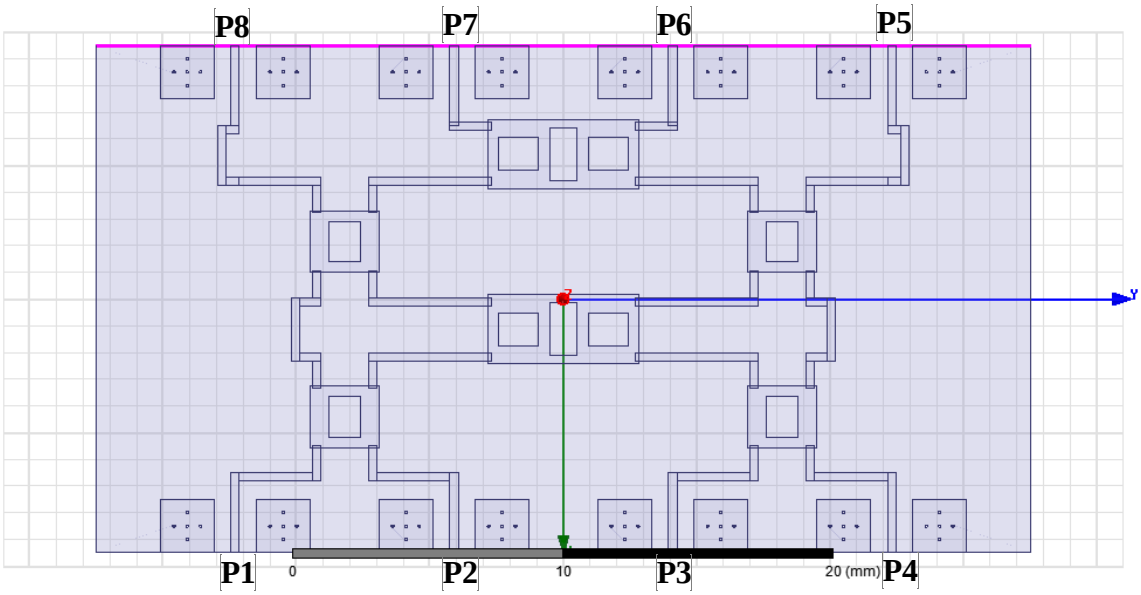

Figure 84 Layout of Butler-Stage III

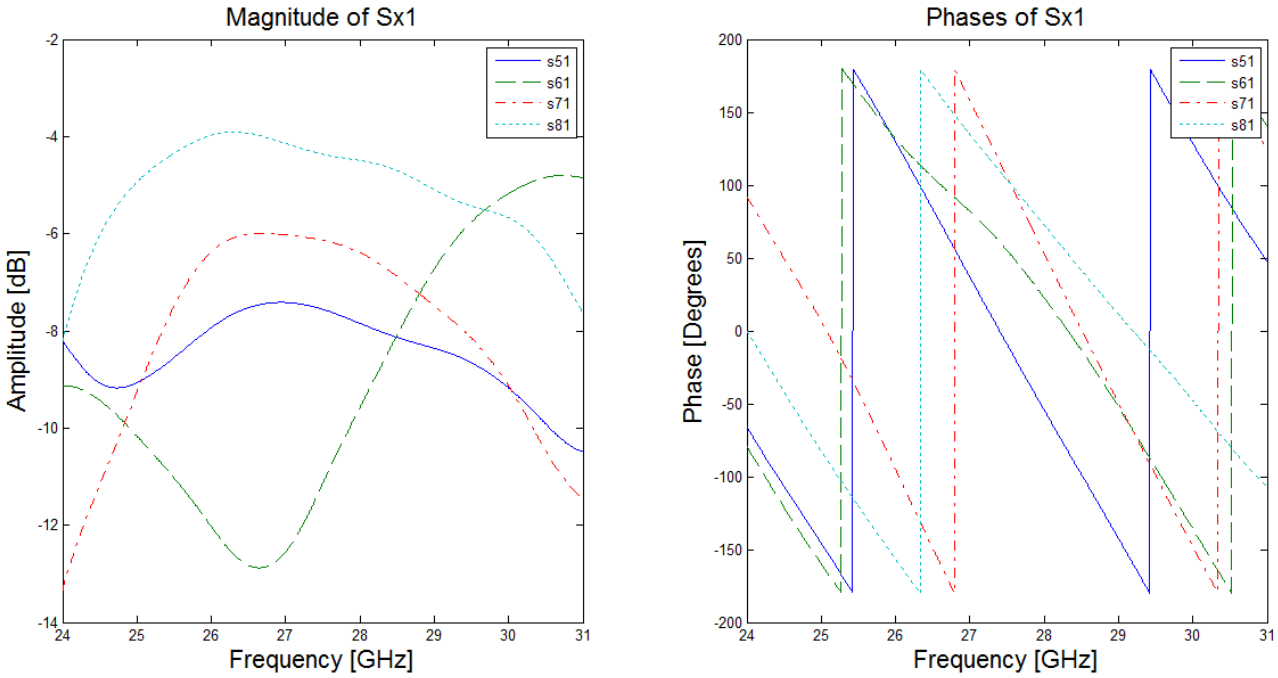

Figure 85 Butler Output responses when port 1 is excited

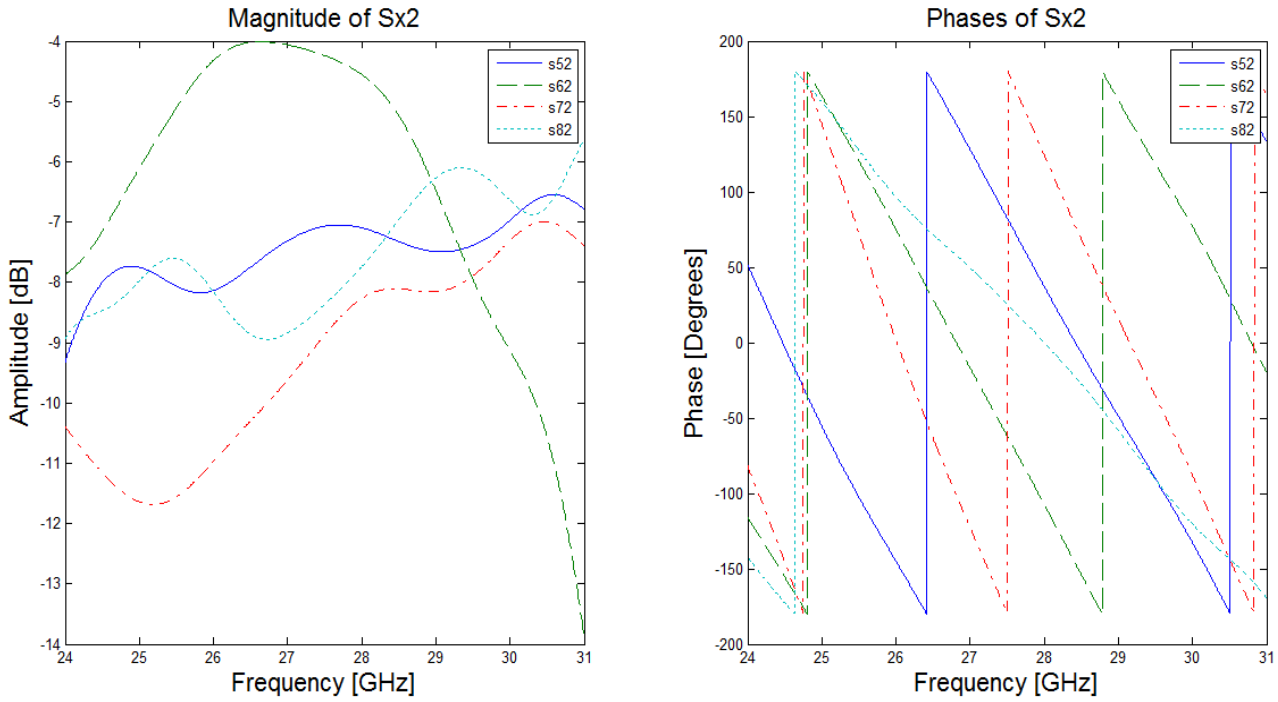

Figure 86 Butler Output responses when port 2 is excited

The equal power split is no longer available with the current system. When any port is excited, the system will end up having a variation up to 6 dB difference between the output ports, at the cost of having better reflection coefficients. When port 1 is excited, -4.2 dB is detected at port 8 while on the other hand -10 dB is received at port 6. Port 5 will receive -8.1 dB while port 7 will get -6.3 dB. When port 2 is excited, the variation at the output is 5 dB, 1 dB better than port 1. It must be noted that it is important to have equal power split between the outputs but it is not as important as having the right phase difference between adjacent ports. When port 1 is excited, the phase difference between ports 5 and 6 is 46.8 degrees. It is 46.4 degrees between ports 6 and 7, and 26 degrees between ports 7 and 8. It can be stated that we are having an average phase error of 9.76 degrees when port 1 is excited. The average errors are 19.77, 19.57 and 9.66 degrees for ports 2, 3 and 4, respectively.

In Figure 87, the reflection coefficients of the current Butler are shown, where S11 and S44 are resonating at 28.8 GHz and S22 and S33 are resonating at 28.2GHz. But all of them are having values less than -20 dB at 28.5GHz. Another factor forced us to redesign Butler network is the step where it will be connected to an antenna array radiating at 28.5 GHz. So, it is desired to have both systems; Butler and the antenna to resonate at the same frequency.

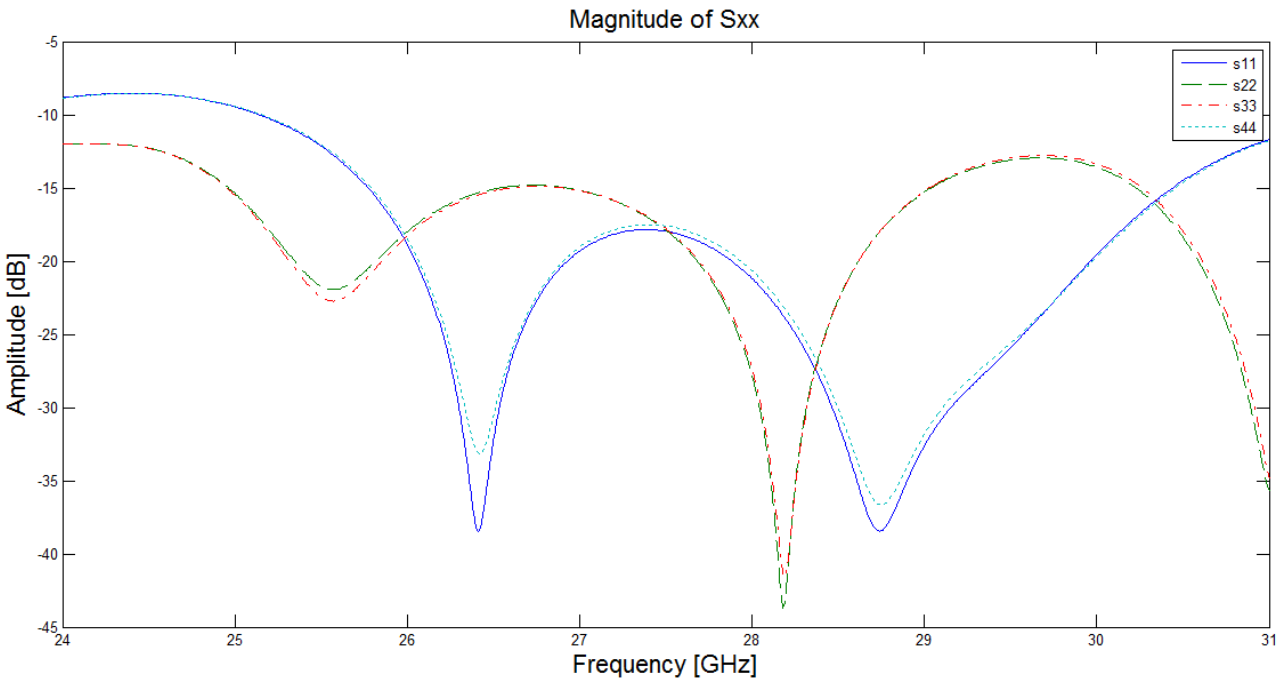

Figure 87 Reflection Coefficients of Butler-Stage III

4.4 Conclusions

In this chapter, a Butler feed network was designed from its basic components. Starting by the Hybrid coupler, the Crossover and ending with the complete structure for Butler Network. The design procedure passed through many stages, out of which the most important three ones were shown. Simulation results were shown for each stage and it had been concluded to go on with Stage III design for our final integrated system. The Butler network based on stage III occupied a volume of 35 x 19 x 0.13 mm^3. The BW of the system was almost 1 GHz from 28 to 29 GHz which was determined by the phase response. When port 1 is excited, the phase difference between port 5 and 6 is 46.85 degrees; introducing an error of 1.85 degrees. The errors between the other adjacent two ports are 1.43 and 26 degrees; introducing an average error of 9.76 degrees. The average errors when port 2, 3 or 4 is excited are 19.77, 19.57 and 9.66 degrees, respectively.

CHAPTER 5

COMPLETE MM-WAVE FEED NETWORK AND

ANTENNA ARRAY SYSTEM

After designing Butler network, we still need two more sub-systems to complete the proposed system in Figure 2. The two sub-systems are the 4x4 antenna array and the power-splitter/combiner needed to connect Butler to the antenna array. In this section, single element patch and slot antennas will be designed and simulated first. Then a linear 1x4 antenna array will be designed to check the performance of Butler Network before going to the full scale of having a 4x4 antenna array integrated with Butler feed network.

5.1 Single Element Antennas at mm-wave

A single patch and a single slot will be designed in this step. This part will help to choose which antenna type to go on with. Different parameters will be considered when comparing the two types, i.e. bandwidth, directivity, reflection coefficient, size, and geometry.

5.1.1 Single element patch antenna at mm-wave

The structure of the patch antenna has been explained in section 2.4.2. The dimensions of our patch antenna were found to be 2.98 by 3.65 mm^2 when operating with a center frequency of 28.5 GHz. The edge feeding point has been shifted inside the patch by an inset of 1.1mm to match the impedance of the transmission line to the 50 ohm point of the patch. The layout of the single patch antenna is shown in Figure 88 (a). The reflection coefficient achieved was -31.8 dB at 28.5GHz, with a bandwidth of 300 MHz and a Gain of 7.8 dB as illustrated in Figure 88 (b) and Figure 89.

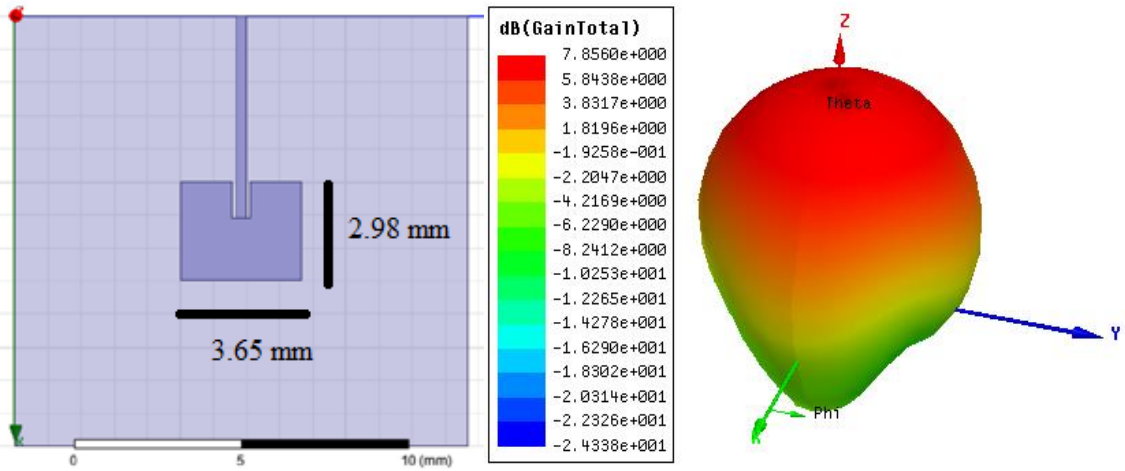

Figure 88 Layout of a single patch antenna and its radiation

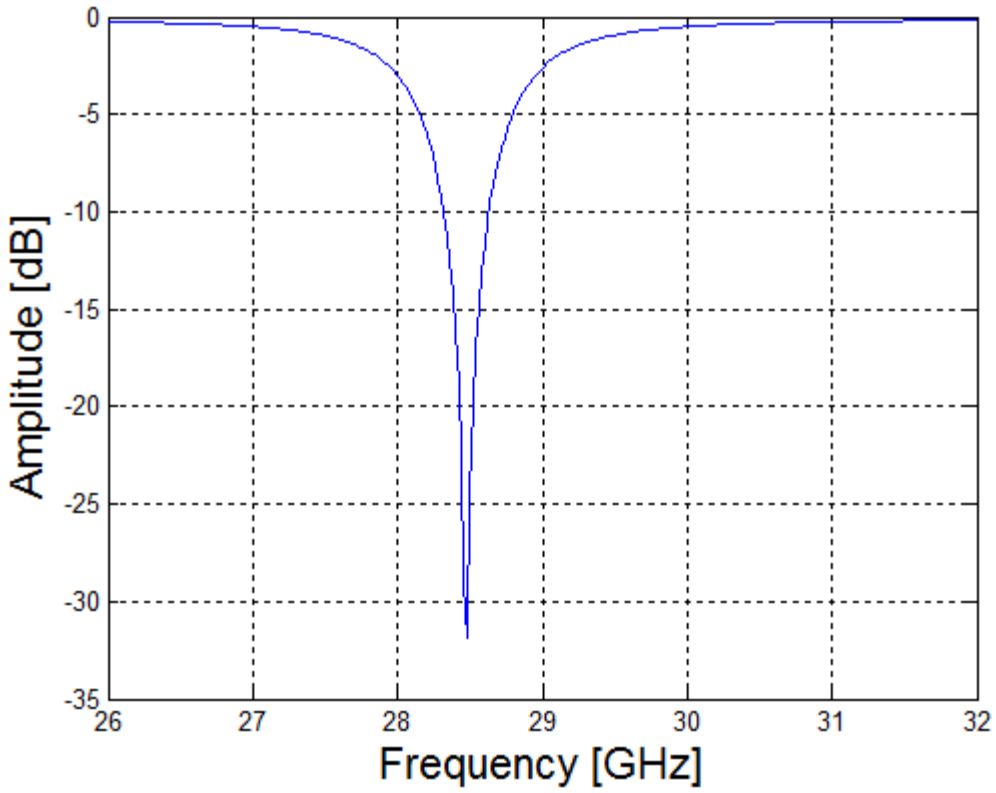

Figure 89 Reflection Coefficient of a single patch antenna

5.1.2 Single element slot antenna at mm-wave

Having an effective wavelength of 6.73 mm, the slot length is theoretically half-wavelength; 3.34mm. But after tuning the slot size in HFSS to have higher gain and resonance frequency closer to 28.5 GHz, the slot actual length was

3.75mm. The slot will cover an area of 3.75x0.5 mm^2 on the ground plane. It will be fed by aperture coupling from a transmission line very close to one edge of the slot. The reflection coefficient attained was -26.4dB at 28.5 GHz. Another big advantage offered by the slot antenna beside its geometrical structure, is the very wide BW. Our design will offer a bandwidth of almost 4 GHz from 27 to 31 GHz. On the other hand, gain is barely 3 dB and the pattern has front and back radiation instead of one when it is compared to patch antenna. Layout, radiation pattern and reflection coefficient are shown in Figure 90 and Figure 91 respectively.

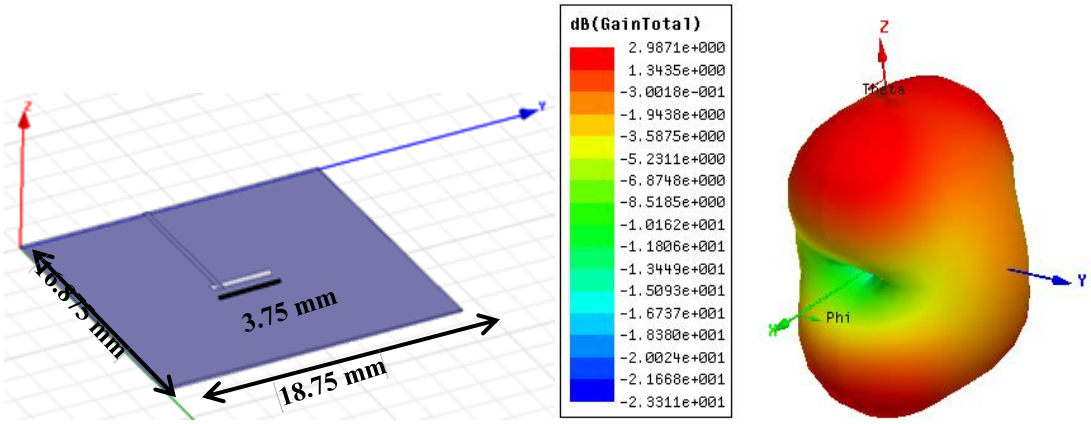

Figure 90 (a) Layout and (b) radiation pattern of a single slot antenna

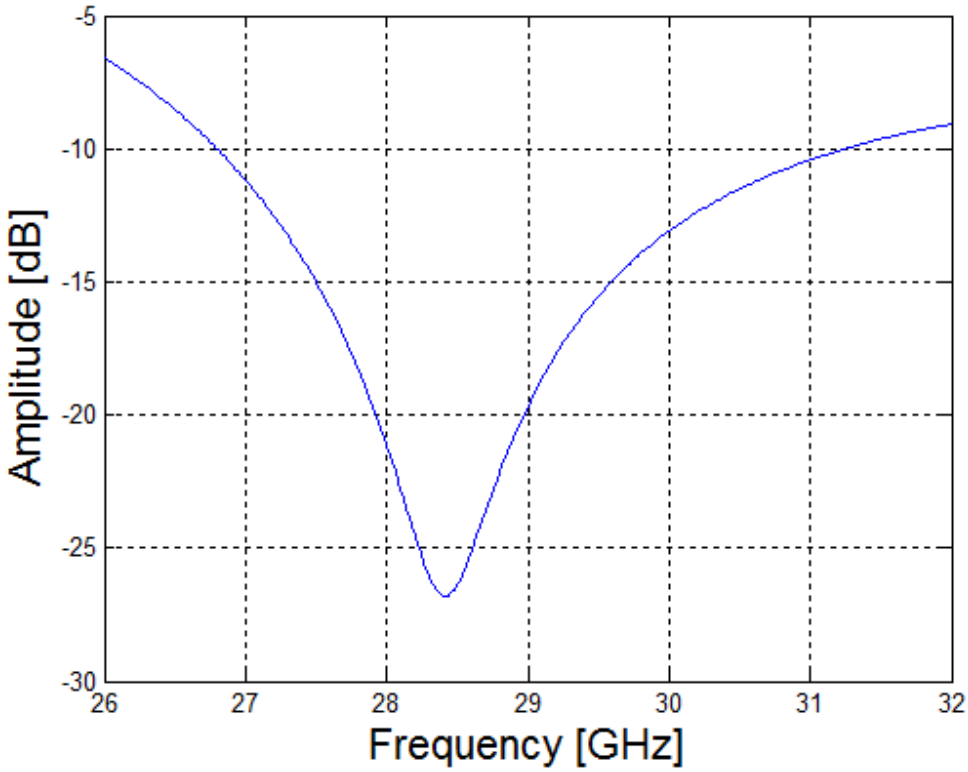

Figure 91 Reflection Coefficient of a single slot antenna

5.2 Linear Antenna Array (1x4) at mm-wave

When designing the single element antenna, size had been taken into account in order to be able to place several elements next to each other. The Butler network integrated with these upcoming linear 1x4 antenna arrays is based on stage II design, where the problem of reflection coefficient has not been stated yet in the measurements.

For the linear patch antenna, the spacing between the output ports had been changed to 5mm to accommodate having the patches next to each other with small gaps in between. The layout of the integrated system is in Figure 92. The dimensions used for the substrate are 30 x 34 mm^2. Radiation patterns are shown when ports 1 and 2 are excited in Figure 93 and when ports 3 and 4 are excited in Figure 94.

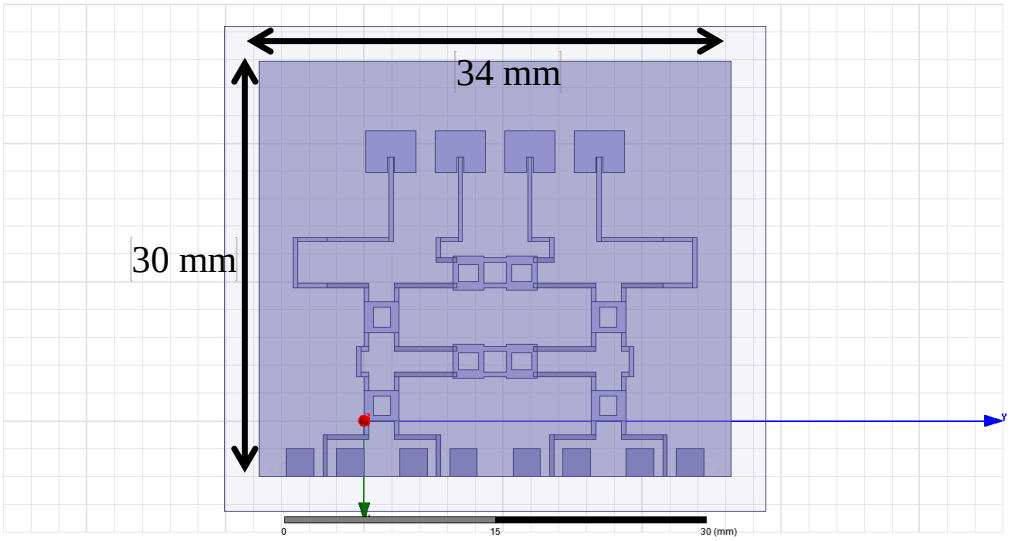

Figure 92 Layout of Butler + Linear patch antenna array

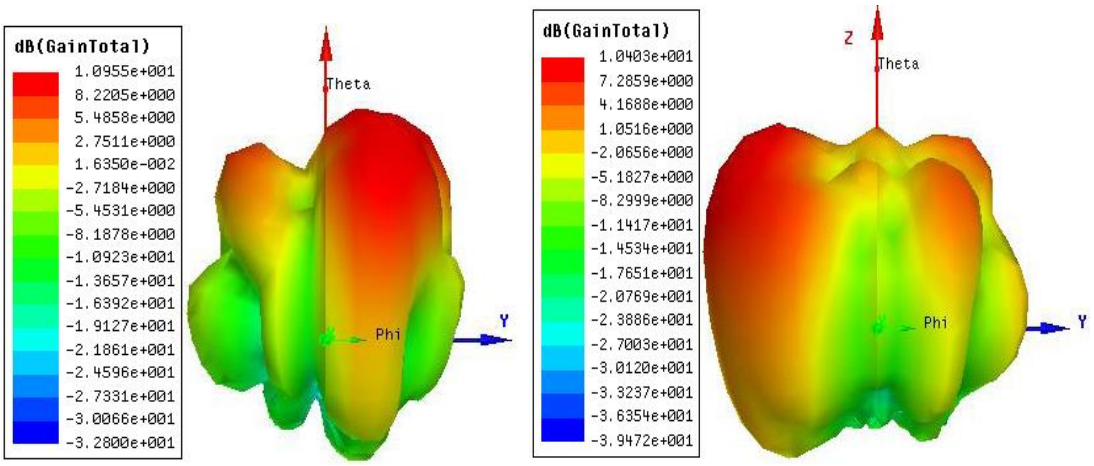

Figure 93 Radiation patterns when port (a) 1 (b) 2 is excited for Butler+Linear patch array

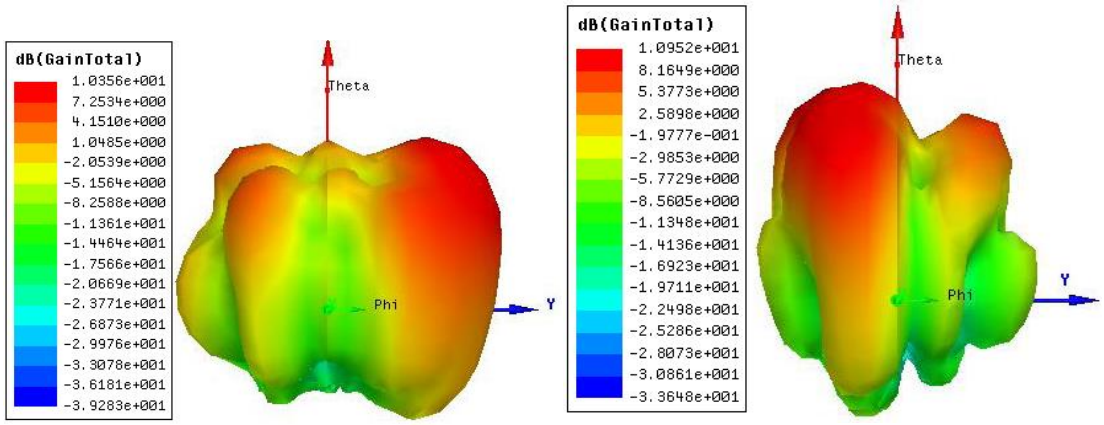

Figure 94 Radiation patterns when port (a) 3 (b) 4 is excited for Butler+Linear patch array

The gain obtained from a linear 1x4 patch antenna array was 10 dB for all cases. Although side lobes exist in undesired locations, it still can be observed that the maximum of the pattern is steering depending on which input is excited.

The spacing between the output ports for the linear slot antenna array has been set to three quarters of a wavelength, which is almost 5.6mm after tuning. The layout is shown in Figure 95. Figure 96 and Figure 97 show the obtained gain patterns for the excitation of various ports. The dimension of the system is 33.76 x 35.63 mm^2. A gain of 8.3 dB is achieved when ports 1 or 4 is excited. While the gain drops to 6 dB for port 3 and to 5.3 dB for port 2. Moreover, the problem of side lobes still exists in undesired locations. However, the peak of the beam is rotating according to which input is excited. So, Butler is behaving acceptably for both types of linear arrays.

Next, the feed network feeding the antenna elements will be discussed.

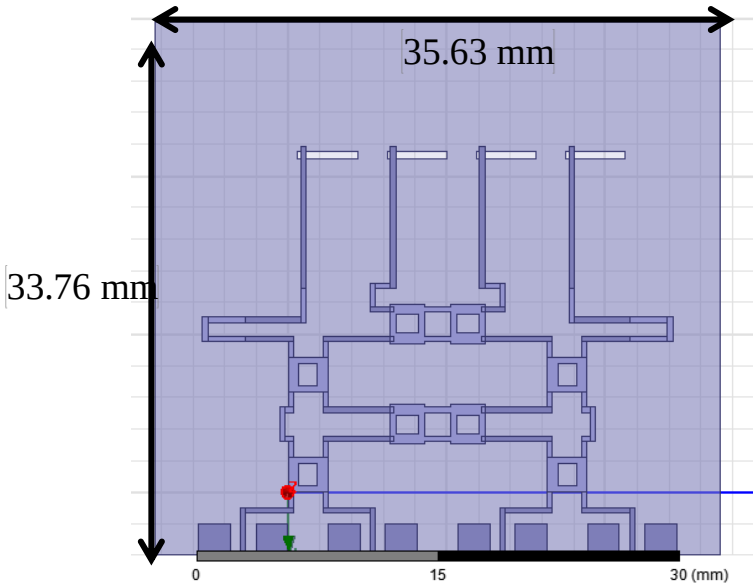

Figure 95 Layout of Butler + Linear Slot antenna array

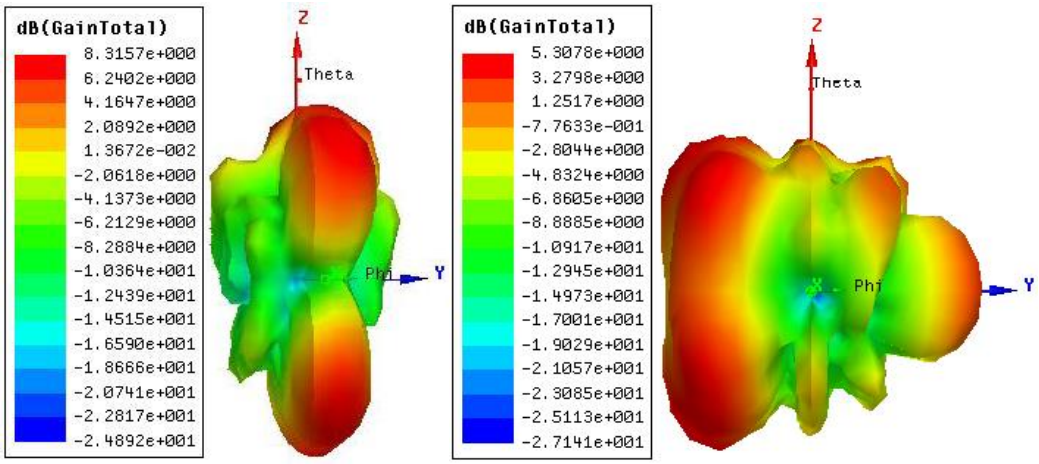

Figure 96 Radiation patterns when port (a) 1 (b) 2 is excited for Butler+Linear slot array

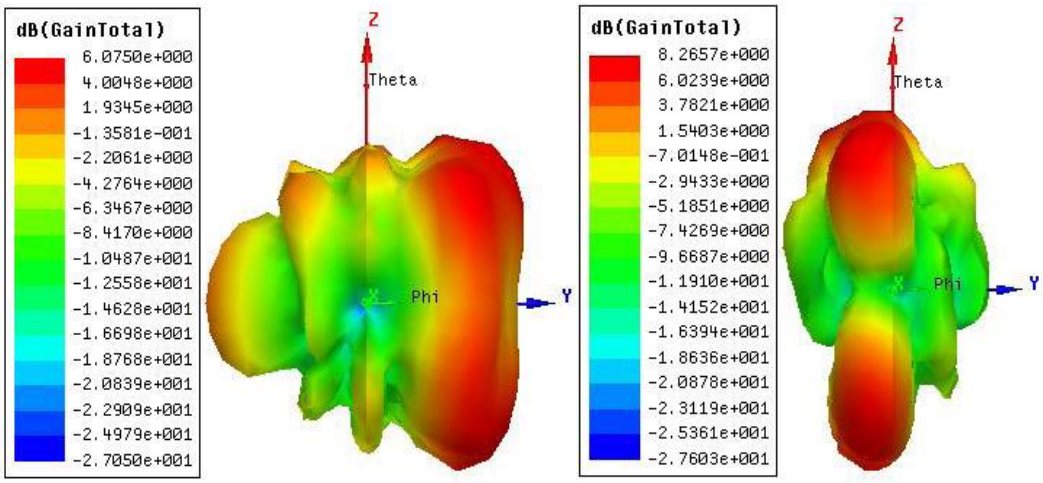

Figure 97 Radiation patterns when port (a) 3 (b) 4 is excited for Butler+Linear slot array

5.3 Power Splitter/Combiner

Feeding a linear antenna array of 4 elements was an easy task; it was implemented previously without the need to explain it. Now, before going to design a 4x4 antenna, we need to know how to feed them. The feed network should deliver equal power and should not introduce phase difference between adjacent antenna elements in order to keep the scheme of patterns produced by Butler as it is.

There are two general types of feeding networks; series feed and corporate feed networks as illustrated by Figure 98. The advantages of using corporate feed network are the equal power split received at each antenna element, as well as the phase of the signal. On the other hand, using corporate network will consume a lot of space. Moreover, quarter-wavelength impedance transformer must be used to ensure matching the microstrip lines with the antenna elements as can be noticed from Figure 99. It can be done using tapered lines instead.

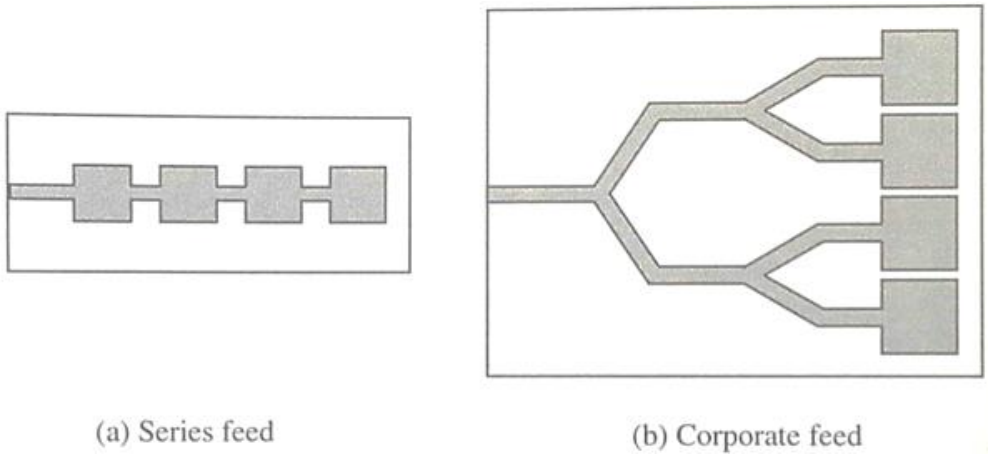

Figure 98 Types of feeding systems [6]

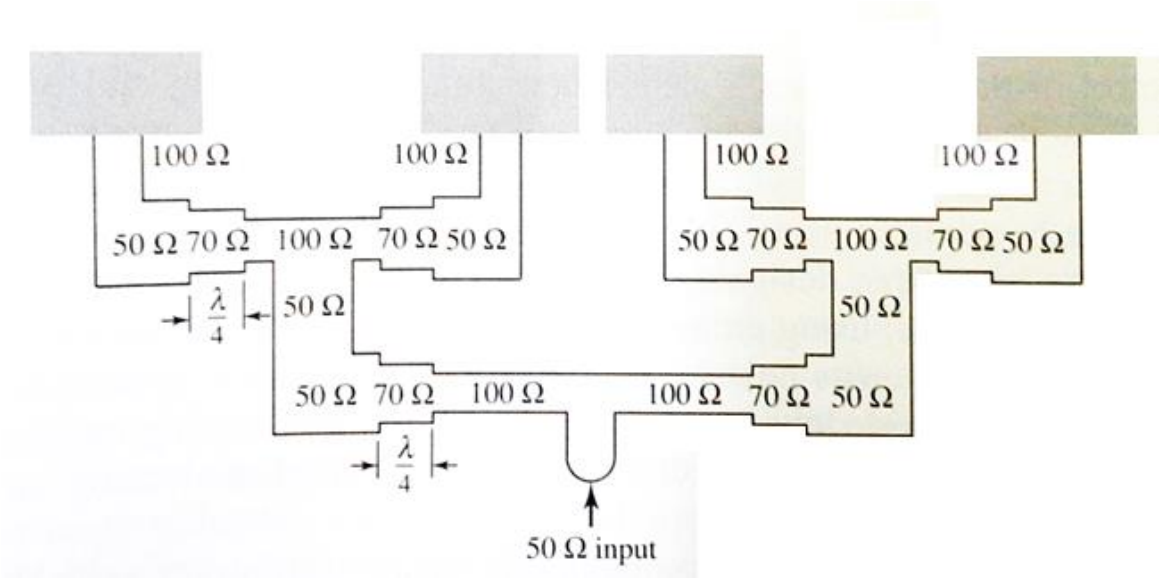

Figure 99 Lambda/4 transformers needed for corporate network [6]

In terms of space, series feed networks consume the least. But they do not guarantee equal power delivery between the elements. The same can be said about the phase since it will produce some progressive phase shift with each antenna element it feeds, since there will be some distance of microstrip lines between the elements. Even though it is not like the corporate feed network in delivering equal phases, the important requirement for the beams to be steered is to have the phase difference between adjacent elements, not the phase value. So, let's say that we used series feed lines connected to the output ports of our Butler. The phase difference between the first element on the line fed by port 5 and the first element on the line fed by port 6 will be 45 degrees (for example). As long as we keep the inter-element spacing fixed for all lines, the phase difference between the second element on the line fed by port 5 and the second

element on the line fed by port 6 is still 45 degrees, since the signals in both of them have experienced the same progressive phase shift. Thus, even though the amplitudes are not equal, the phase differences will provide the required beam steering (this has been investigated).

5.4 Planar 4x4 Antenna Array

On one hand, the patch antenna, when compared to slot antenna, has better reflection coefficient and higher gain, thus, higher directivity. On the other hand, it consumes more space and has much narrower bandwidth. Regarding the slot antenna, the problem of low gain can be diminished since we will use a 4x4 antenna array that will increase the gain. Thus, due to bandwidth, size and solved gain-issue, the slot antenna has been chosen to be used in our integrated system.

Also, due to the space saved when using the series feed network, it has been preferred over the corporate feed network. The duty in designing the series feed is to optimize the inter-element spacing between the elements such that it will reduce the power reflected. The layout of the designed 4x4 slot array is displayed in Figure 100.

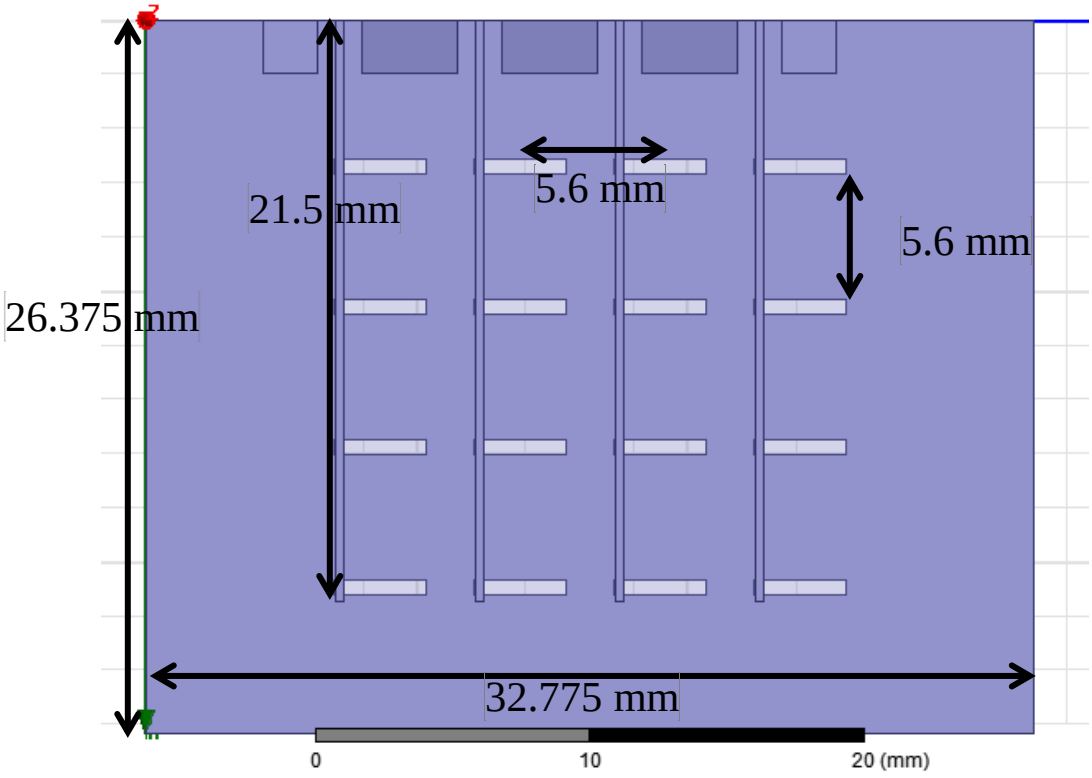

Figure 100 Layout of 4x4 slot antenna array

The inter-element spacing is the same of the Linear 1x4 slot antenna array; 5.6 mm after tuning. After building this array, its radiation patterns will be analyzed after feeding the ports with an ideal Butler output. So, to mimic the outputs of Butler when its first port is excited, equal power will be distributed between the ports. Also, a phase difference of 45 degrees will be forced between them. Then the 3D pattern of the radiation will be plotted. The same procedure applies when mimicking port 2 as illustrated in Figure 101. Port 3 will be identical to port 2 and port 4 is similar to port 1. Of course, reflection coefficient was considered when designing the inter-element spacing and slot size. All feed lines have reflection coefficients lower than -17 dB centered at 28.5 GHz as shown in Figure 102. A BW of 1 GHz is clearly seen.

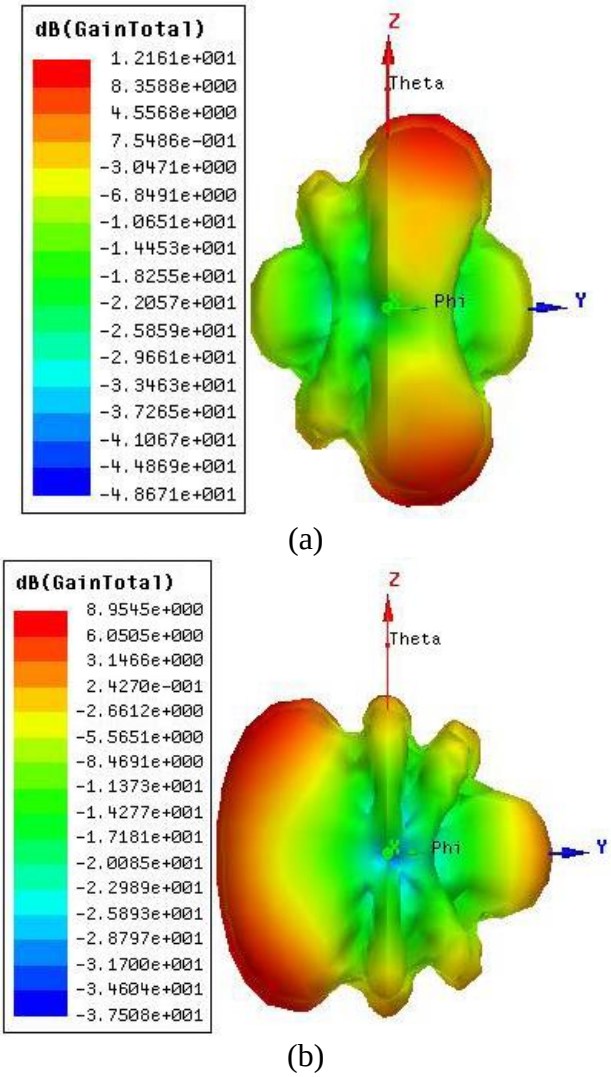

Figure 101 Radiation pattern when port (a) 1 (b) 2 is excited

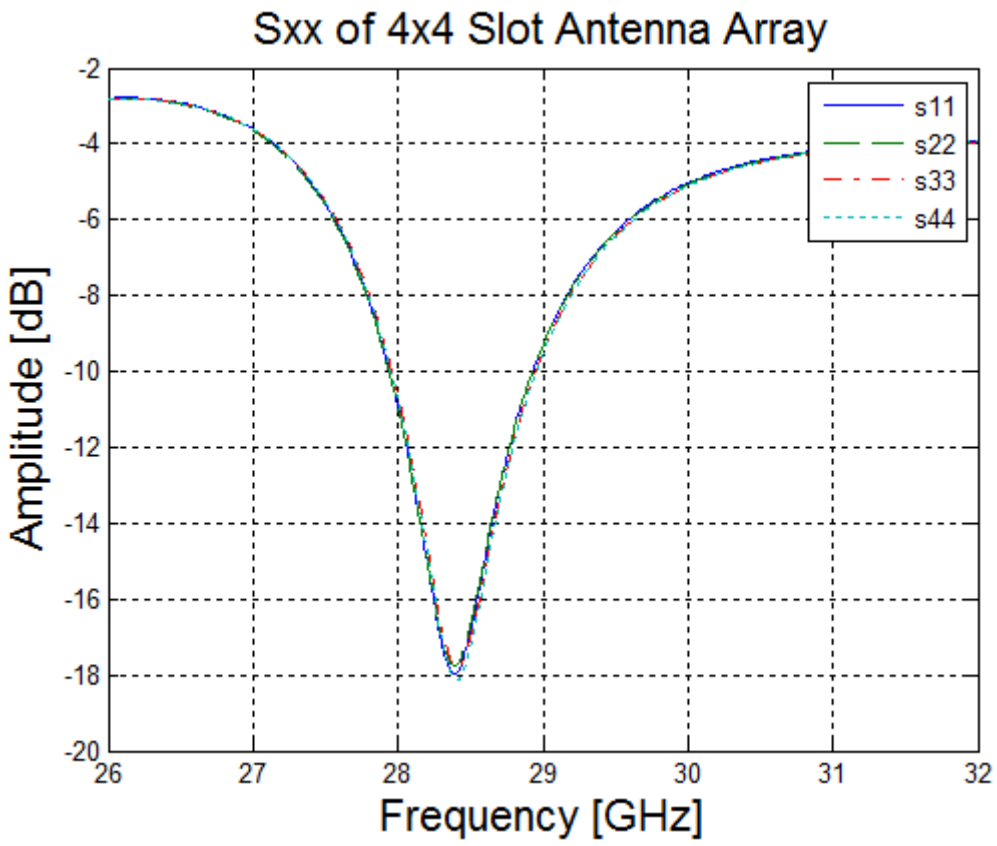

Figure 102 Reflection Coefficients of 4x4 slot antenna array

5.5 Complete integrated mm-wave System

The last part of this section is integrating the full 4x4 slot antenna array with the re-designed Butler as can be seen in Figure 103, where the overall dimensions were 43 x 35 mm^2. The system shows acceptable response and the beams are tilted depending on which input is selected.

When port 1 is excited, Table 3 shows the patterns of the integrated system for three different frequencies side by side with the pattern produced by the 4x4 slot antenna array fed by an ideal Butler output. It can be seen that the maximum gain obtained when the 4x4 slut antenna is fed with an ideal Butler output is 11.4 dB, while the gain obtained from the complete integrated system is 1 dB only less than the ideal case at 28.5 GHz. The system covers almost 1 GHz of bandwidth as can be seen in the table.

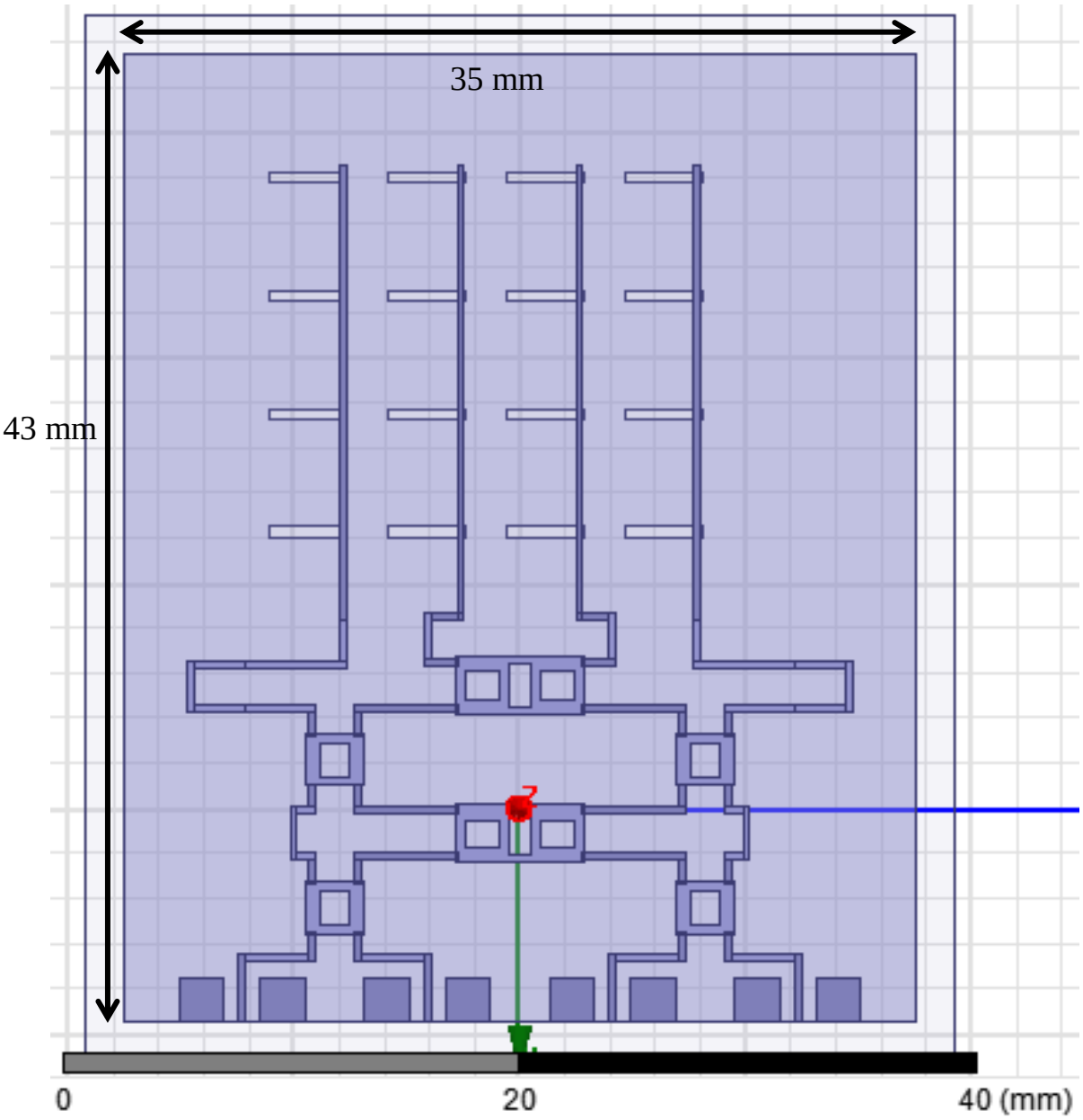

Figure 103 The complete integrated system

Table 4 shows the case when the second port of Butler is excited. There is a 0.5 dB difference between the ideal case and the complete system. The pattern of the system has a gain 8.5 dB. But it still suffers from high side lobes due to the phase errors and the non-equal power splits at Butler's outputs. Table 5 and Table 6 show the two cases when ports 3 and 4 are excited, respectively. At 28.5 GHz, the gain difference was 1.7 dB when port 3 is excited and 0.6 dB when port 4 is excited.

Table 3 Patterns of complete system VS slot array when port 1 of Butler network is excited

Port 1	4x4 Slot Antenna Array	Complete Integrated System
@ 28 GHz	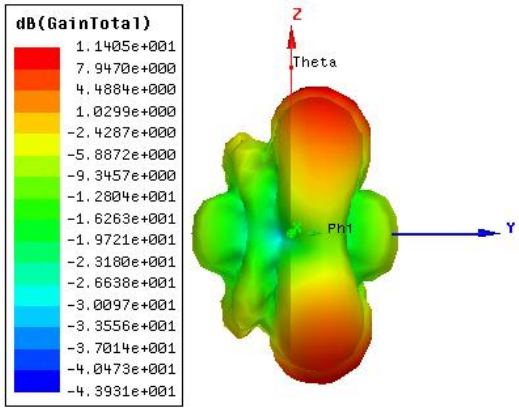	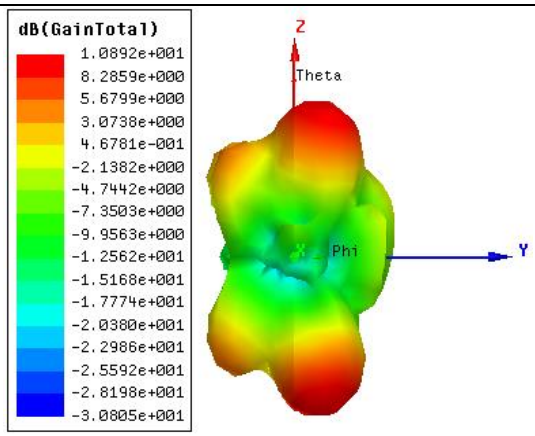
@ 28.5 GHz	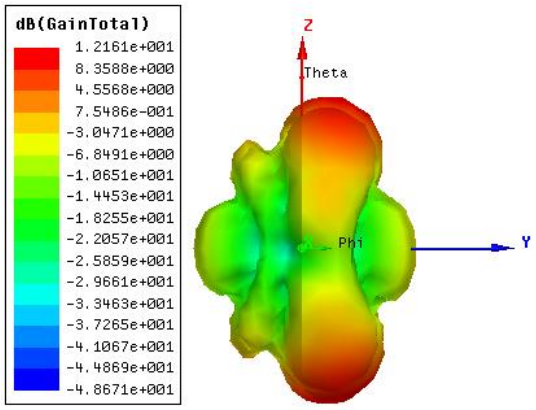	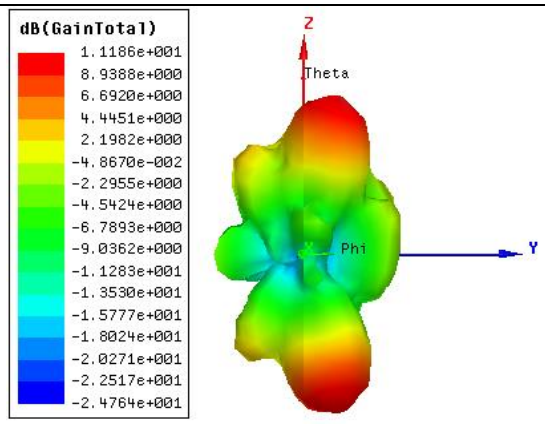
@ 29 GHz	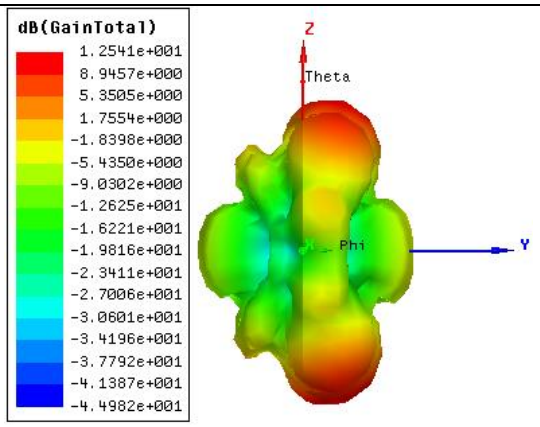	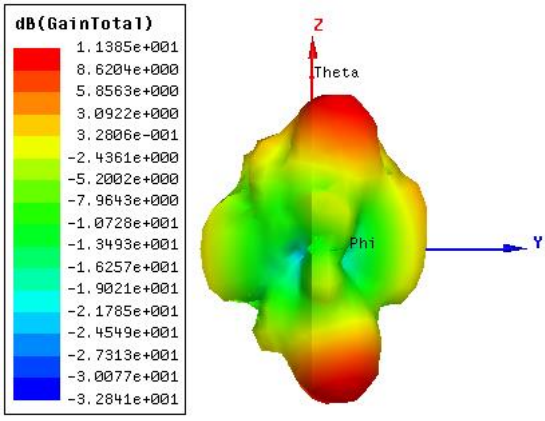

Table 4 Patterns of complete system VS slot array when port 2 of Butler network is excited

Port 2	4x4 Slot Antenna Array	Complete Integrated System
@ 28 GHz	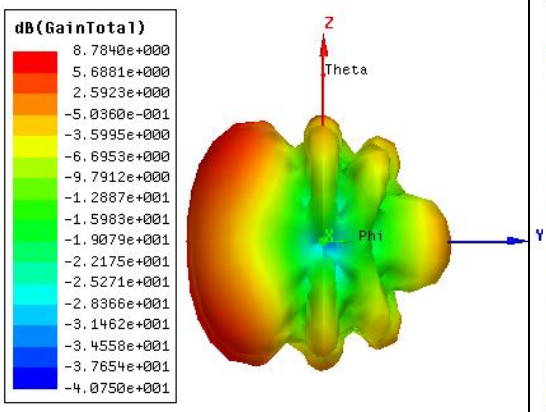	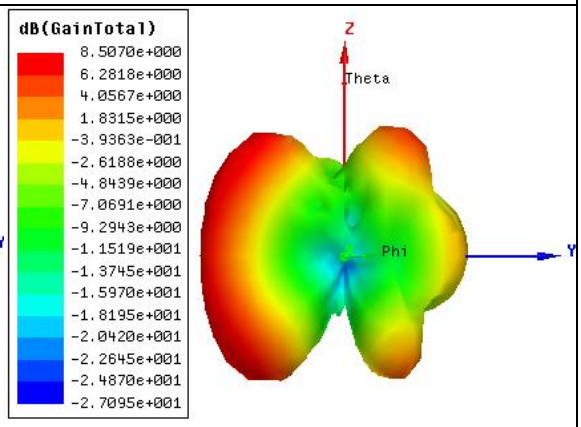
@ 28.5 GHz	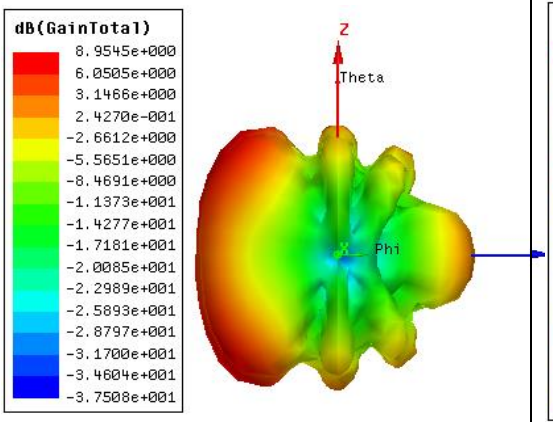	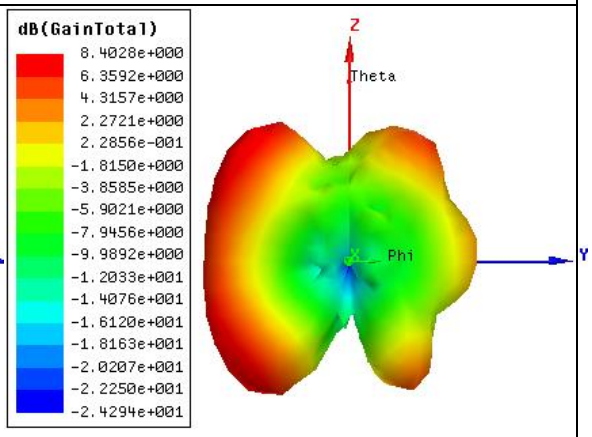
@ 29 GHz	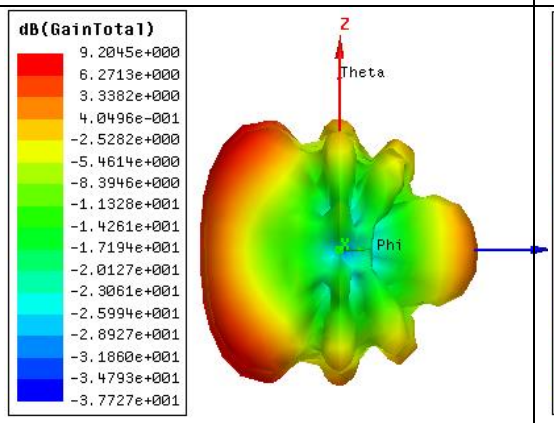	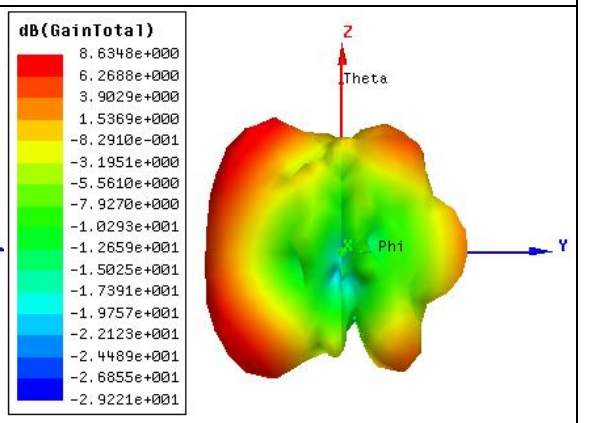

Table 5 Patterns of complete system VS slot array when port 3 of Butler network is excited

Port 3	4x4 Slot Antenna Array	Complete Integrated System
@ 28 GHz	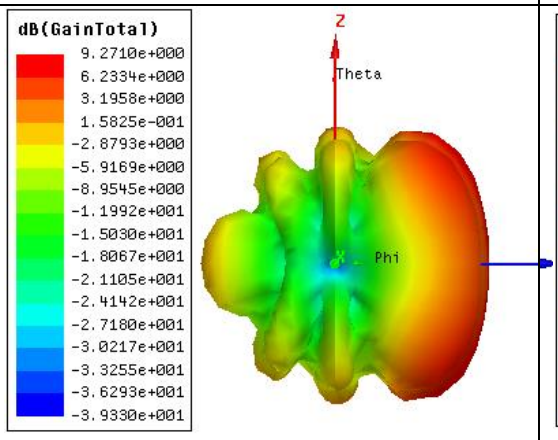	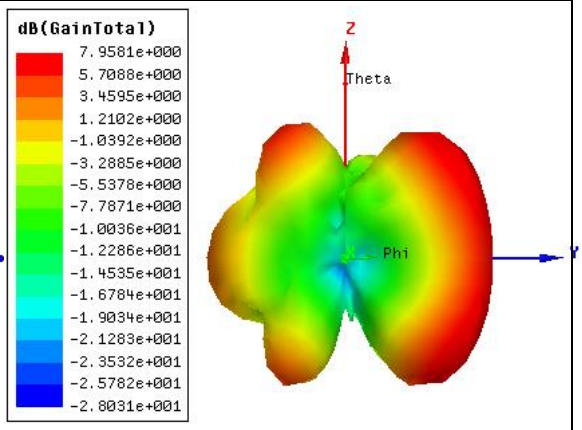
@ 28.5 GHz	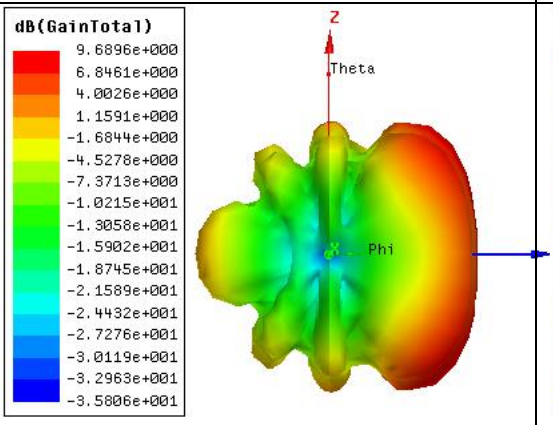	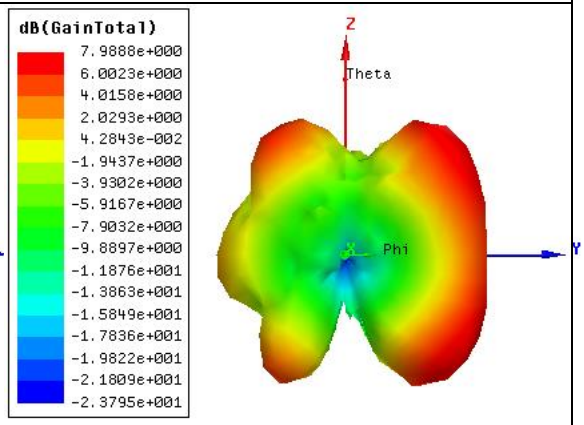
@ 29 GHz	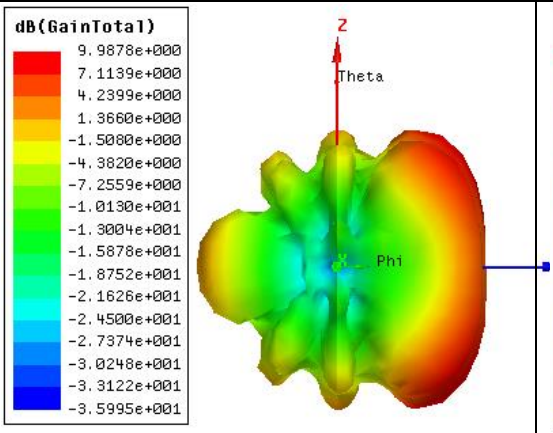	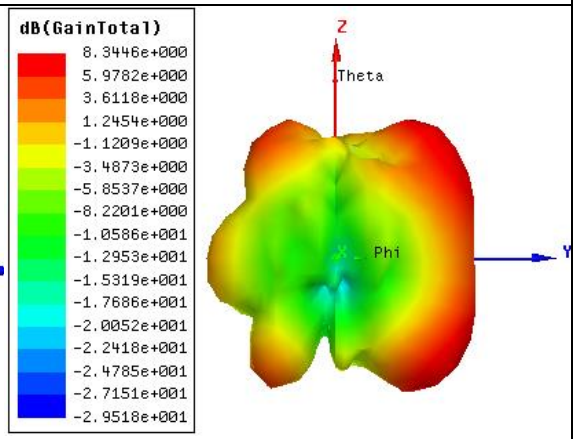

Table 6 Patterns of complete system VS slot array when port 4 of Butler network is excited

Port 4	4x4 Slot Antenna Array	Complete Integrated System
@ 28 GHz	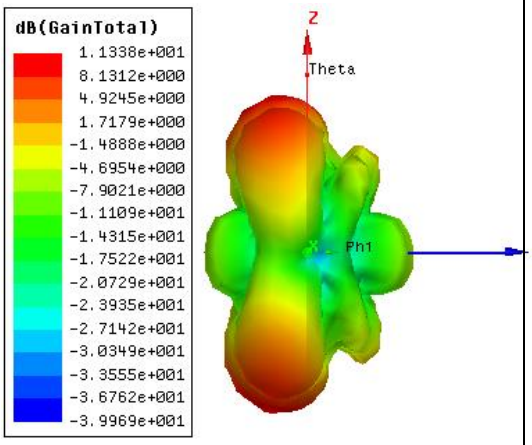	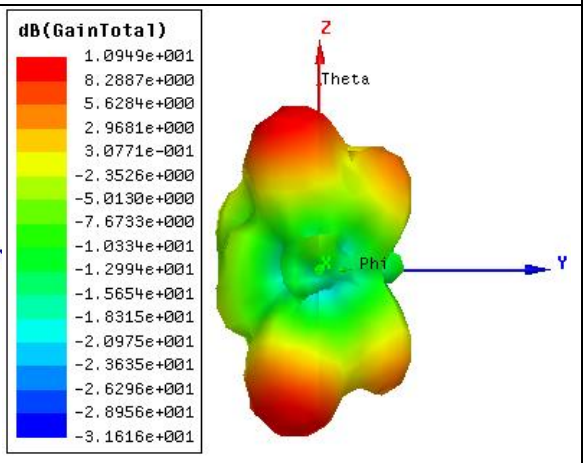
@ 28.5 GHz	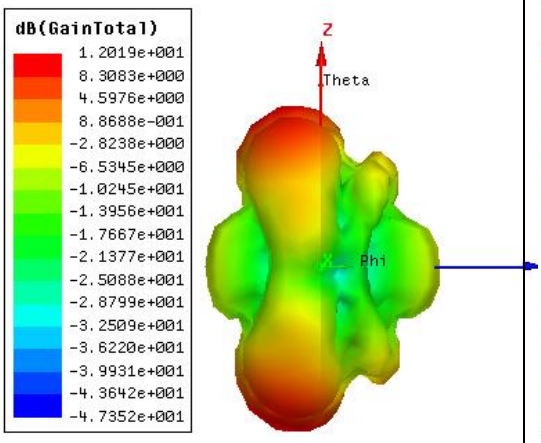	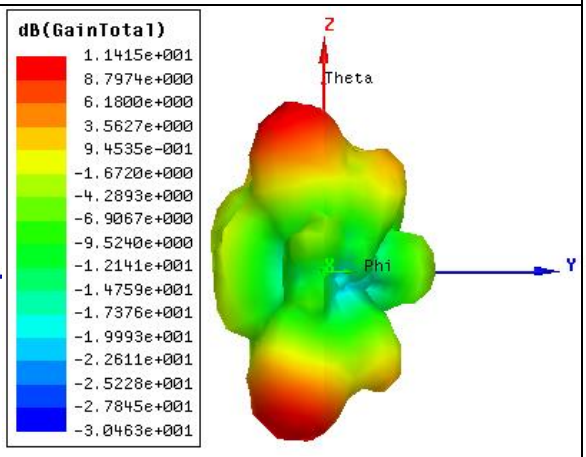
@ 29 GHz	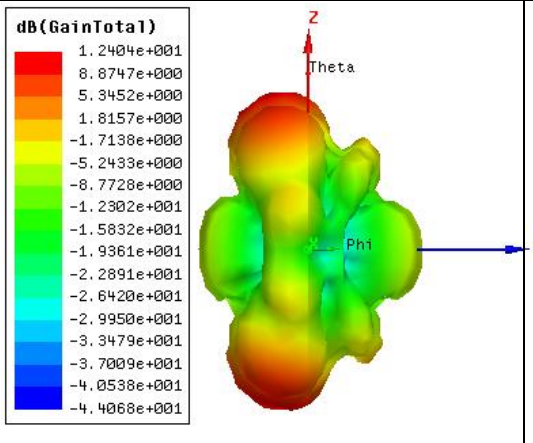	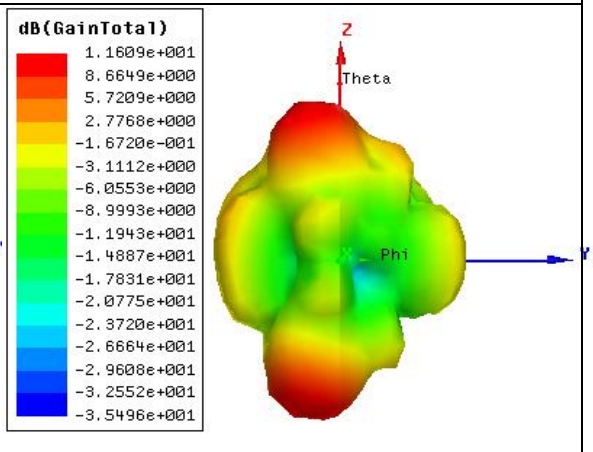

The 2D polar plots for the radiation patterns at 28.5 GHz are shown in Figure 104. Figure (a) shows the pattern when port 1 is excited and (b) is when port 2 is excited. The patterns for ports 3 and 4 are almost identical to ports 1 and 2 due to the system's symmetrical structure.

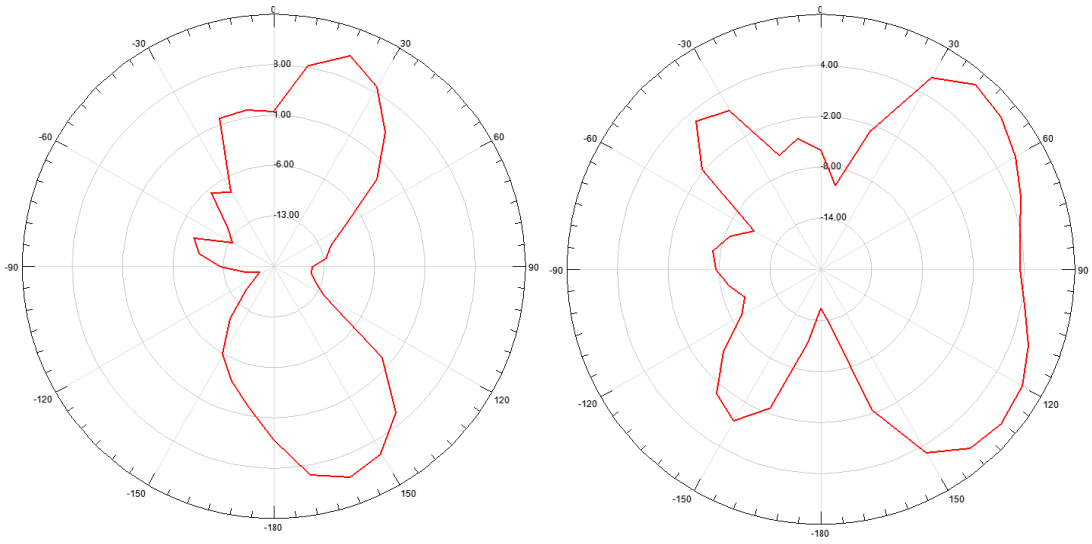

Figure 104 2D Polar plots for the radiation patterns when port (a) 1, (b) 2 is excited

5.6 Conclusions

In this chapter, the complete integrated system; consisting of the Butler feeding network, power splitter and the 4x4 slot antenna array, was designed and simulated. The concept of steering the beams have been confirmed and illustrated. The integrated system occupied a volume of 43 x 35 x 0.13 mm^3 of Roger 3003 substrate with dielectric constant of 3. The beams were steered to four locations, covering ±20˚ and ±45˚. The maximum gain obtained is 11.4 dB at 28.5GHz when port 4 is excited, while the minimum gain was 7.98 dB which happens when port 3 is excited. The integrated system has shown steady performance in simulation over 1 GHz of BW as illustrated by the tables.

CHAPTER 6

FABRICATION & MEASUREMENTS

In this chapter, we present the attempted fabrications and designs as well as the obtained measurements. The successful and unsuccessful measurements of the Butler network, antenna array and the integrated system are presented.

6.1 Butler - Stage I - Failed Attempts

Figure 105 will summarize all of the failed attempts to fabricate Butler network that was based on Stage I at the Antennas and Microwave Structure Design Laboratory (AMSDL) at the Electrical Engineering Department at KFUPM. We had to replace the etching tool with every attempt as the line width is only 0.3mm, and any used etching tool (even if it was used once) will etch out the complete copper on the PCB. One of the attempt almost succeeded but we failed to insert a via of the diameter as the holes in the pads.

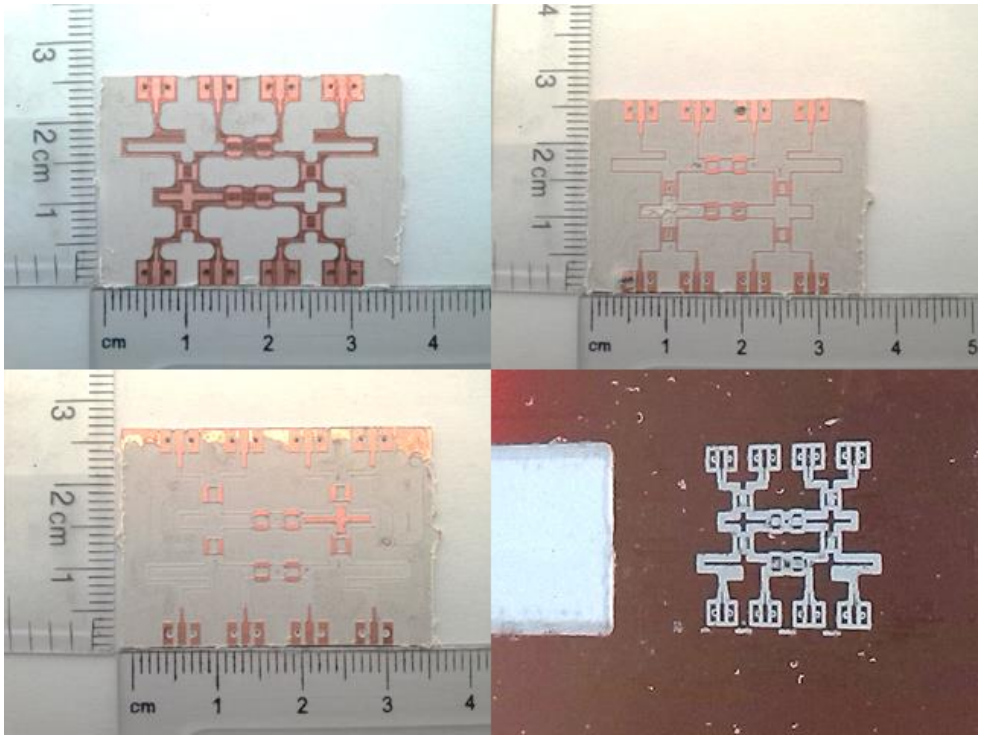

Figure 105 Butler PCB design based on Stage I

6.2 Butler - Stage II

After succeeding with getting results in simulation very close to the ideal case in Butler design stage II, we decided to manufacture the PCB in the UK. It is important to note that the thickness of this design is 0.13mm. If you stack up 2 A4 papers, their combined thickness is 0.1mm. The fabricated design with assembled ports is shown in Figure 106.

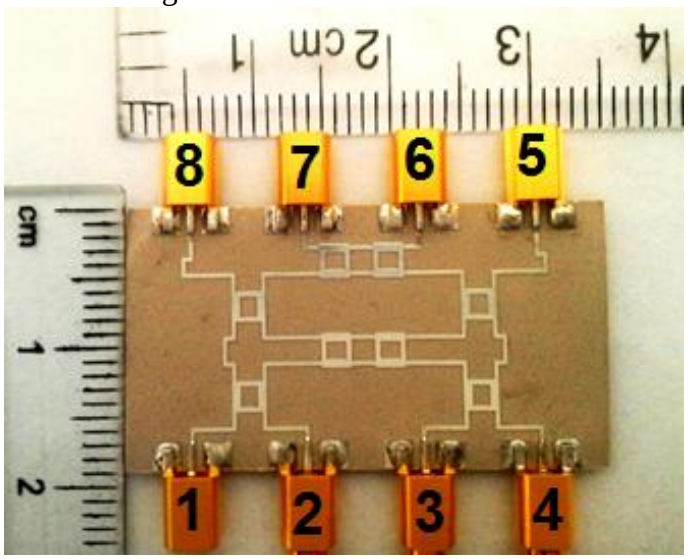

Figure 106 Fabricated Butler based on Stage II

Measuring S-parameter for this PCB was an extremely difficult task due to the fragile structure. A bend will be introduced by just holding it in the hand, it can be imagined the damage caused when trying to insert a 50 ohm SMP termination by pushing force. Unfortunately, the amplitude response was damaged and it was not close to the simulation values (Please check the appendix for this and other encountered challenges). Nevertheless, phase responses were measured and plotted in Figure 107. Compared with simulations, measured phase differences when port 1 is excited has experienced an average error of 17.75, which is 4.7 degrees far from the response acquired by simulation. While when port 2 is excited, the average error was 20 degrees, again 4.5 degrees away from the simulated response.

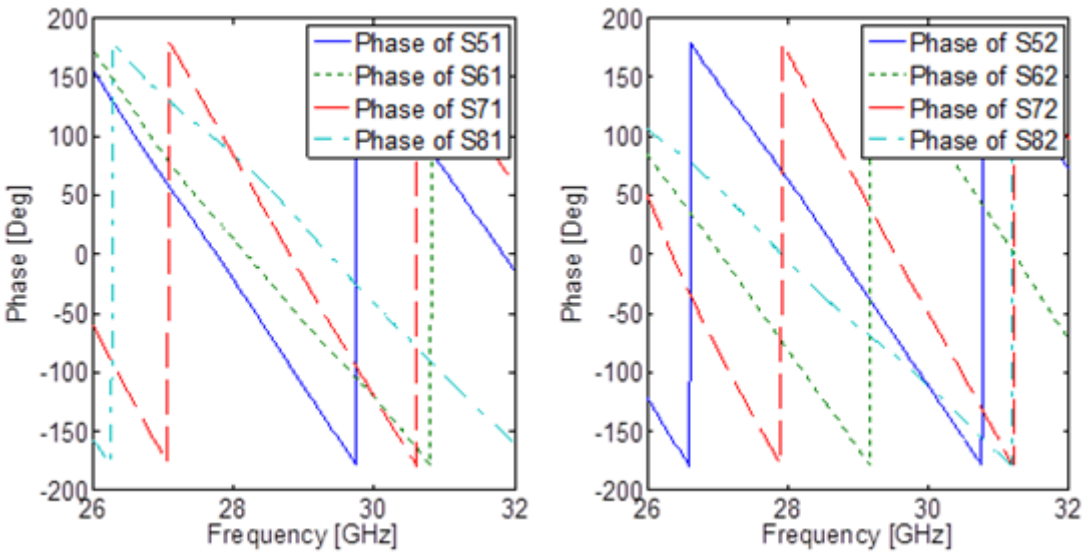

Figure 107 Phase response when port (a) 1 (b) 2 is excited

6.3 Butler Integrated with Linear Array

This attempt was made to fabricate the Butler network with a linear antenna array where the Butler acquired in the second stage was used. The fabrication process was also done in the UK and the boards were sent to the University of Michigan, Ann Arbor, USA, where Prof. Kamal Sarabandi conducted the measurements for us. This time, in order to avoid the issue of damaging the structure again, a metalized sheet was attached to the back side of the substrate as shown in Figure 108. Of course, this metalized sheet was not covering the slots and was placed a little less than 2 cm away from them.

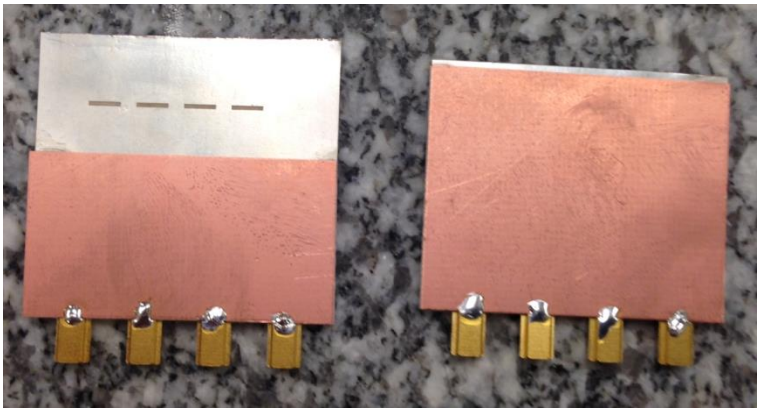

Figure 108 Metallic sheet attached to support the fragile substrate

Reflection coefficients were measured for both systems (see Figure 109). Unfortunately, both systems were having resonance at different frequencies. For the Butler integrated with linear patch array, ports 1 and 4 were resonating at 29.5 GHz while ports 2 and 3 were resonating at 29.2 GHz. All of them were resonating well at 32.5 GHz while they were -7dB at 28.5 GHz, as shown in Figure 110. That was the reason behind redesigning Butler and going into Stage 3 (as mentioned in section 4.3). We needed to redesign the Butler to ensure that all of Sxx are resonating closer to 28.5 GHz with accepted values. Figure 111shows the results for the integrated system with a linear slot antenna array. Ports 2 and 3 were -13 dB at 28 GHz while ports 1 and 4 were around -11 dB at 29 GHz. All ports were only -7 dB around 28.5 GHz.

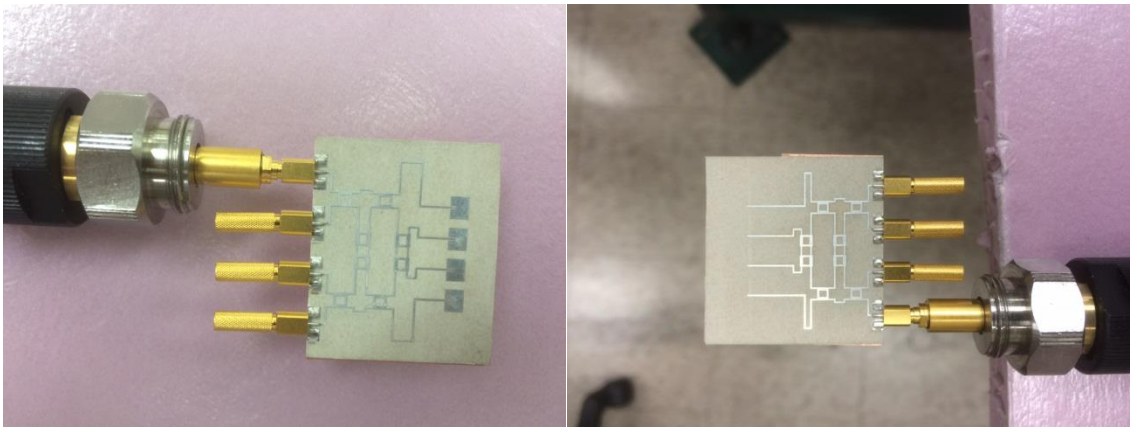

Figure 109 Exciting port 1 while others are terminted

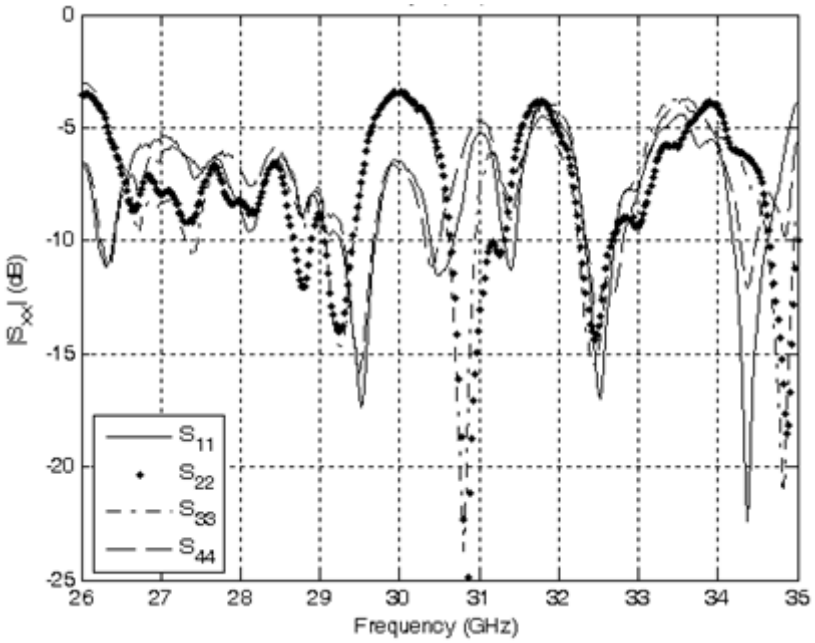

Figure 110 Measured reflection coefficients for Butler+Linear Patches when port 1 is excited

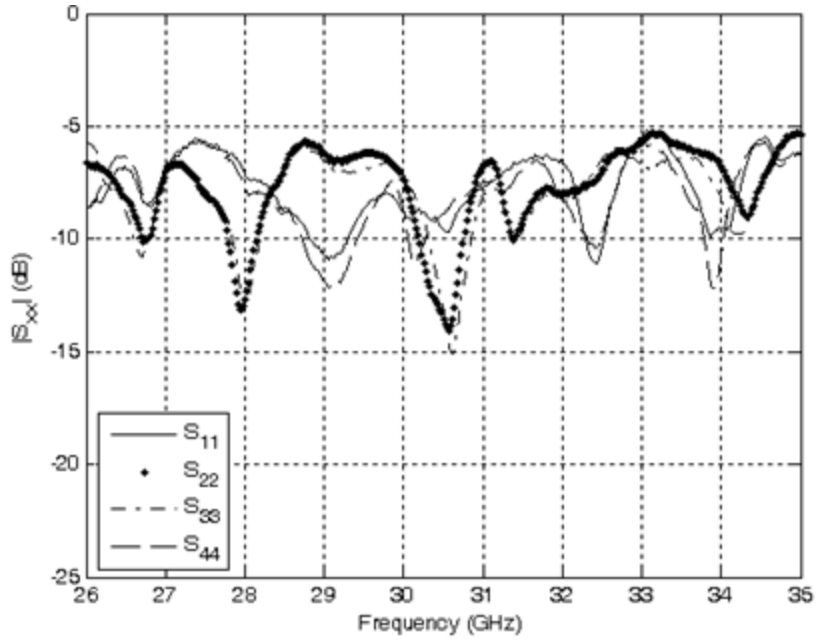

Figure 111 Measured reflection coefficients for Butler+Linear Slots when port 1 is excited

6.4 Butler – Stage III

Figure 112 shows the fabricated Butler network that was based on stage III. As shown in Figure 113, the reflection coefficients for the input ports are barely reaching the -10dB point. It must be noted that for all the coming measurements, the loss encountered in the wires as well as the adapters have not been included. Thus, BW would be slightly larger than the one shown in Figure 113. While the system is having better performance at 27 GHz with reflection coefficient of -14 dB and an input -10dB BW of 200 MHz.

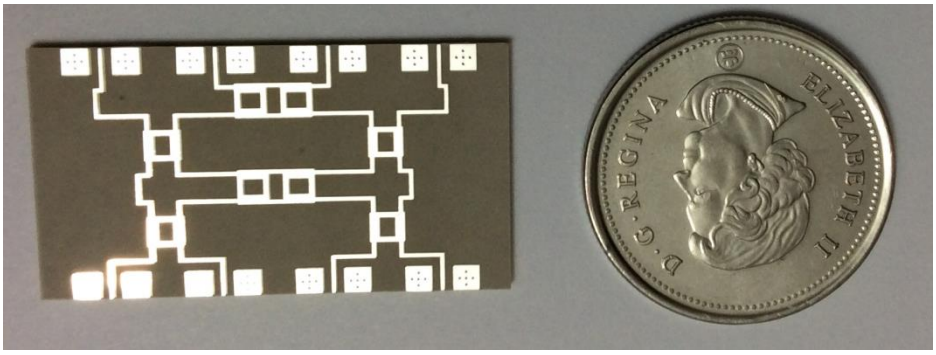

Figure 112 Fabricated Butler Network based on Stage III

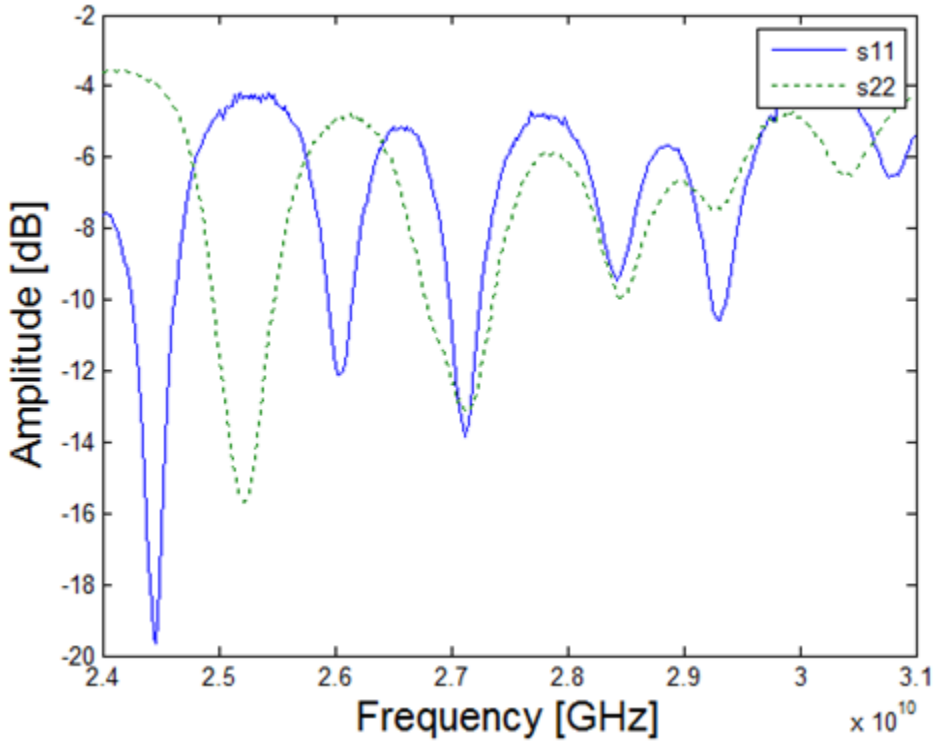

Figure 113 Measured input reflection coefficients of Butler-Stage III

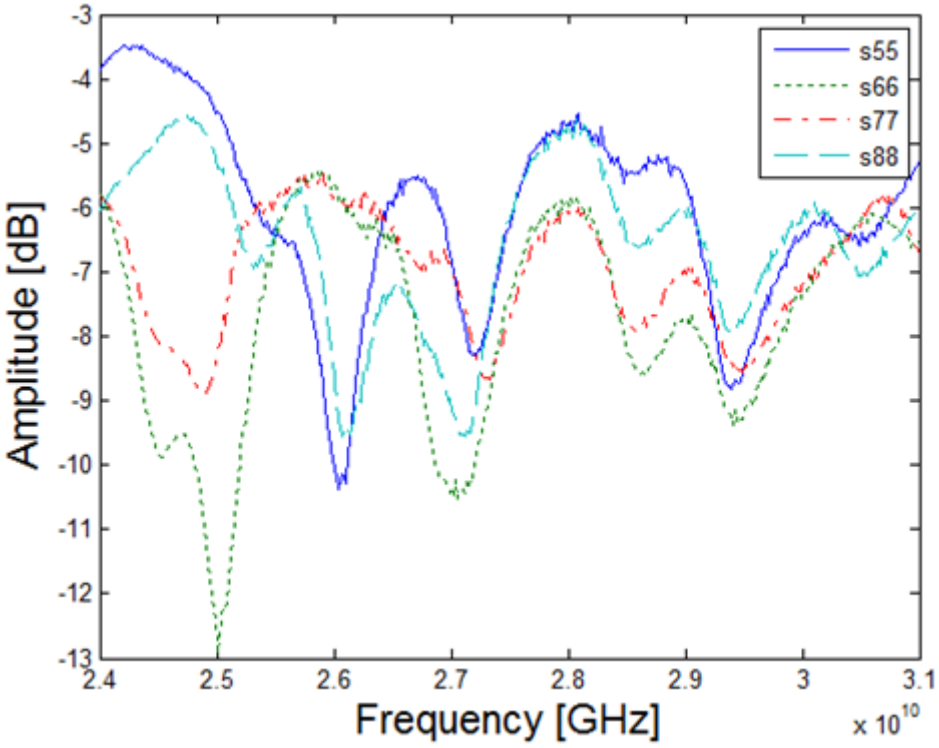

Figure 114 Measured output reflection coefficients of Butler-Stage III

The output reflection coefficients are shown in Figure 114. It can be noticed that the lowest values appear at 27 GHz where all output ports experienced reflections of -8 to -10 dB.

Figure 115 and Figure 116 shows the detected power level at the four output ports when port 1 or 2 is excited, respectively. When port 1 is excited, there are two bands where the levels are kind of close to each other; at 28.5 and at 27 GHz. It can be easily noted that the performance is better at 27 GHz because of the less attenuation in the power. In simulations, there was 4 dB variation between the output ports as shown in Figure 85. This 4 dB variation holds for the band from 28.5 to 29 GHz. As has been noticed before, the performance at 27 GHz is better where signal levels are around -11dB. But the 4dB variation at the outputs holds for narrower BW that what is found at 28.5 GHz. When port 2 is excited, the performance of the system is not well at 28.5 GHz. On the other hand, better and steady response is found at 27 dB. In simulations, the variation between the output ports was found to be about 3 dB as shown in Figure 86. This 3 dB variation holds for about 600 MHz about 27 GHz as can be observed from Figure 116.

In Figure 117 and Figure 118, the phase responses are shown for ports 1 and 2, respectively. Unfortunately, there is non-linearity behavior in all output ports that made us unable to notify any region of operation in the entire band. It should be noted that the effects of the physical ports and the supporting back plane are not considered in the simulations.

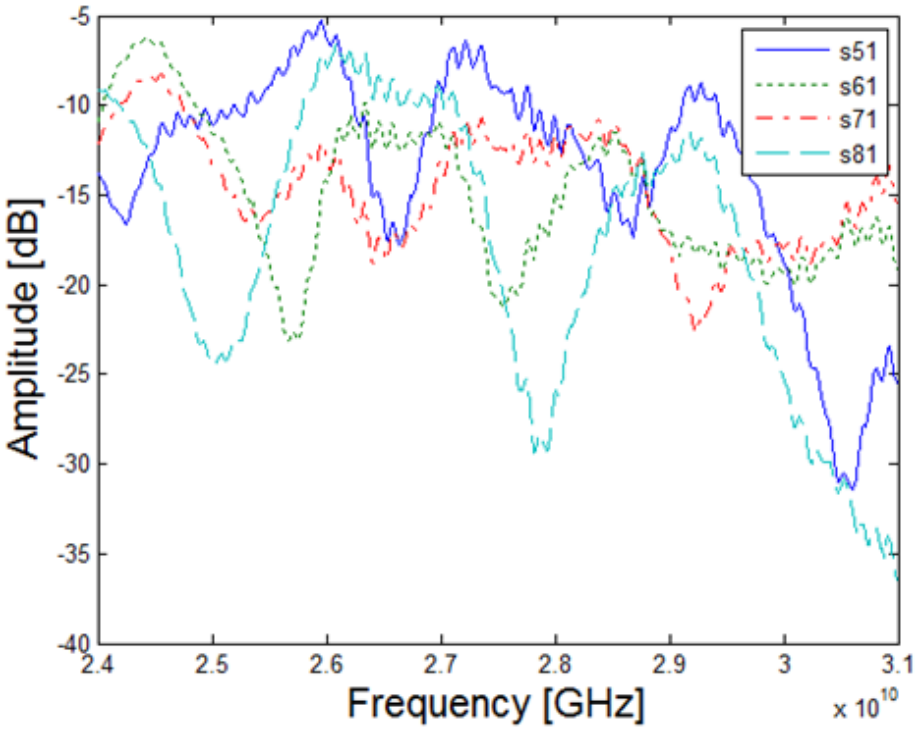

Figure 115 Measured output response of Butler-Stage III when port 1 is excited

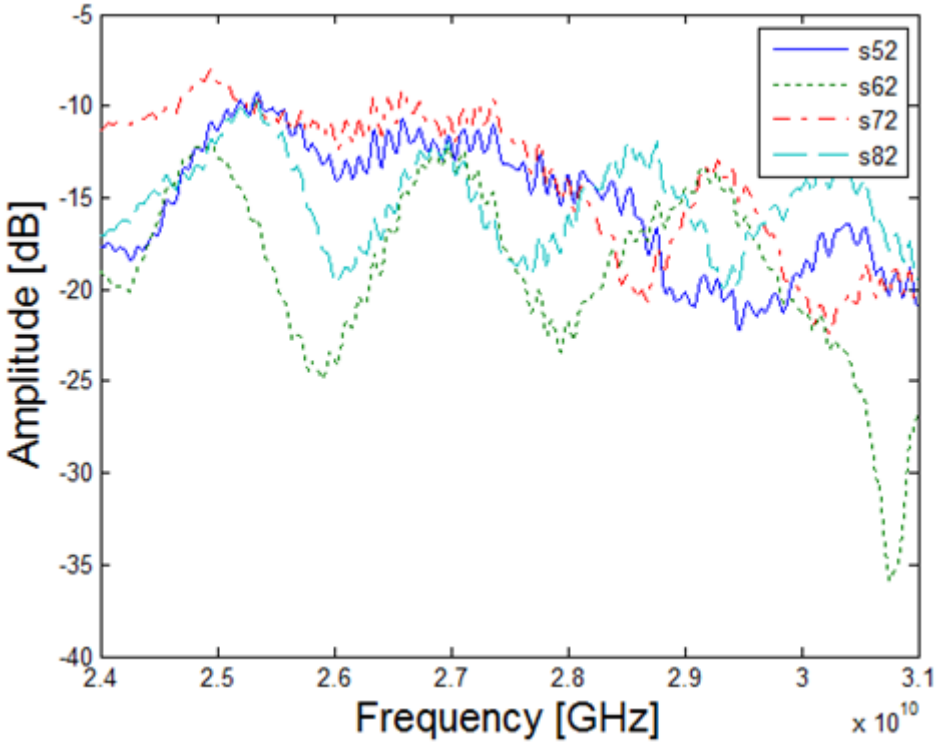

Figure 116 Measured output response of Butler-Stage III when port 2 is excited

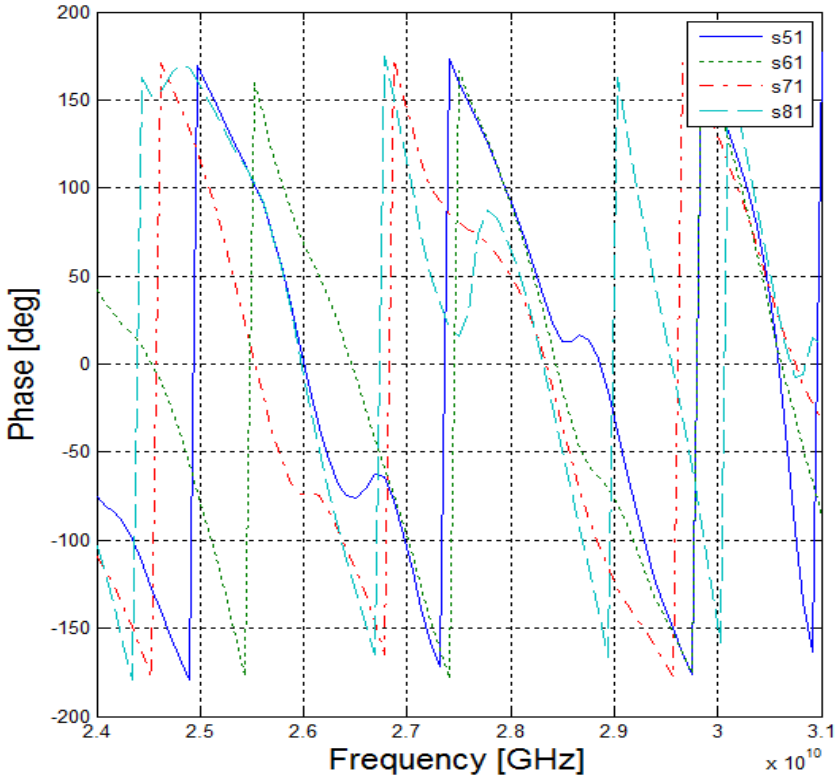

Figure 117 Measured output phase response of Butler-Stage III when port 1 is excited

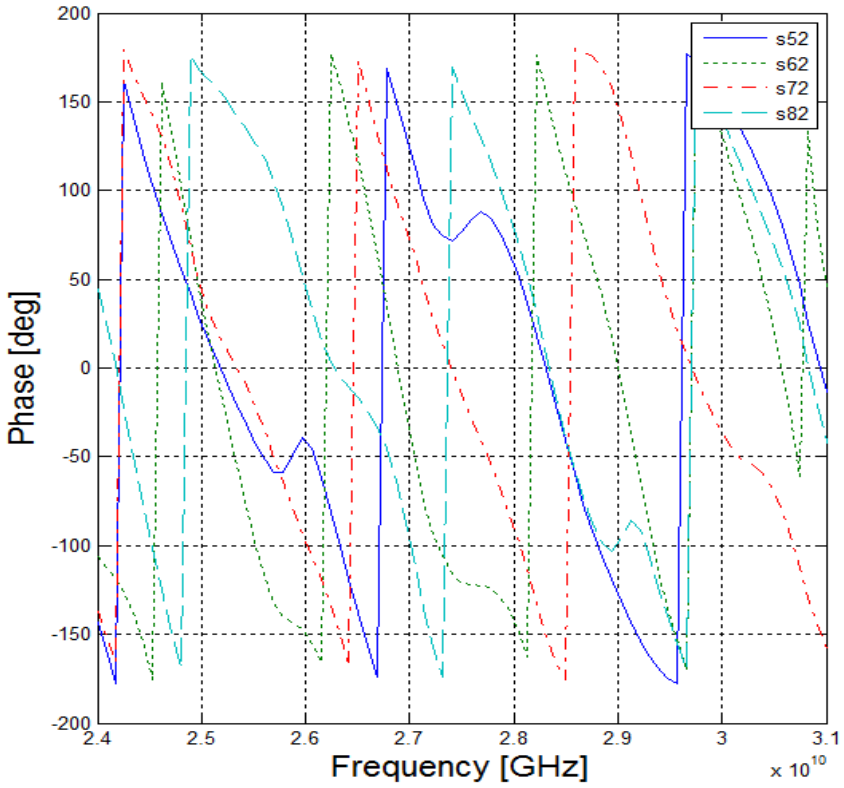

Figure 118 Measured output phase response of Butler-Stage III when port 2 is excited

6.5 Linear Slot Antenna Array

The fabricated 4x4 Slot antenna array is shown in Figure 119. It appeared that the reflection coefficients have shifted 3 GHz down to 25.5 instead of 28.5 GHz as illustrated in Figure 120 while Figure 121 shows a comparison between the simulated and the measured reflection coefficient. Taking 25.5 GHz as the operating band, the reflection coefficients were -18 dB for all of the ports. The -10dB BW was 500 MHz. There were two other resonances at 28 and 30 GHz, but they were barely reaching the -10 dB point. It is expected that when this fabricated antenna array is integrated with the Butler network, it would not provide the optimum performance, since their operating points are now different after fabrication. It must be noted that a plastic backing material was mounted on the area around the connectors to make the substrate more rigid and capable of withstanding the pressure when attaching the cables to the ports, as the substrate is very thin and cannot take any small force.

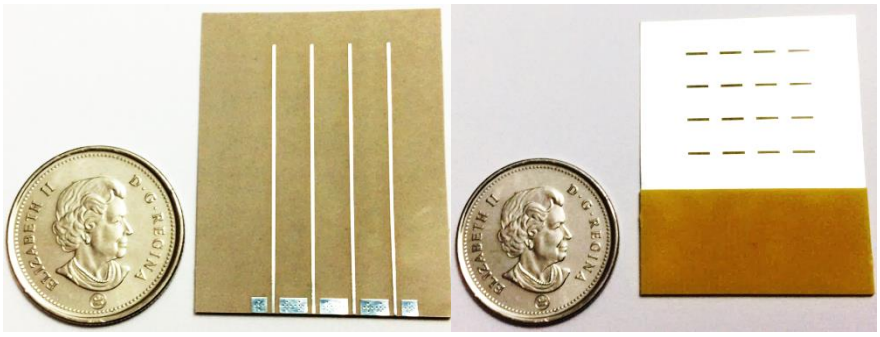

Figure 119 The fabricated 4x4 Slot Antenna Array

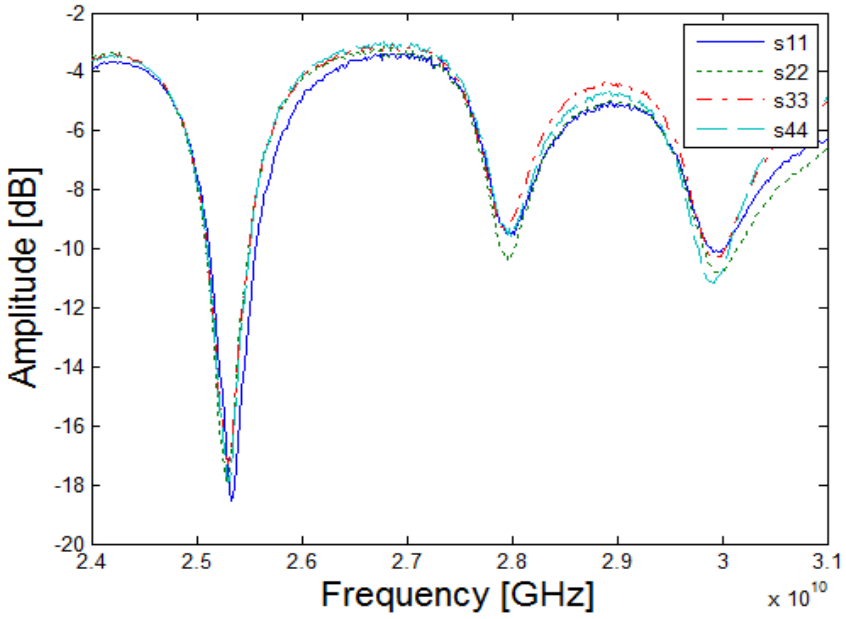

Figure 120 The measured reflection coefficients of the4x4 slot antenna array

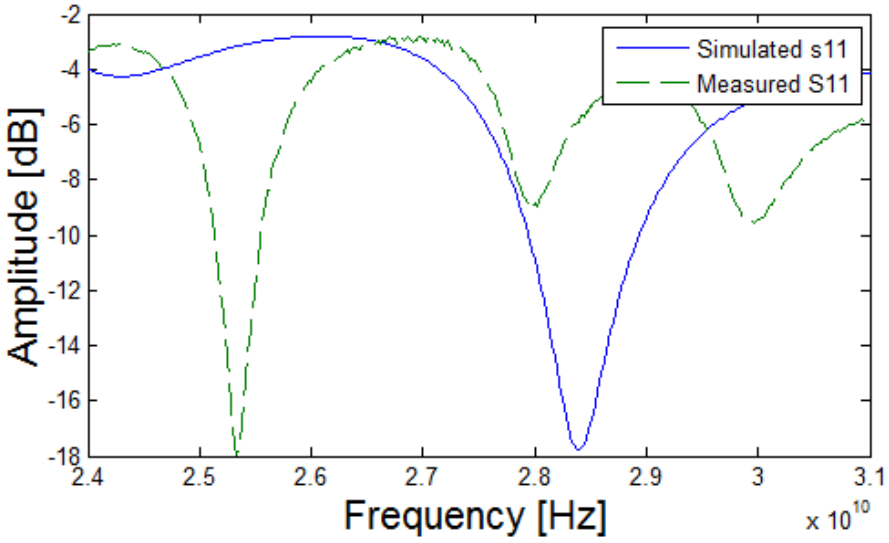

Figure 121 Comparison between Simulated and Measured reflection coefficient S11

6.6 Complete Integrated System

Since the fabricated antenna array operated at 25.5 GHz instead of 28.5 GHz, it is expected that this integrated system would not behave as intended at 28.5 GHz. The fabricated complete integrated system is shown in Figure 122 and its measured reflection coefficients are plotted in Figure 123. The system is having almost -8dB of reflected power at the input ports at 27.5 and at 29 GHz. When port 2 is excited, the reflection coefficients of ports 2 and 3 are -13 dB. The -10 dB BW is almost 400 MHz; from 25 to 25.5 GHz.

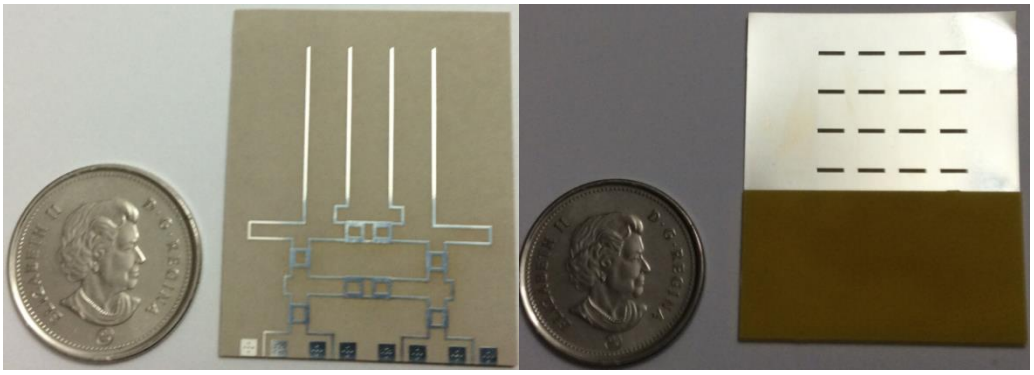

Figure 122 The fabricated complete integrated system

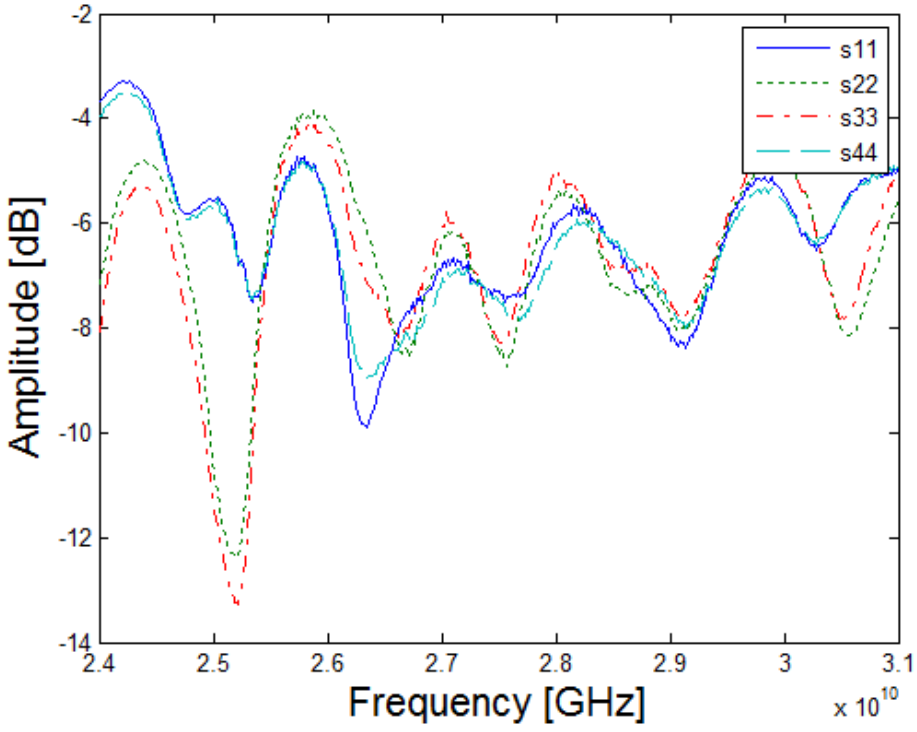

Figure 123 The measured reflection coefficients for the complete integrated system

6.7 Conclusions

In this chapter, fabrications and measurements were shown for different designs; the successful and the unsuccessful ones. First, it showed the failed attempt to fabricate Butler network at AMSD lab and then moved to the measurement conducted for the first successful fabricated model of Butler. Then, measurements have shown that our design of Butler needed to be reconsidered after having higher reflected power than what should be at the input ports of the linear antenna arrays integrated with the Butler network (Stage-II). After that, the Butler network (Stage-III) was measured and found to have a reflection coefficient of -9 dB while it had a -14 dB at 27 GHz. The antenna array was resonating at 25.25 with -18 dB.

It can be concluded that the system operated well at 25.3 GHz with a BW 400 MHz, and that holds only when ports 2 or 3 are excited. Unfortunately, the fabricated system is not operating well at 25.3 GHz when port 1 or 4 is excited. We can conclude that we had a frequency shift in the performance, where the operating point has shifted 3.2 GHz from 28.5 to 25.3 GHz, that is almost 10 % error. Just to mention that in [18], they designed their system at 60 GHz and they got it at 62 GHz, which is 3.4 % error. For the same reasons here, the shift was introduced due to the fabrication process, where a single 0.1mm extra distance in the dimensions can introduce a shift in this very-small size system.

CHAPTER 7

THESIS CONCLUSIONS

7.1 Conclusions

In this Thesis, a beam-steering system was designed, analyzed and fabricated. The design procedure started with its major part which is the Butler network that was fully discussed and analyzed, followed by the design and analysis of the 4x4 slot antenna array alongside with its series feed network as a power splitter. The final complete integrated system has been optimized to operate at 28.5 GHz in simulations. The gain achieved was 11 dB when port 1 or port 4 is excited. While the beams were steered at 4 different locations depending on which input port is excited. In measurement, a 3.2 GHz shift was introduced making the system to operate at 25.2 GHz. Unfortunately, only ports 2 and 3 operated at 25.2 GHz while the others did not.

The Butler feed network has been designed in many stages, summarized by the three mentioned ones in this work. The first Butler network occupied a volume of 0.5 x 25.5 x 36.5 mm^3 while it suffered from huge loss due to the relatively large thickness of the substrate. In the second stage, the thickness has been reduced to 0.13 and the output levels were much more acceptable. Its size was 0.13 x 18.72 x 34 mm^3. The biggest loss experienced at port 6 when port 1 is excited and it was only 2dB (compared to 16 dB loss in the first stage). For the phase responses, the average errors will vary from 13 to 15 degrees, which will not affect the final performance of the integrated system. The last Butler network was designed to enhance the input reflection coefficients of the previous model. It was achieved at the expense of increasing the variation of the detected power at the output ports; they are not as equal as before. Phase errors were in the range which will still not affect the steering mechanism. For the final fabricated Butler Network, there was a difference from 6 to 7.5 dB between the simulated and measured output power levels. Measured phase response was unclear to compare with simulations due to non-linearity behavior exhibited by the network.

After finishing the feed network, the focus was given to the antenna array that will be designed and integrated with the Butler network. Patch and slot antenna were investigated and analyzed. A 1x4, 2x4, 3x4 and 4x4 slot antenna array were designed, where the last one is selected due to its higher gain. (2x4 and 3x4 are shown in Appendix D). In simulations, a reflection coefficient of -18 dB centered at 28.5 GHz with a -10dB BW of 1 GHz is achieved by the 4x4

Slot antenna array. While in measurements, the reflection coefficient was -18.4 dB with a BW of almost 400 MHz and it was shifted down to 25.2 GHz. After that, the complete system (Butler with Antenna Array) was designed and simulated.

Finally, the thesis was concluded with measurements that showed undesired shift in the frequency of operation, keeping in mind that a variation of 0.1 mm in fabrication would introduce considerable frequency shifts. Bearing in mind that the physical ports, backing plate and adapters were not accounted in the simulation, and their effect is quite considerable to the results.

7.2 Future Work

1- Re-optimize the complete integrated system to reduce the frequency shift as much as possible by re-simulating the system and considering finite conducting sheets instead of perfect layers.

2- Try to investigate the energy levels supplied to each slot using the series feed approach and characterize the effect of the end stub on this coupled power levels and phases.

3- Investigate the feasibility of the proposed arrays with MIMO (Multi-input-Multi-Output) systems.

APPENDIX (A) – CHALLENGES

In this section, I would like to mention some difficulties I have faced during this work and how I managed to take over them. Most of the points were mentioned throughout the thesis. But emphasizing them in this section would give clearer pictures about the issues.

The first point encountered was when I was trying to tune the Hybrid Coupler. It is important to note that the minimum peaks of S11 and S41 will not be exactly the same. Ideally, we would like both of them to be minimal, as S11 will affect the reflection coefficient and S41 will affect the coupling between adjacent ports. The key is to concentrate on S11 and make its negative peak centered at 28.5 GHz, then we compromise for S41 making it as low as possible. We will end up with an excellent Hybrid coupler operating at 28.5 GHz.

Another major issue was to choose the right material for the substrate. It is known that for microstrip-based network, it is desired to have high dielectric constant and very thin thickness in order to keep the electric field in the substrate as much as possible. While for microstrip-based antennas, it is recommended to lower the dielectric constant and to increase the thickness of the substrate as we want the electric field to radiate away and not to be captured. For our system, we had both; Butler network and a 4x4 Slot antenna array. So, we had to compromise. Unfortunately, failure of our Butler (Stage I) has forced us to select the thinnest substrate available, ignoring the effect on the radiation performance of the antenna array. Otherwise, the system will not even function properly.

Even after choosing the right material for our system, tuning the early versions of Butler was difficult and would mess up the output amplitude if phases are fixed. However, it was stated that the Schiffman Phase shifter was not used at this high frequency. So, I tried replacing it with a regular transmission lines and it worked. It appears that the Schiffman Phase Shifter was having loosened reflection coefficient that would reflect huge part of the signal passing through it. Due to the high frequency, there also might be some coupling between the small stubs in the small C-section that might end the shifter up to resonate like an antenna instead of a regular phase shifter.

Also, after choosing the appropriate material with the right thickness, and after replacing the Schiffman Phase Shifter by regular transmission lines, tuning the Butler network to have the correct phase differences between the output ports cannot be accomplished to the full limit. Still, if you try to make the phases completely correct when a certain port is excited, you will end up introducing more errors when another port is excited. So, the catch is to compromise. It is recommended to lower the phase errors between the ports that have more power than the ports which have less power.

One of the most difficult obstacles faced in this work was when I tried to make the reflection coefficients for all input ports of Butler resonate to resonate at 28.5 GHz. Even though all individual components were designed to operate at 28.5 GHz, the final Butler was resonating at a frequency higher than 30 GHz. So, I had to redesign all the components at different frequencies in order to have the final Butler resonating at 28.5 GHz. This was solved by enormous optimization based simulations. It happened by having some couplers resonating at 27.2 GHz and crossovers are resonating at 28 GHz. Using these new designs will produce a Butler that has reflection coefficients closer to 28.5 GHz.

For the 4x4 Slot antenna array, there was only one way to control the resonance of the antenna array, which was the inter-element spacing between the elements. Using stub matching is not a recommended choice as the space between adjacent lines is already small. Even if we fit a stub in between, this stub is too close to the next line that it might couple some power from it and affect the performance.

One last point about the measurements, since the substrate is so thin, it is recommended to attach a thick plastic or metalized sheet to the back of the PCB, mounted on the ground. And it is always recommended to use tools and holders for the connection. Never use your bare hands for anything. As shown in Figure 124, a tool holding the entire system is highly recommended when connecting the wires and pushing in the 50 ohm terminations. Also, the wires and the substrate must both be taped before the connection. As the force of a moving wire is enough to destroy the system as shown in Figure 125.

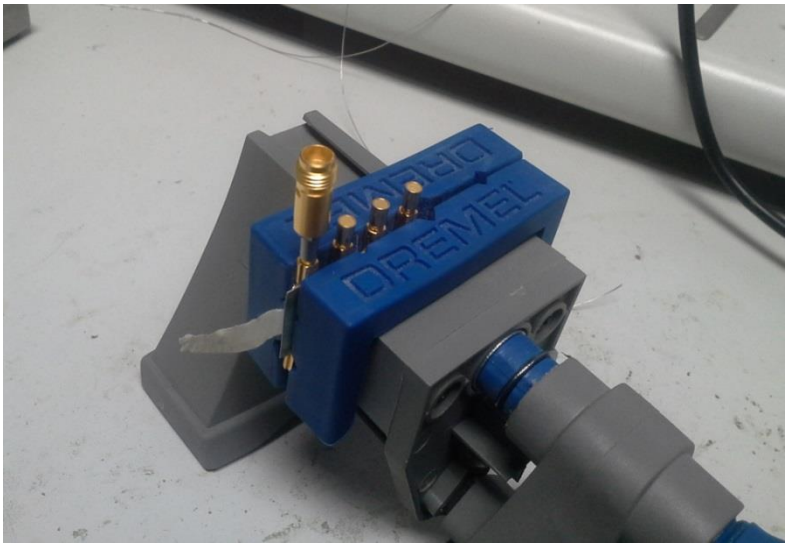

Figure 124 Holder for the complete structure

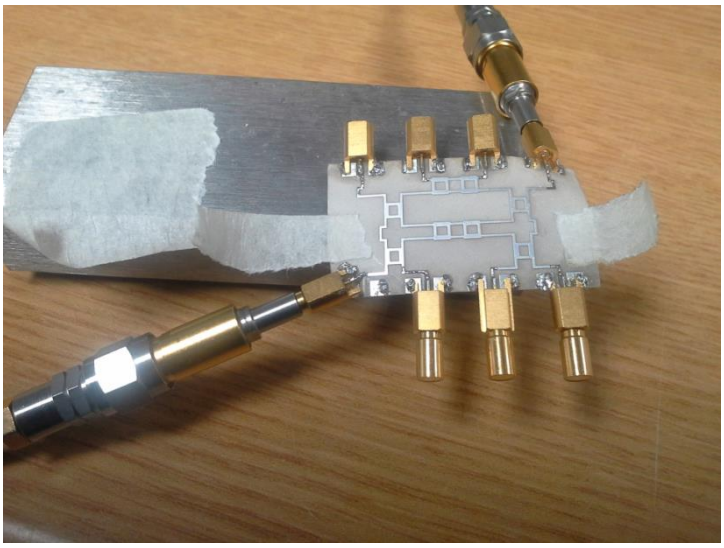

Figure 125 Damaged board due to unmounted cables

APPENDIX (B) – PHASED ARRAY

Given that for an ideal Butler network, the output power levels should be equal and the phase difference between them is controlled. This will result in having a phased antenna array that will provide maximum radiation at certain directions.

The array factor of a linear antenna array can be expressed as:

$$AF = \sum_{n=1}^{N} e^{j(n-1)\psi} \ ;$$

Given that d is the inter-element spacing of the antenna array, β is the phase difference between adjacent elements, N is the number of elements, θ is the elevation angle, the following equations are used:

$$\psi = kd\cos\theta + \beta$$

$$k = {}^{2\pi}/_{\lambda}$$

$$d = {}^{\lambda}/_{2} \text{ (Selected to be half a wavelength)}$$

The next MATLAB code shows the expected patterns when an ideal Butler is connected to a linear 1x4 antenna array. Figure 126 shows the patterns when the phase difference between the ports is varied.

```
clear all
clc
t = -pi:0.01:pi;
deg = t*180/pi;
N = 4 ; % Number of elements
j = sqrt(-1);
z = zeros(size(t));
Beta = [-pi/4, 3*pi/4, -3*pi/4, pi/4];
AFi = zeros(length(Beta), length(t));
%%%%%%%%%%%%%%%%%%%%%%%%%%%%%%%%%%%%%%%%%%%%%%
for ij=1:1:length(Beta)
    AF1=zeros(1,N);
    AF2=zeros(1,length(t));
    for mm=1:1:length(t)
        sum = 0;
        for n=1:1:N
            AF1(n) = exp(j*(n-1)*(pi*cos(t(mm))+Beta(ij)));
            sum = sum+AF1(n);
        end
        AF2(mm) = sum;
    end
AF2max = max(AF2);
```

```
AF2 = AF2/AF2max;
AFi(ij,:) = AF2(1,:);
end
%%%%%%%%%%%%%%%%%%%%%%%%%%%%%%%%%%%%%%%%%%%%
figure(1)
subplot(2,2,1), polar(t,AFi(1,:))
title('Beta = -45 Degrees');
subplot(2,2,2), polar(t,AFi(2,:))
title('Beta = 135 Degrees');
subplot(2,2,3), polar(t,AFi(3,:))
title('Beta = -135 Degrees');
subplot(2,2,4), polar(t,AFi(4,:))
title('Beta = 45 Degrees');
```

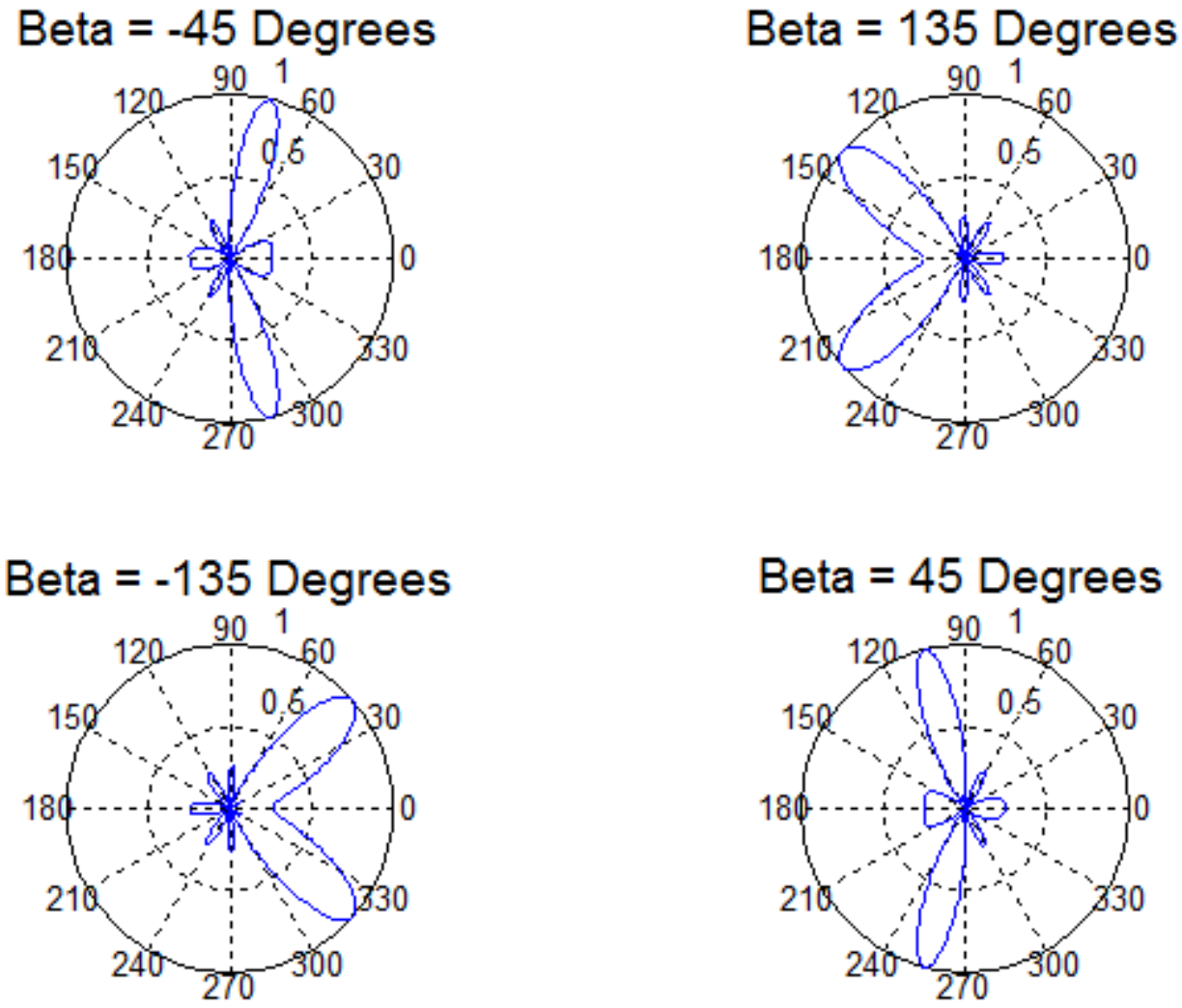

Figure 126 Radiation patterns of a 1x4 linear antenna array connected to an ideal Butler network

APPENDIX (C) – SOFTWARE TOOLS

In this work, two software tools were used to simulate the results for the designs. They were High Frequency Structural Simulator (HFSS) and Microwave Office (MWO). Computational Electromagnetics have several numerical techniques that can be applied to acquire solutions with certain tolerance.

HFSS is one of the commercial industrial tools used to solve the structures for the 3D full wave electromagnetic properties. Its solver is based on a numerical technique that will divide the required structures into small parts and finds the incremental electric and magnetic field components and then sums them geometrically for the whole structure to find to total fileds. This technique is the Finite Element Method (FEM). In FEM the partial differential equations are approximated to find solutions for boundary value problems. Depending on the structure and the case, HFSS also uses integral equation solvers as well as hybrid methods to provide solutions for a wide variety of problems. It is commonly used when designing antennas, microwave circuits and printed circuits.

MWO is a comprehensive tool that provides a variety of different design levels. It can be used to simulate all types of microwave and radio frequency circuits. Its system-level environment can enable designers to build complete system architecture and then observe the performance while optimizing its components. It also has a 3D FEM electromagnetic simulator that will be able to assist the designers to confirm the performance of their circuits. It can optimize and characterize passive components on RF printed circuit boards, monolithic microwave integrated circuit as well as antennas.

APPENDIX (D) – 2x4 & 3x4 SLOT ANTENNA ARRAY

In this appendix, the design and simulations of a 2x4 and a 3x4 slot antenna array will be shown. These array sizes were considered first to evaluate the gain, BW, reflection coefficients and physical dimensions to decide which one could fit within handheld small devices with minimal characteristics.

In Figure 127, the layout with the dimensions of the 2x4 slot antenna array is shown. The wavelength was set to 6.2mm while the slot's width was 0.5mm. A -28dB reflected power is detected at the input ports at 28.5 GHz as noted in Figure 128 where the -10dB BW is 1 GHz. The gain obtained when port 1 is excited is 9.5 dB while it dropped to 7.8 dB with a relatively high back lobe when port 2 is excited. The radiation patterns when ports 1 & 2 are excited are shown in Figure 129.

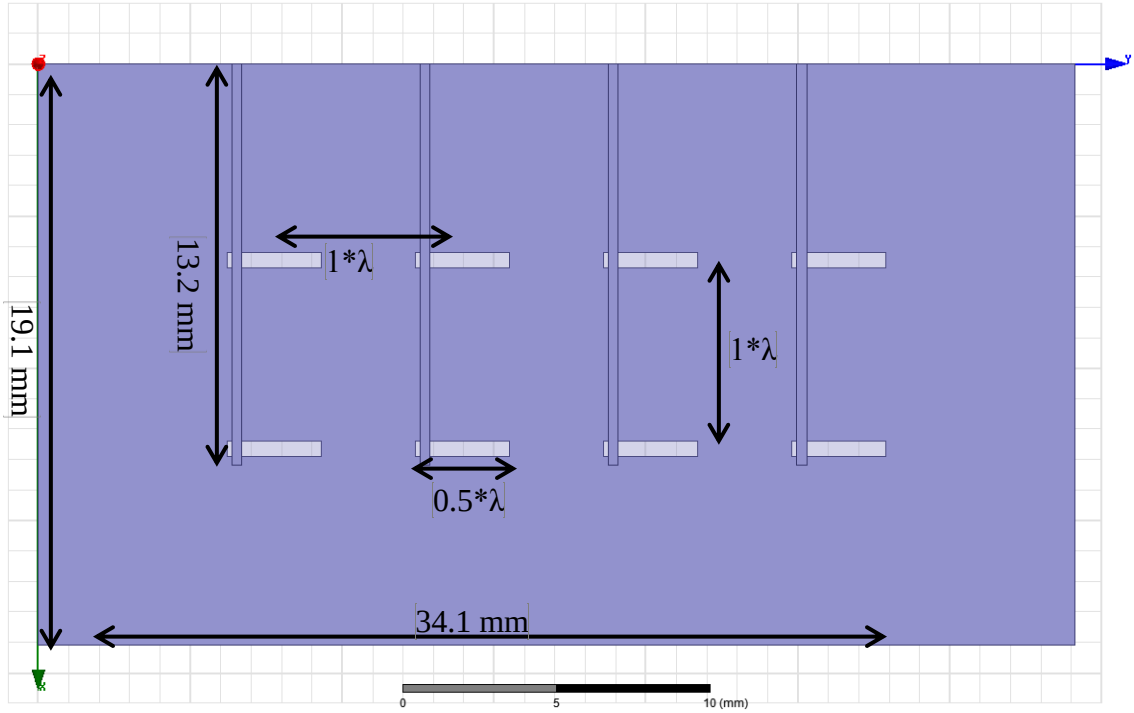

Figure 127 Layout of the 2x4 SLot Antenna Array

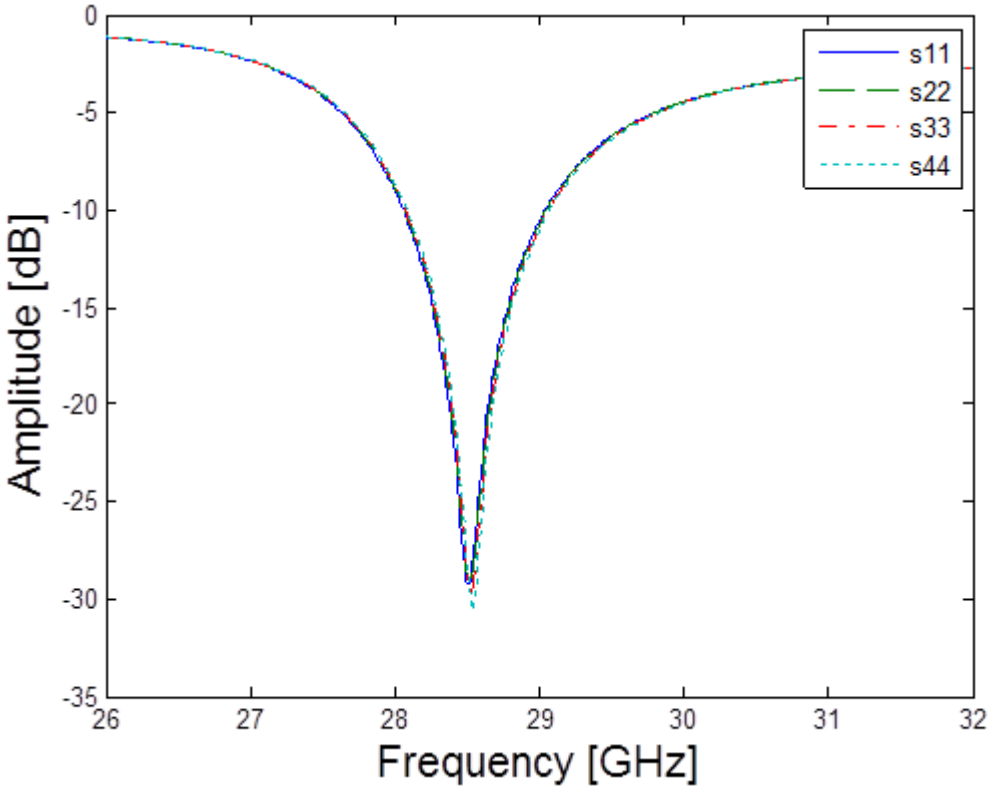

Figure 128 Reflection Coefficients of the 2x4 Slot Antenna Array

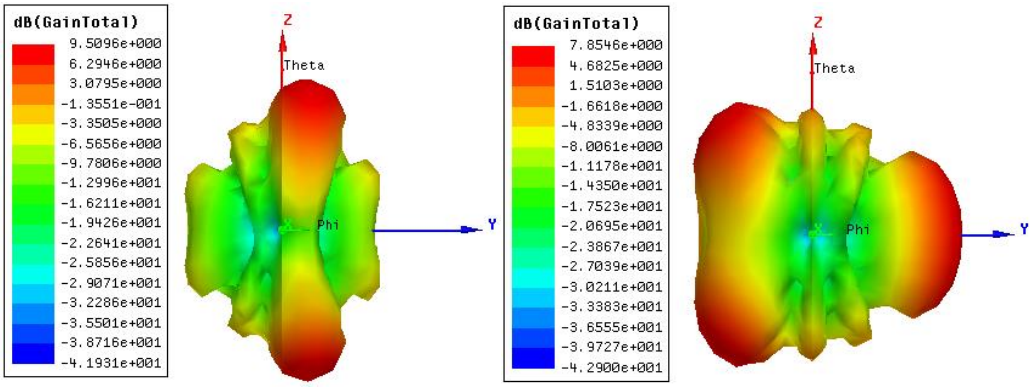

Figure 129 Radiation patterns when port (a) 1 (b) 2 is excited for the 2x4 slot antenna array

The layout shown in Figure 130 is for the 3x4 slot antenna array. Using 12 slots spaced a wavelength apart, the antenna array is resonating at 28.5 GHz with reflection coefficients lower then -20dB for all of the four ports. The slot width was optimized to 0.6mm and the wavelength to 6.55mm. The -10dB BW for this antenna array is 640 MHz; from 28.3 to 28.94 GHz as can be observed from Figure 131.

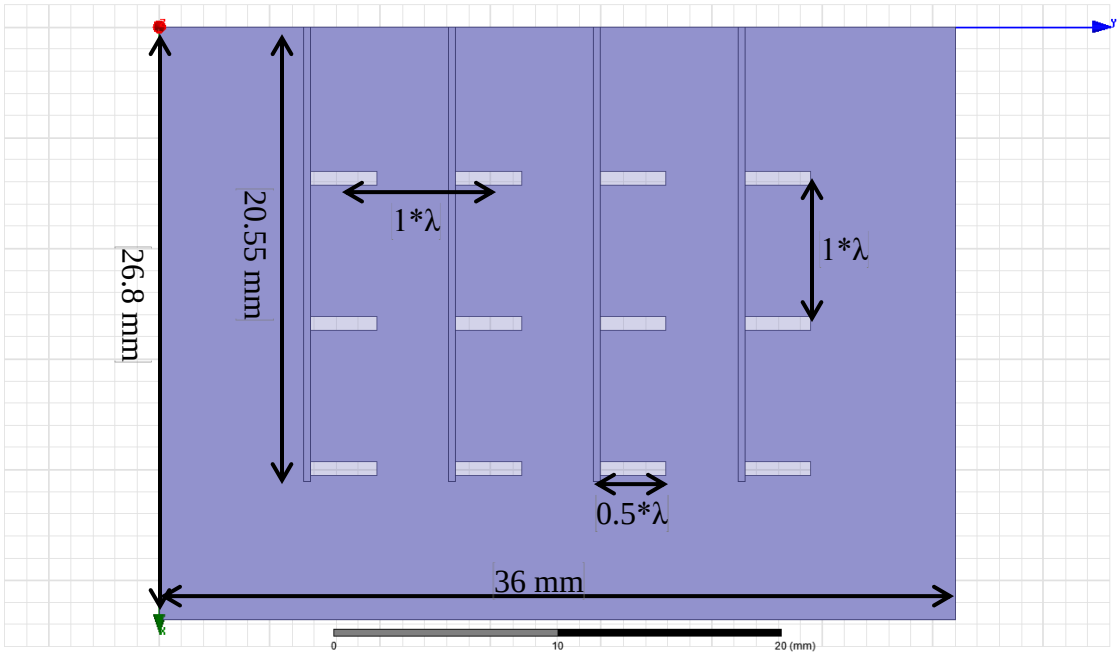

Figure 130 Layout of the 3x4 Slot Antenna Array

Figure 132 shows the radiation patterns when ports 1 & 2 are excited. The maximum gain obtained was 11.4 dB when port 1 is excited. Unfortunately, a relatively high back lope exists when port 2 is excited, while having a gain of 9 dB in the desired direction. Results when ports 3 & 4 are very similar.

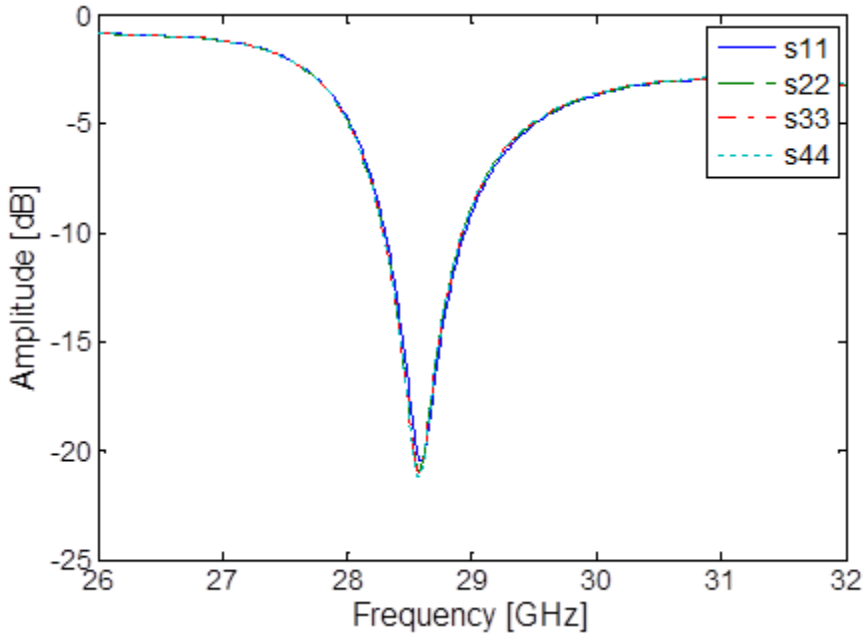

Figure 131 Reflection Coefficients of the 3x4 Slot Antenna Array

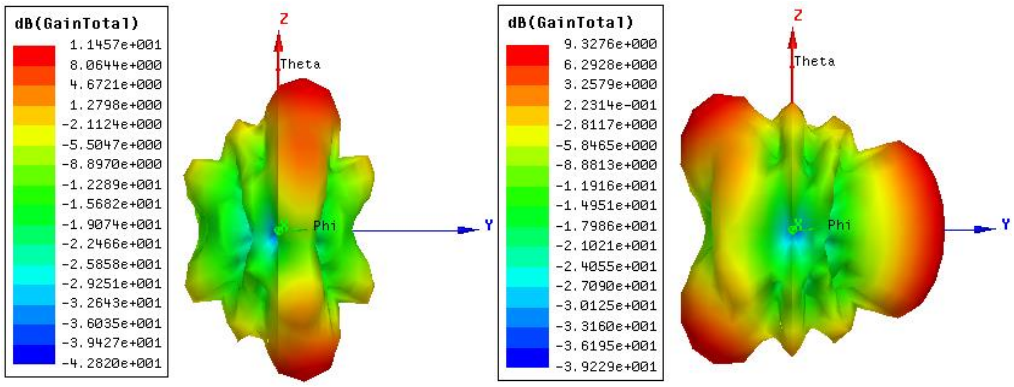

Figure 132 Radiation patterns when port (a) 1 (b) 2 is excited for the 3x4 slot antenna array

References

[1] K.-C. Huang and D. J. Edward, Millimeter Wave Antennas for Gigabit Wireless Communications, Wiley, 2008.

[2] T. S. Rappaport, S. Sun, R. Mayzus, H. Zhao, Y. Azar, K. Wang, G. N. Wong, J. K. Schulz, M. Samimi and F. Gutierrez, "Millimeter Wave Mobile Communications for 5G Cellular: It Will Work!," *IEEE Access*, pp. 335 - 349, 2013.

[3] T. Rappaport, F. Gutierrez, E. Ben-Dor, J. Murdock, Y. Qiao and J. Tamir, "Broadband Millimeter-Wave Propagation Measurements and Models Using Adaptive-Beam Antennas for Outdoor Urban Cellular Communications," *Antennas and Propagation, IEEE Transactions on (Volume:61 , Issue: 4)*, pp. 1850 - 1859, 2013.

[4] S. E. DEIF, "DESIGN OF A PROGRAMMABLE WIDEBAND MICROWAVE FEED NETWORK," Electrical Engineering Department, KFUPM, 2013.

[5] A. Rahimian and R. a. A., "Enhanced RF steerable beamforming networks based on butler matrix and rotman lens for ITS applications," in *IEEE Region 8 International Conference on Computational Technologies in Electrical and Electronics Engineering (SIBIRCON)*, July 2010.

[6] C. A. Balanis, Antenna Theory Analysis and Design, John Wiley & Son, Inc., 1997.

[7] A. Grebennikov, RF AND MICROWAVE TRANSMITTER DESIGN, New Jersey: A JOHN WILEY & SONS, INC., PUBLICATION, 2011.

[8] O. P. Gandhi, "Univerity of Utah - ece class notes," [Online]. Available: http://www.ece.utah.edu/~ece5324/supp.pdf. [Accessed 26 11 2014].

[9] J. Butler and R. Howe, "Beamforming matrix simplifies design of electronically scanned antennas," *Elec. Design, vol. 9*, 1961.

[10] C.-C. Chang, R.-H. Lee and T.-Y. Shih, "Design of a Beam Switching/Steering Butler Matrix for Phased Array System," *Antennas and Propagation, IEEE Transactions on, vol. 58, no. 2*, p. 367 –374, Feb. 2010.

[11] C. Liu, S. Xiao, Y.-X. Guo, M.-C. Tang, Y.-Y. Bai and B.-Z. Wang, "Circularly Polarized Beam-Steering Antenna Array With Butler Matrix Network," *Antennas and Wireless Propagation Letters, IEEE, Volume: 10*, pp. 1278 - 1281, 2011 .

[12] K. Wincza and K. Sachse, "Broadband 4×4 Butler matrix in microstrip multilayer technology designed with the use of three-section directional couplers and phase correction Networks," in *Microwave Radar and Wireless Communications (MIKON), 2010 18th International Conference*, 2010.

[13] R. De Lillo, "A high performance 8-input, 8-output Butler matrix beamforming network for ultra-broadband applications," in *Antennas and Propagation Society International Symposium, 1993. AP-S. Digest*, 1993.

[14] M. Withers, "Frequency-insensitive phase-shift networks and their use in a wide-bandwidth Butler matrix," *Electronics Letters Volume: 5, Issue: 20* , pp. 496 - 498, 1969.

[15] S. Gruszczynski, K. Wincza and K. Sachse, "Broadband 4 × 4 Butler matrices utilizing tapered-coupled-line directional couplers," in *Microwaves, Radar and Remote Sensing Symposium (MRRS), 2011* , 2011 .

[16] K. Ding, F. He, X. Ying and J. Guan, "A compact 8×8 Butler matrix based on double-layer structure," in *Microwave, Antenna, Propagation and EMC Technologies for Wireless Communications (MAPE), 2013 IEEE 5th International Symposium*, 2013 .

[17] N. Jizat, S. Rahim and T. Rahman, "Dual Band Beamforming Network Integrated with Array Antenna," in *Mathematical/Analytical Modelling and Computer Simulation (AMS), 2010 Fourth Asia International Conference*, 2010 .

[18] C.-H. Tesng, C.-J. Chen and T.-H. Chu, "A Low-Cost 60-GHz Switched-Beam Patch Antenna Array With Butler Matrix Network," *IEEE Antennas and Wireless Propagation Letters, vol. 7*, p. 432 –435, 2008.

[19] P. Chow and D. Davies, "Wide bandwidth Butler matrix network," *Electronics Letters Volume:3 , Issue: 6*, pp. 252 - 253, 1967.

[20] M. Bona, L. Manholm, J. P. Starski and B. Svensson, "Low-loss compact Butler matrix for a microstrip antenna," *Microwave Theory and Techniques, IEEE Transactions on, vol. 50, no. 9*, p. 2069 – 2075, 2002.

[21] D. Titz, F. Ferrero, C. Luxey, G. Jacquemod, C. Laporte and H. Ezzeddine, "Design of a miniaturized Butler matrix in IPD process for 60 GHz switched-beam antenna arrays," in *Antennas and Propagation Society International Symposium (APSURSI), 2012 IEEE*, 2012.

[22] S. Gruszczynski and K. Wincza, "Broadband 4x4 Butler Matrices as a Connection of Symmetrical Multisection Coupled-Line 3-dB Directional Couplers and Phase Correction Networks," *Microwave Theory and Techniques, IEEE Transactions on Volume: 57, Issue: 1,*

pp. 1 - 9, 2009.

[23] T. G. Kwang and P. Gardner, "4x—4 Butler Matrix Beam Forming Network using Novel Reduced Size Branchline Coupler," in *Microwave Conference, 2001. 31st European* , 2001.

[24] O. Haraz and A.-R. Sebak, "Two-layer butterfly-shaped microstrip 4×4 Butler matrix for ultra-wideband beam-forming applications," in *Ultra-Wideband (ICUWB), 2013 IEEE International Conference*, 2013 .

[25] K. Wincza and S. Gruszczynski, "A broadband 4×4 Butler matrix for modern-day antennas," in *Microwave Conference, 2005 European, Volume: 2*, 2005.

[26] S. Gruszczynski, K. Wineza and K. Sachse, "Compact broadband Butler matrix in multilayer technology for integrated multibeam antennas," *Electronics Letters, Volume: 43, Issue: 11,* pp. 635 - 636, 2007.

[27] T.-Y. Chin, S.-F. Chang, C.-C. Chang and J.-C. Wu, "A 24-GHz CMOS Butler Matrix MMIC for multi-beam smart antenna systems," *Radio Frequency Integrated Circuits Symposium,* p. 633 –636, 2008.

[28] C.-C. Chang, T.-Y. Chin, J.-C. Wu and S.-F. Chang, "Novel Design of a 2.5-GHz Fully Integrated CMOS Butler Matrix for Smart-Antenna Systems," *Microwave Theory and Techniques, IEEE Transactions on, vol. 56, no. 8,* p. 1757 –1763, Aug. 2008.

[29] K. Park, W. Choi, Y. Kim, K. Kim and Y. Kwon, "A V-band switched beam-forming network using absorptive SP4T switch integrated with 4×4 Butler matrix in 0.13-μm CMOS," in *Microwave Symposium Digest (MTT), 2010 IEEE MTT-S International*, 2010 .

[30] T. Mbarek and Gharsallah, "Mutual Coupling in Phased Arrays For 3×4 Butler Matrices Antenna Network," in *International Conference on Signals, Circuits and Systems*, 2008.

[31] K. Staszek, S. Gruszczynski and K. Wincza, "Broadband Measurements of -Parameters With the Use of a Single 8 8 Butler Matrix," *Microwave Theory and Techniques, IEEE Transactions, vol: 62, issue: 2,* pp. 352 - 360, 2014.

[32] L. M. Abdelghani, T. Denidni and M. Nedil, "Ultra-broadband 4×4 compact Butler matrix using multilayer directional couplers and phase shifters," in *Microwave Symposium Digest (MTT), 2012 IEEE MTT-S International* , 2012.

[33] I. Fanyaev and V. Kudzin, "Beamforming network for eight-element antenna array," in *Ultrawideband and Ultrashort Impulse Signals (UWBUSIS), 2012 6th International Conference*, 2012 .

[34] T. Djerafi and K. Wu, "A Low-Cost Wideband 77-GHz Planar Butler Matrix in SIW Technology," *Antennas and Propagation, IEEE Transactions, Volume: 60, Issue: 10* , pp. 4949 - 4954 , 2012 .

[35] L. Weisgerber and A. Popugaev, "Multibeam antenna array for RFID applications," in *Microwave Conference (EuMC), 2013 European*, 2013.

[36] S. K. Abdul Rahim and P. Gardner, "Beamforming networks using cascaded Butler Matrices," in *Asia-Pacific Conference on Applied Electromagnetics*, APACE, 2007.

[37] C. E. Patterson, W. T. Khan, G. E. Ponchak, G. S. May and J. Papapolymerou, "A 60-GHz Active Receiving Switched-Beam Antenna Array With Integrated Butler Matrix and GaAs Amplifiers," *IEEE Transactions on Microwave Theory and Techniques, vol. no. 99*, p. 1 –10, 2012.

[38] C. Rusch, C. Karcher, S. Beer and T. Zwick, "Planar Beam Switched Antenna with Butler Matrix for 60 GHz WPAN," in *Antennas and Propagation (EUCAP), 2012 6th European Conference*, 2012.

[39] A. P. Thakare and R. N. Shelke, "Planar implementation of Butler Matrix feed network for a switched multibeam antenna array," in *TENCON 2009 - 2009 IEEE Region 10 Conference*, 2009.

[40] M. Nedil, T. Denidni and L. Talbi, "Design and implementation of a new Butler matrix using slot line technology," in *Radio and Wireless Symposium, 2006 IEEE* , 2006 .

[41] P. Mariadoss, M. Rahim and M. Abd Aziz, "Butler matrix using circular and mitered bends at 2.4 GHz," in *Networks, 2005. Jointly held with the 2005 IEEE 7th Malaysia International Conference on Communication., 2005 13th IEEE International Conference*, 2005.

[42] A. García, M. V. Isasa and M. Pérez, "3×3 Microstrip beam forming network for multibeam triangular array," in *Microwave Symposium (MMS), 2010 Mediterranean*, 2010 .

[43] P. Mariadoss, M. Rahim and M. Aziz, "Design and implementation of a compact Butler matrix using mitered bends," in *Microwave Conference Proceedings, 2005. APMC 2005. Asia-Pacific Conference Proceedings, Volume:5*, 2005.

[44] L. Baggen, M. Bottcher and M. Eube, "3D-Butler matrix topologies for phased arrays," in *International Conference on Electromagnetics in Advanced Applications*, 2007.

[45] F. F. He, K. Wu, W. Hong, L. Han and X.-P. Chen, "Low-Cost 60-GHz Smart Antenna Receiver Subsystem Based on Substrate Integrated Waveguide Technology," *Microwave*

Theory and Techniques, IEEE Transactions vol: 60, issue: 4, pp. 1156 - 1165, 2012.

[46] "www.pasternack.com," 2013. [Online]. Available: http://www.pasternack.com/images/ProductPDF/PE44490.pdf. [Accessed 25 11 2014].

[47] R. Merritt, "Intel Surfs Millimeter Waves to 5G," *EE Times,* 1 October 2014.

[48] A. Ali, F. Coccetti, H. Aubert and N. Fonseca, "Novel multi-layer SIW broadband coupler for Nolen matrix design in Ku band," in *Antennas and Propagation Society International Symposium, 2008. AP-S 2008. IEEE* , 2008.

[49] J. Shelton and J. Hsiao, "Reflective Butler matrices," *Antennas and Propagation, IEEE Transactions Volume: 27, Issue: 5,* pp. 651 - 659 , 1979.

[50] K. U-yen, M. Ahn, Z.-J. Zhang and J. Kenney, "Effects of microwave switch isolation on a Butler matrix beamforming network in smart antenna systems," in *Radio and Wireless Conference, 2004 IEEE,* 2004 .

[51] P. Hall and S. Vetterlein, "Review of radio frequency beamforming techniquesfor scanned and multiple beam antennas, " *Microwaves, Antennas and Propagation, IEE Proceedings H Volume: 137 , Issue: 5* , pp. 293 - 303, 1990.

Vitae

Name	:Ali Tawfiq Rashed Al-Reshaid
Nationality	:Saudi
Date of Birth	:1/29/1990
Email	:ali.alreshaid@gmail.com
Address	:Al-Khobar – Eastern Province – Saudi Arabia
Academic Background	:Bachelor Deg.-Electrical Engineering-May 2012-KFUPM